AD-A189 171   HELICAL GEARS WITH CIRCULAR ARC TEETH: GENERATION   1/1
              GEOMETRY PRECISION AND   (U) ILLINOIS UNIV AT CHICAGO
              CIRCLE F L LITVIN ET AL OCT 87 NASA-CR-4089 NAGS3-655
UNCLASSIFIED   F/G 13/9   NL

②

AD-A189 171

Helical Gears With Circular Arc Teeth: Generation, Geometry, Precision and Adjustment to Errors, Computer Aided Simulation of Conditions of Meshing, and Bearing Contact

Faydor L. Litvin and Chung-Biau Tsay

DTIC
SELECTED
DEC 1 8 1987
E

87 12 1 071

US ARMY
AVIATION
SYSTEMS COMMAND
AVIATION R&T ACTIVITY

NASA

Helical Gears With Circular Arc Teeth: Generation, Geometry, Precision and Adjustment to Errors, Computer Aided Simulation of Conditions of Meshing, and Bearing Contact

Faydor L. Litvin and Chung-Biau Tsay
The University of Illinois at Chicago
Chicago, Illinois

Accession For		
NTIS GRA&I		☒
DTIC TAB		☐
Unannounced		☐
Justification		
By		
Distribution/		
Availability Codes		
Dist	Avail and/or Special	
A-l		

NASA

National Aeronautics
and Space Administration

Scientific and Technical
Information Division

1987

Helical Gears with Circular Arc Teeth: Generation, Geometry,

Precision and Adjustment to Errors, Computer

Aided Simulation of Conditions of Meshing and

Bearing Contact

Table of Contents

Circular Arc Helical Gears: Generation, Geometry, Precision
and Adjustment to Errors, Computer Aided Simulation of Conditions
of Meshing and Bearing Contact.

by Faydor L. Litvin
Professor of Mechanical Engineering
Member ASME

Chung-Biau Tsay
Research Assistant
University of Illinois at Chicago, IL 60680

1. Introduction and Principles of Generation

Circular arc helical gears (Wildhaber - Novikov gears) have
the following advantages over involute helical gears: (a) there
is reduced contacting stresses and (b) the conditions of
lubrication are better. The disadvantages of the circular arc
helical gears are: (a) higer bending stresses, (b) the
sensitivity to the change of center distance and (c) a more
complicated shape of the tool. The bending stresses can be
reduced by appropriate proportions of tooth elements. The effect
of dislocation of the bearing contact due to the change of the
gear center distance can be reduced by appropriate relations
between the principal curvatures of the gears and may even be
compensated technologically. Circular arc gears can be
successfully applied in gear trains with limited weight. The
success of Westland Helicopter Co. which designed and
manufactured these gears is the best evidence of this statement.

The main advantages of the discussed gears-reduced
contacting stresses and improved conditions of lubrication - are
the result of special conditions of the contact of gear tooth

1

surfaces and their meshing. Surfaces of the gear teeth contact each other at a point at every instant, instead of a line; the relations between the principal curvatures of surfaces are free of the limitations which exist for gears having line contact of the surfaces; the point of contact (it is the center of the contacting ellipse) moves over the surface <u>along</u> a helix, and it is due to this motion of the contact point and a favorable orientation of the contacting ellipse that the conditions of lubrication are improved substantially.

Consider that shapes Σ_1 and Σ_2 are in contact at point M (Fig. 1.1); Σ_1 and Σ_2 are the cross-sections of gear tooth surfaces; the instantaneous angular velocity ratio is given by

$$m_{12} = \frac{\omega^{(1)}}{\omega^{(2)}} = \frac{0_2 I}{0_1 I}$$

It is not excluded that m_{12} is not constant, thus $m_{12} = f(\phi_1)$ where ϕ_1 is the angle of rotation of gear 1. The derivative $\frac{df}{d\phi_1}$ is equal to zero if and only if the following equation is satisfied

$$\frac{\rho_2 - \rho_1}{(\rho_1 - \ell)(\rho_2 - \ell)} = \frac{\Delta\rho}{\rho_1^2 - \ell(\rho_1 + \Delta\rho) + \ell^2} = \frac{r_1 + r_2}{r_1 r_2 \sin\psi_c} \qquad (1.1)$$

Here: $\rho_2 = C_2 M$, $\rho_1 = C_1 M$ where C_1 and C_2 are the centers of curvatures of shapes Σ_1 and Σ_2, respectively; $\Delta\rho = \rho_2 - \rho_1$; $\ell = IM$; $r = 0_1 I$ and $r_2 = 0_2 I$; ψ_c is the angle formed by the shapes normal, $\underset{\sim}{n}$, and line m-m. Equation (1.1) results in that the difference of curvature radii, $\Delta\rho = \rho_2 - \rho_1$, depends on r_1, r_2, ψ_c, ℓ, and ρ_1 . Thus, $\Delta\rho$ is not a free design parameter and we

2
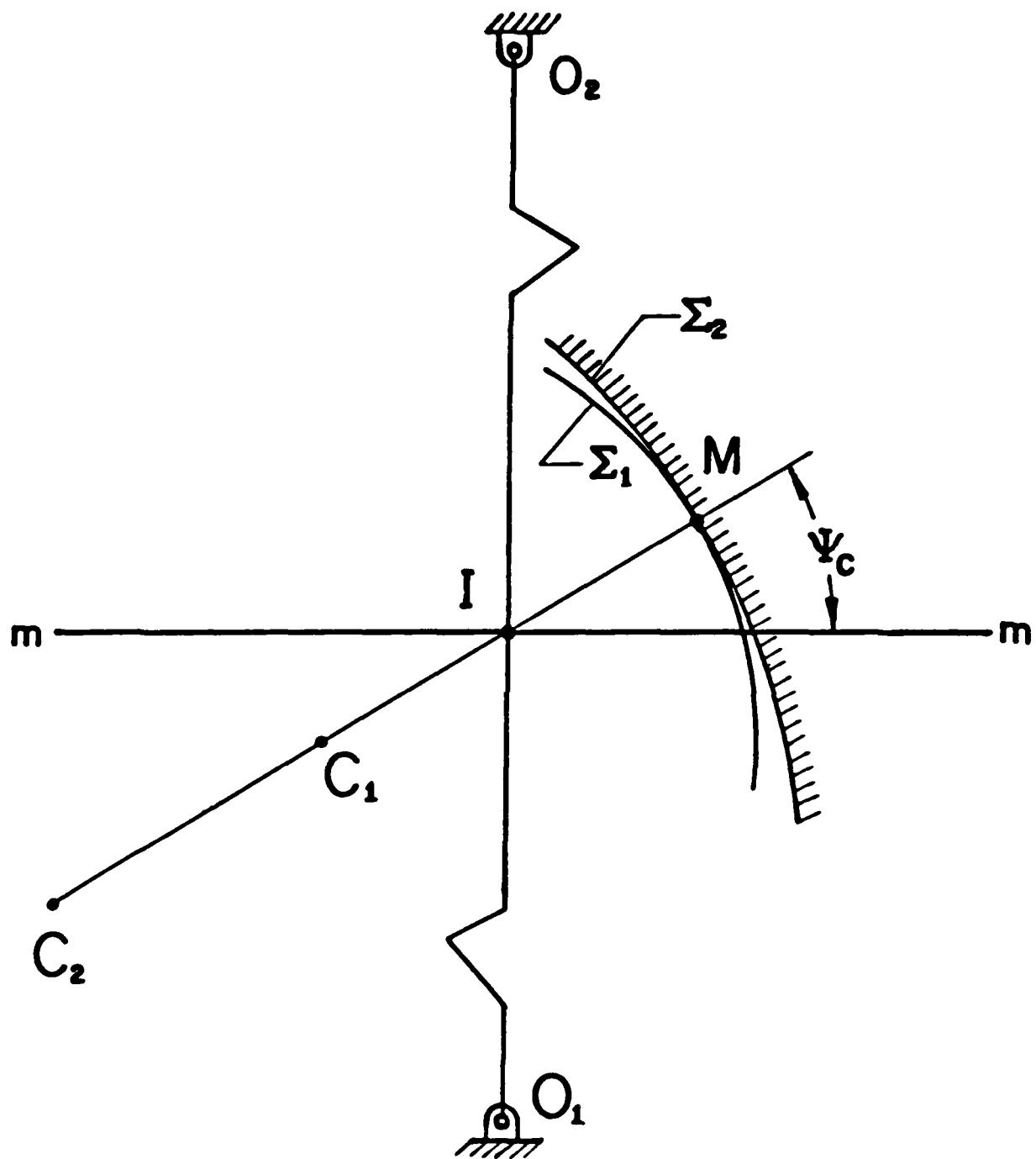
Fig. 1.1

cannot substantially reduce the contacting stress by minimizing $\Delta\rho$. This obstacle can be overcome if the gears are designed as helical gears and the gear tooth surfaces are in point contact.

Consider that the difference of curvature radii, $\Delta\rho$, provides optimal conditions for contacting stresses, but does not satisfy equation (1.1). If the gear tooth surfaces would be designed as spur or helical gears, whose surfaces are in line contact, then such gears would not be able to transform rotation with the constant angular velocity. But if the gears are designed as helcial gears whose surfaces are in point contact, then both requirements - the reduction of contacting stresses and the constancy of gear ratio - can be achieved.

Fig. 1.2 a shows a gear tooth surface of a helical gear. This surface may be generated by a planar curve Σ in its screw motion about axis 0-0.

Consider two cross-section of the gear tooth surface formed by cutting the surface by two planes, P_1 and P_2 (Fig. 1.2a,b). Shapes $\Sigma^{(1)}$ and $\Sigma^{(2)}$ lie in planes P_1 and P_2, respectively. The location and orientation of $\Sigma^{(2)}$ with respect to $\Sigma^{(1)}$ is determined by the axial displacement and rotation of $\Sigma^{(1)}$ in its screw motion while it generates the screw surface of the gear. We assume that in such a screw motion of $\Sigma^{(1)}$, the gear is at rest.

Now, consider that two helical gears are in mesh and their screw surfaces contact each other at point M initially (Fig. 1.2 b). The shapes of gears 1 and 2 have a common normal n^* at M, which passes through point I - the point of intersection of the

4

(a)

(b)

LINE OF ACTION

Fig. 1.2

5
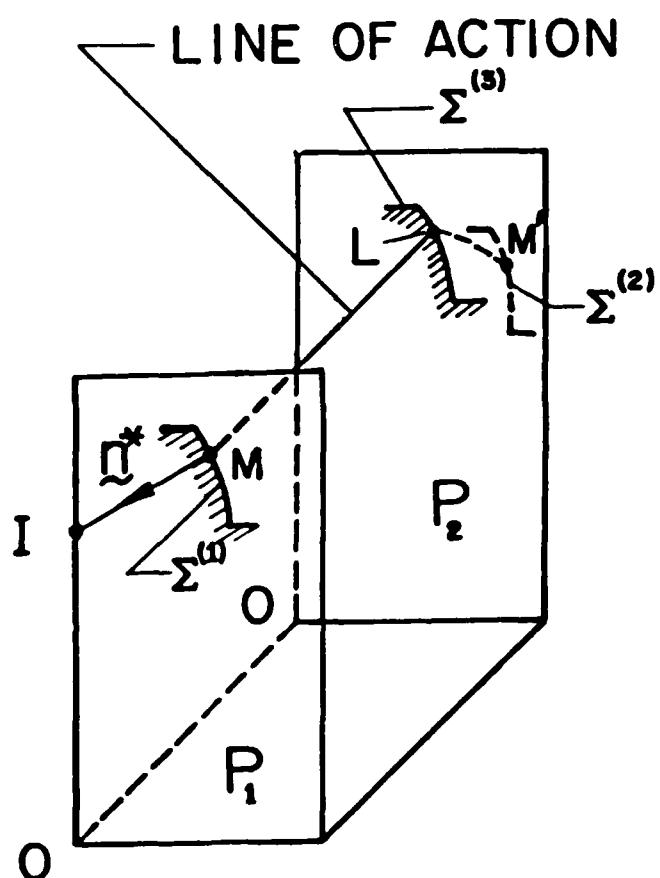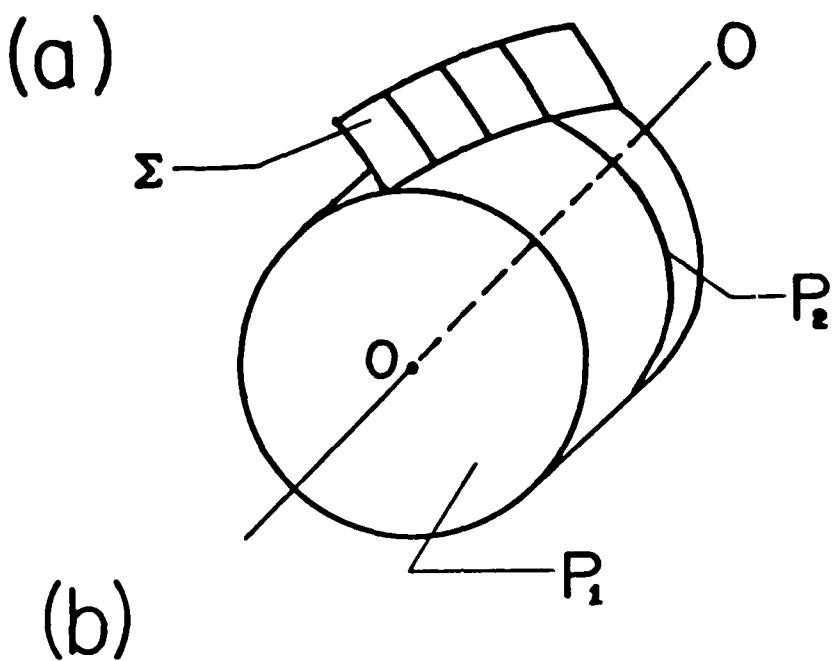
instantaneous axis of rotation I - I with the plane P_1. Shape $\Sigma^{(2)}$ of the screw surface of gear 1 will come in contact with the corresponding shape of gear 2 if the gears will be rotated through certain angles about their axes. For instance, shape $\Sigma^{(2)}$ of gear 1 will come in tangency with the mating shape of gear 2 if shape $\Sigma^{(2)}$ takes the position of $\Sigma^{(3)}$. This position can be reached if the gear with its screw surface (thus with the shapes $\Sigma^{(1)}$ and $\Sigma^{(2)}$) is rotated about axis 0-0. Shapes $\Sigma^{(3)}$ and $\Sigma^{(1)}$ have the same orientation but lie in different plane P_1 and P_2, respectively. In the process of meshing of helical gears with the type of point contact described above, the gear tooth surfaces contact each other at every instant at a point along the line ML, which is parallel to the axes of gear rotations. Line ML is the line of action of gear tooth surfaces.

It is known that a screw surface of a helical gear may be generated by a cylindrical surface Σ_c whose generatrix are parallel to plane π and form a certain angle with the gear axis (Fig 1.3 a). Plane π is the tangent plane to the gear cylinder of radius r. While the generating surface Σ_c translates with plane π, with velocity $\underset{\sim}{v}$, the gear rotates with angular velocity ω, where $\omega = v \div r$. Plane π and the cylinder of radius r are the axodes.

To generate gears having point contact of their surfaces, we have to use two generating cylindrical surfaces, $\Sigma_c^{(1)}$ and $\Sigma_c^{(2)}$ (Fig. 1.3 a), which contact each other along a straight line. While plane π translates with velocity $\underset{\sim}{v}$, the gears rotate with angular velocities, $\underset{\sim}{\omega}^{(1)}$ and $\underset{\sim}{\omega}^{(2)}$ respectively (Fig. 1.3 b).
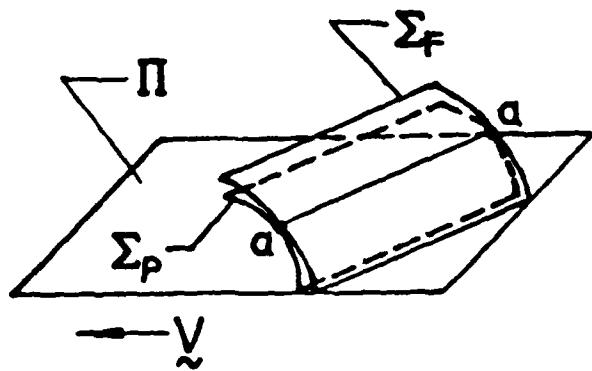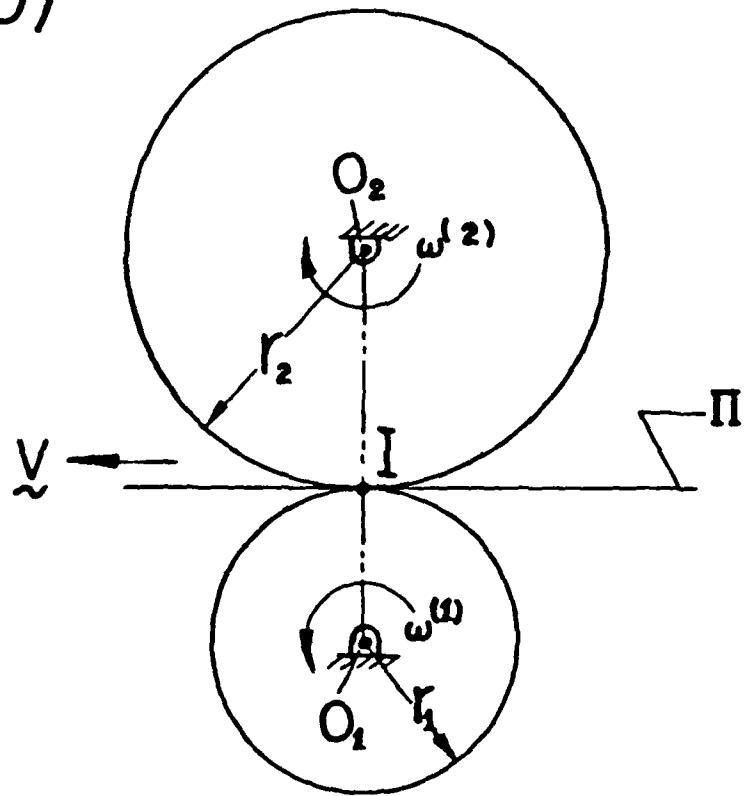
Fig. 1.3

We may imagine that surface $\Sigma_c^{(1)}$ generates the screw surface of gear 1, and $\Sigma_c^{(2)}$ generates the screw surface Σ_2 of gear 2. The surfaces of helical gears, Σ_1 and Σ_2, will be in point contact and their line of action will be the line ML (Fig 1.2 b).

We have to emphasize that surfaces $\Sigma_c^{(i)}$ and Σ_i (i = 1,2) are in _line_ contact and Σ_i is generated as an envelope of the family surfaces $\Sigma_c^{(i)}$. Using two different generating surfaces, $\Sigma_c^{(1)}$ and $\Sigma_c^{(2)}$, we may generate screw surfaces for both helical gears with a point contact of the gear tooth surfaces, and overcome the limitation of the difference of the curvatures determined by equation (1.1). The described method of generation is the key to the problem of synthesis of helical gears with reduced contacting stresses.

2. Generating Surfaces

Fig. 2.1 shows the normal section of the _space_ of rack cutter F which generates the tooth of gear 1. The shapes of the rack cutter for each of its sides represent two circular arcs centered at C_F and $C_F^{(f)}$, respectively. The circular arc of radius $\rho_F^{(f)}$ with center at $C_F^{(f)}$ generates the fillet surface of the gear 1 while the circular arc of radius ρ_F with center at C_F generates the working surface. Point $0_a^{(F)}$ lies in plane π (Fig. 1.3).

Fig. 2.2 shows the normal section of the _tooth_ of the rack cutter P which generates the space of gear 2. The shape of the rack cutter for each side represents two circular arcs centered

Fig. 2.1

9

Fig. 2.2

10
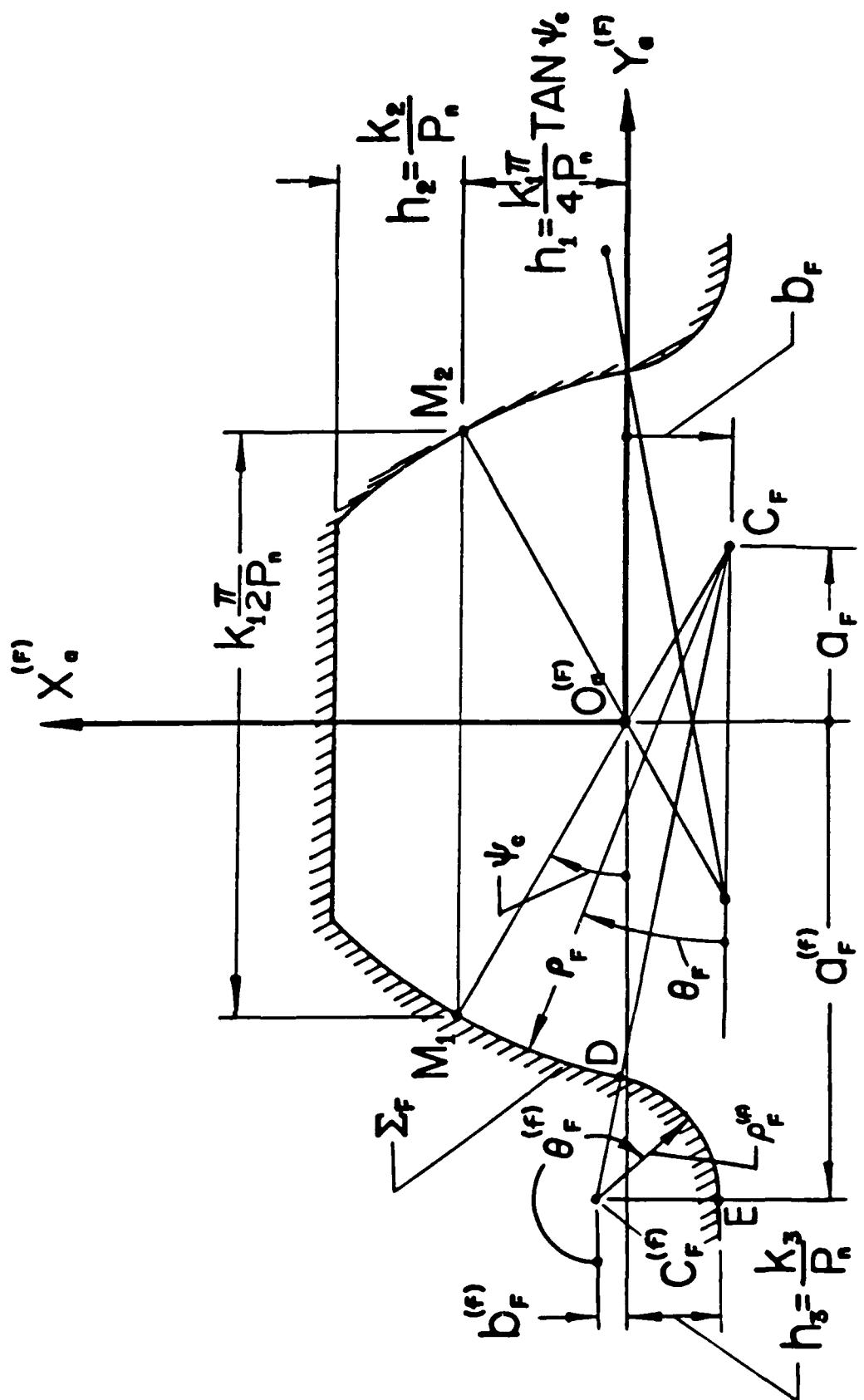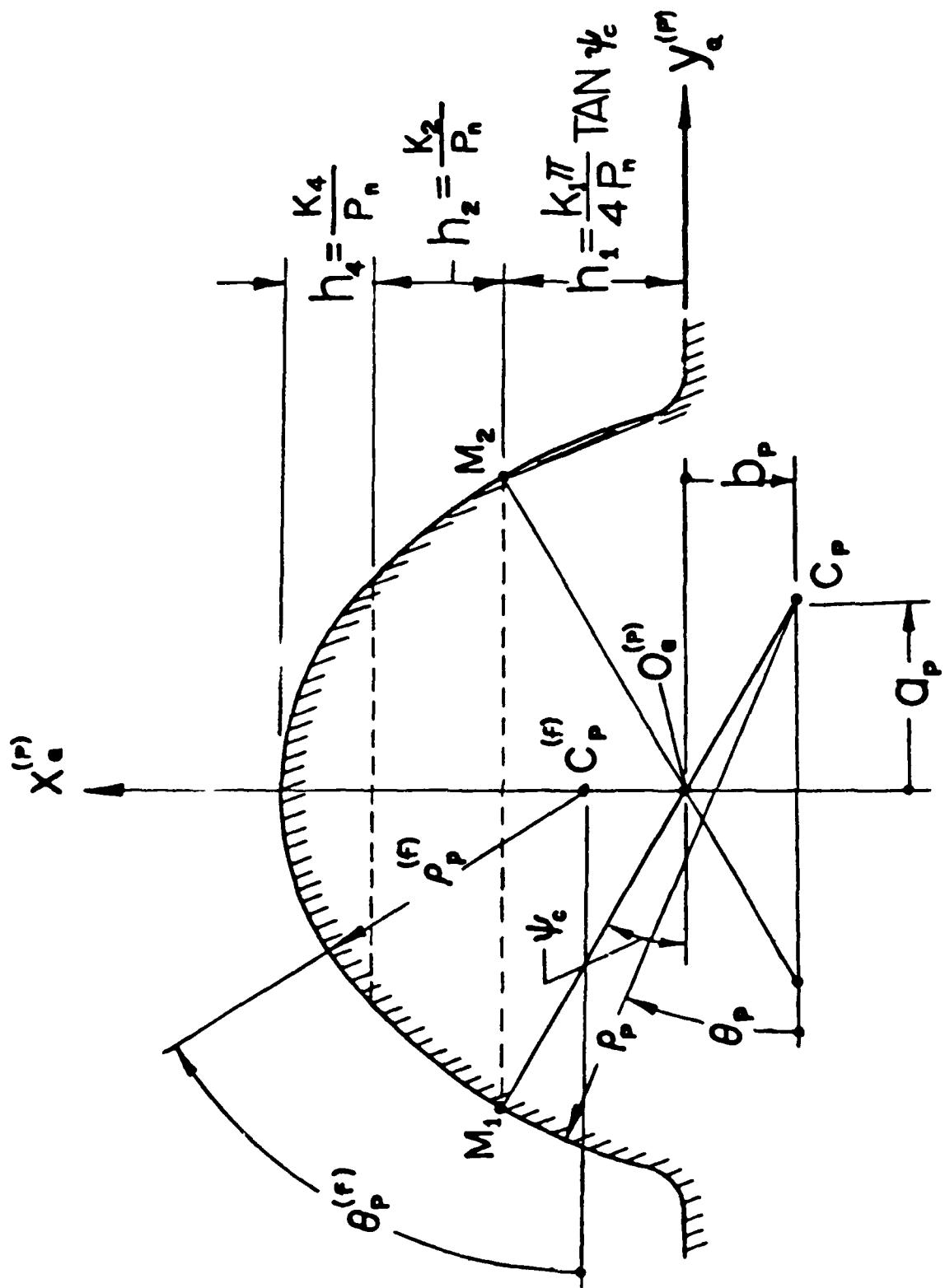
at C_p and $C_p^{(f)}$, respectively. The circular arc of radius $\rho_P^{(f)}$ with center at $C_p^{(f)}$ generates the fillet surface of gear 2 while the circular arc of radius ρ_P with center at C_p generates the working surface.

The shapes of the mating rack cutters do not coincide; rather they are in tangency at points M_1 and M_2.

We may represent all four circular arcs in the coordinate system $S_a(x_a, y_a, z_a)$ by the same equations

$$x_a^{(i)} = \rho_i \sin\theta_i - b_i, \quad y_a^{(i)} = -(\rho_i \cos\theta_i - a_i), \quad z_a^{(i)} = 0 \qquad (2.1)$$

Here: ρ_i is the radius of the circular arc, a_i and b_i are algebraic values which determine the location of the center of the circular arc; θ_i is the variable parameter which determines the location of a point on the circular arc (θ_i is measured clockwise from the negative axis y_a); P_n is the diametral pitch in the normal section; and ψ_c is the pressure angle. The element proportions of rack cutters h_1, h_2, h_3 and h_4 are expressed in terms of the normal diametral pitch, P_n.

It was mentioned above that equations (2.1) represent all four circular arcs - the shapes of both rack cutters. Thus equations

$$x_a^{(F)} = \rho_F \sin\theta_F - b_F, \quad y_a^{(F)} = -(\rho_F \cos\theta_F - a_F), \quad z_a^{(F)} = 0 \quad (2.2)$$

represent the circular arc centered at C_F (Fig. 2.1).

Knowing the normal section of the rack cutter, we may derive

11

equations of the generating surface using the matrix form of coordinate transformation. Consider that a rack cutter shape is represented in the coordinate system $S_a^{(i)}$ (Fig. 2.3 b) while the coordinate system $S_a^{(i)}$ translates along the line $0_c^{(i)}$ $0_a^{(i)}$ with respect to $S_c^{(i)}$; $0_c 0_a = u_i$ is a variable parameter. Using the matrix equation

$$
\begin{bmatrix} x_c^{(i)} \\ y_c^{(i)} \\ z_c^{(i)} \\ 1 \end{bmatrix} = \begin{bmatrix} 1 & 0 & 0 & 0 \\ 0 & \sin\lambda_i & \cos\lambda_i & u_i\cos\lambda_i \\ 0 & -\cos\lambda_i & \sin\lambda_i & u_i\sin\lambda_i \\ 0 & 0 & 0 & 1 \end{bmatrix} \begin{bmatrix} x_a^{(i)} \\ y_a^{(i)} \\ z_a^{(i)} \\ 1 \end{bmatrix} \quad (2.3)
$$

we obtain ($i = F, P$)

$$
\left.
\begin{aligned}
x_c^{(i)} &= \rho_i \sin\theta_i - b_i \\
y_c^{(i)} &= -(\rho_i \cos\theta_i - a_i)\sin\lambda_i + u_i\cos\lambda_i \\
z_c^{(i)} &= (\rho_i \cos\theta_i - a_i)\cos\lambda_i + u_i\sin\lambda_i
\end{aligned}
\right\} \quad (2.4)
$$

In the derivation of equations (2.4), we assumed that $a_i > 0$ and $b_i > 0$. The unit normal to the rack cutter surface is given by the equations

$$
n_c^{(i)} = \frac{N_c^{(i)}}{\left| N_c^{(i)} \right|} \ , \ N_c^{(i)} = \frac{\partial r_c^{(i)}}{\partial \theta_1} \times \frac{\partial r_c^{(i)}}{\partial u_1} \quad (2.5)
$$

Equations (2.4) and (2.5) yield

$$
[n_c^{(i)}] = \begin{bmatrix} \sin\theta_1 \\ -\cos\theta_1\sin\lambda_1 \\ \cos\theta_1\cos\lambda_1 \end{bmatrix} \quad (2.6)
$$

12

(a)

(b)
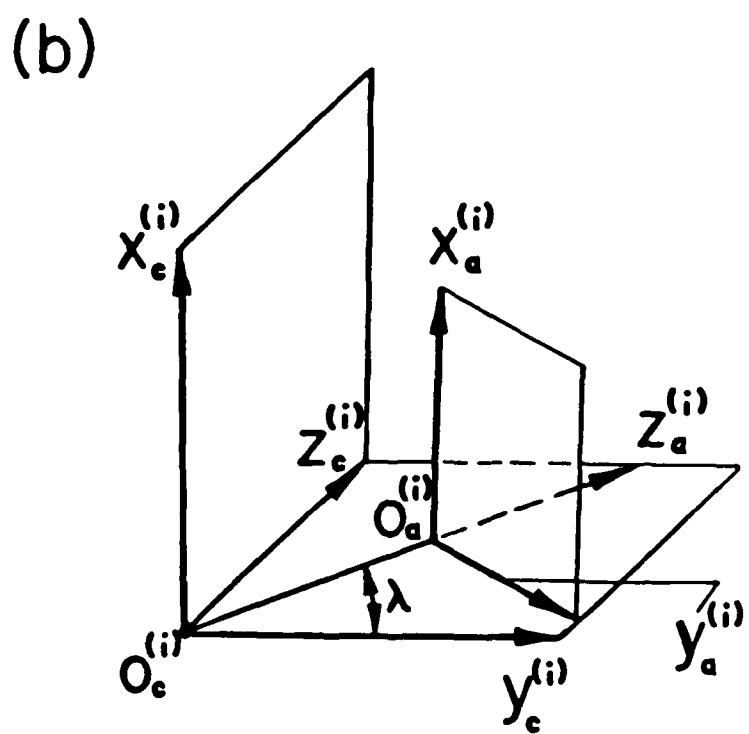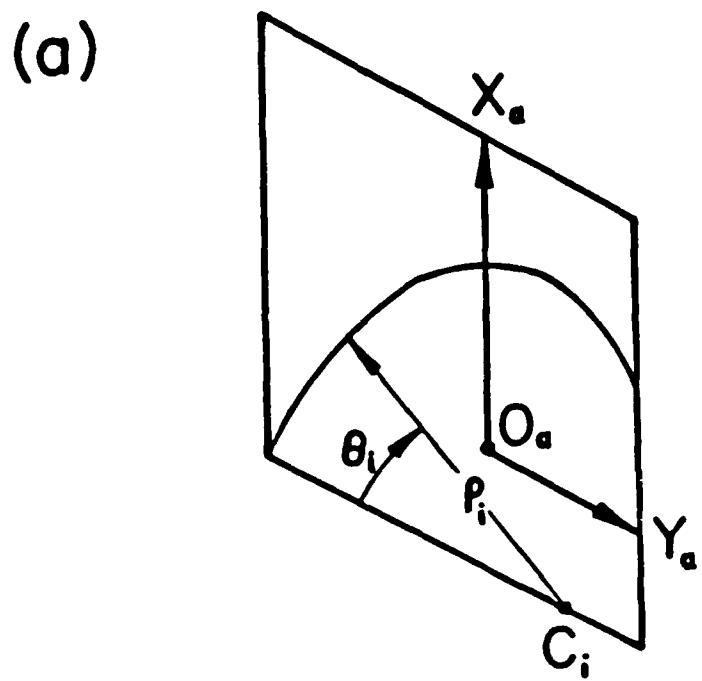
Fig. 2.3

13

Consider that coordinate systems $S_c^{(F)}$ and $S_c^{(P)}$ coincide. Surfaces $\Sigma_c^{(F)}$ and $\Sigma_c^{(P)}$ will be in tangency if the following equations are satisfied

$$x_c^{(F)} = x_c^{(P)} , \quad y_c^{(F)} = y_c^{(P)} , \quad z_c^{(F)} = z_c^{(P)} \qquad (2.7)$$

$$n_{xc}^{(F)} = n_{xc}^{(P)} , \quad n_{yc}^{(F)} = n_{yc}^{(P)} \quad n_{zc}^{(F)} = n_{zc}^{(P)} \qquad (2.8)$$

Equations (2.4), (2.6), (2.7) and (2.8) yield that surfaces Σ_F and Σ_p are in tangency along a straight line a-a (Fig. 1.3, a) if the following conditions are satisfied.

$$\theta_F = \theta_P = \psi_c , \quad u_F = u_P, \quad \lambda_F = \lambda_P, \quad (\rho_P - \rho_F)\sin\psi_c = b_p - b_F,$$

$$(\rho_P - \rho_F)\cos\psi_c = a_P - a_F \qquad (2.9)$$

Here: ψ_c is the pressure angle.

The normal sections of the gear teeth do not coincide with the corresponding normal sections of the rack cutters. Neglecting this difference we may identify the normal sections of gear teeth with the normal sections of rack cutters. The shapes of the gear teeth in the normal section are shown in Fig. 2.4. These shapes are in tangency at points M_1 and M_2. Considering the two sides of the teeth, we have to consider two pairs of surfaces, Σ_F and Σ_P. Each pair of these surfaces is in tangency along a straight line a-a (Fig. 1.3 a) and point $M_i (i = 1, 2)$ lies on a-a. The shape normals at M_1 and M_2 pass through point I which lies on the instantaneous axis of rotation and coincides

14
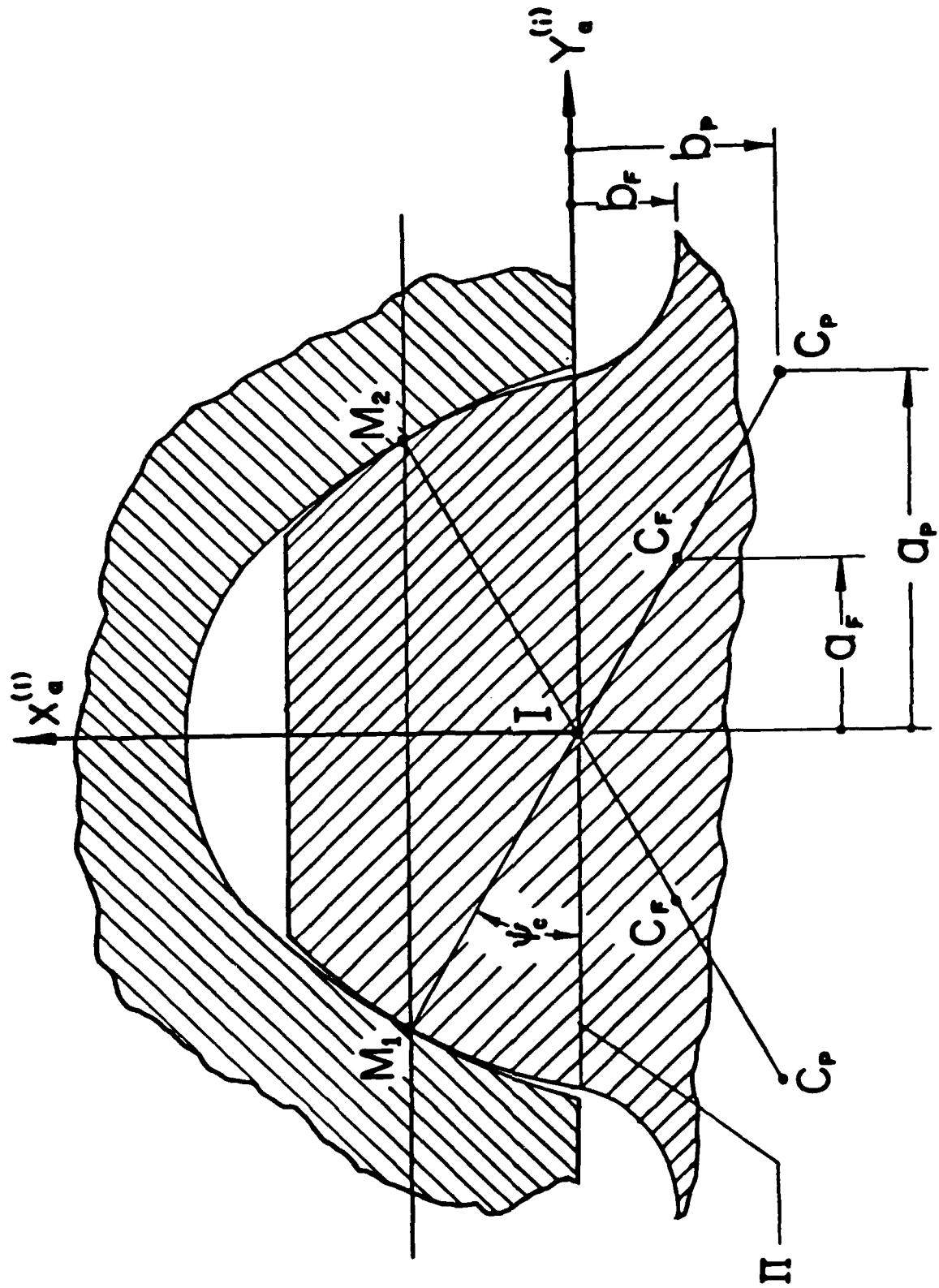
Fig. 2.4

with the origins $0_a^{(F)}$ and $0_a^{(P)}$ for the position shown in Fig. 2.1 and Fig. 2.2

3 Tooth Surfaces of Gear 1 and Gear 2

We set up three coordinate systems: S_c and S_1 rigidly connected to the rack cutter and gear 1, respectively, and the fixed coordinate system S_f (Fig. 3.1, a). Note that in Fig. 3.1 a, the fixed coordinate system S_f coincides with the auxiliary coordinate system S_h.

The derivation of the gear tooth surface Σ_1 is based on the following considerations: (Here Σ_1 represents gear 1 tooth surface, see also Appendix I)

The line of contact of the generating surface Σ_c with the gear tooth surface Σ_1 may be determined in the coordinate system S_c by using the following equations:

$$
\begin{aligned}
\underset{\sim}{r}_c &= \underset{\sim}{r}_c(u_i, \theta_i) \ \varepsilon \ c^1 \\
\underset{\sim}{N}_c \cdot \underset{\sim}{V}_c^{(c1)} &= f(u_i, \theta_i, \phi_1) = 0
\end{aligned}
\tag{3.1}
$$

Here: $\underset{\sim}{r}_c(u_i, \theta_i)$ is the vector function which represents in the coordinate system S_c, the generating surface; $\underset{\sim}{N}_c$ is the normal to the generating surface; and $\underset{\sim}{V}_c^{(c1)}$ is the relative velocity. The subscript "c" designates that the vector components are represented in the coordinate system S_c. In the case of transformation of motions represented in Fig. 3.1 a, the axodes are the plane π and the cylinder of radius r_1, and I-I is the instantaneous axis of rotation in relative motion. We may derive

16

Fig. 3.1

17
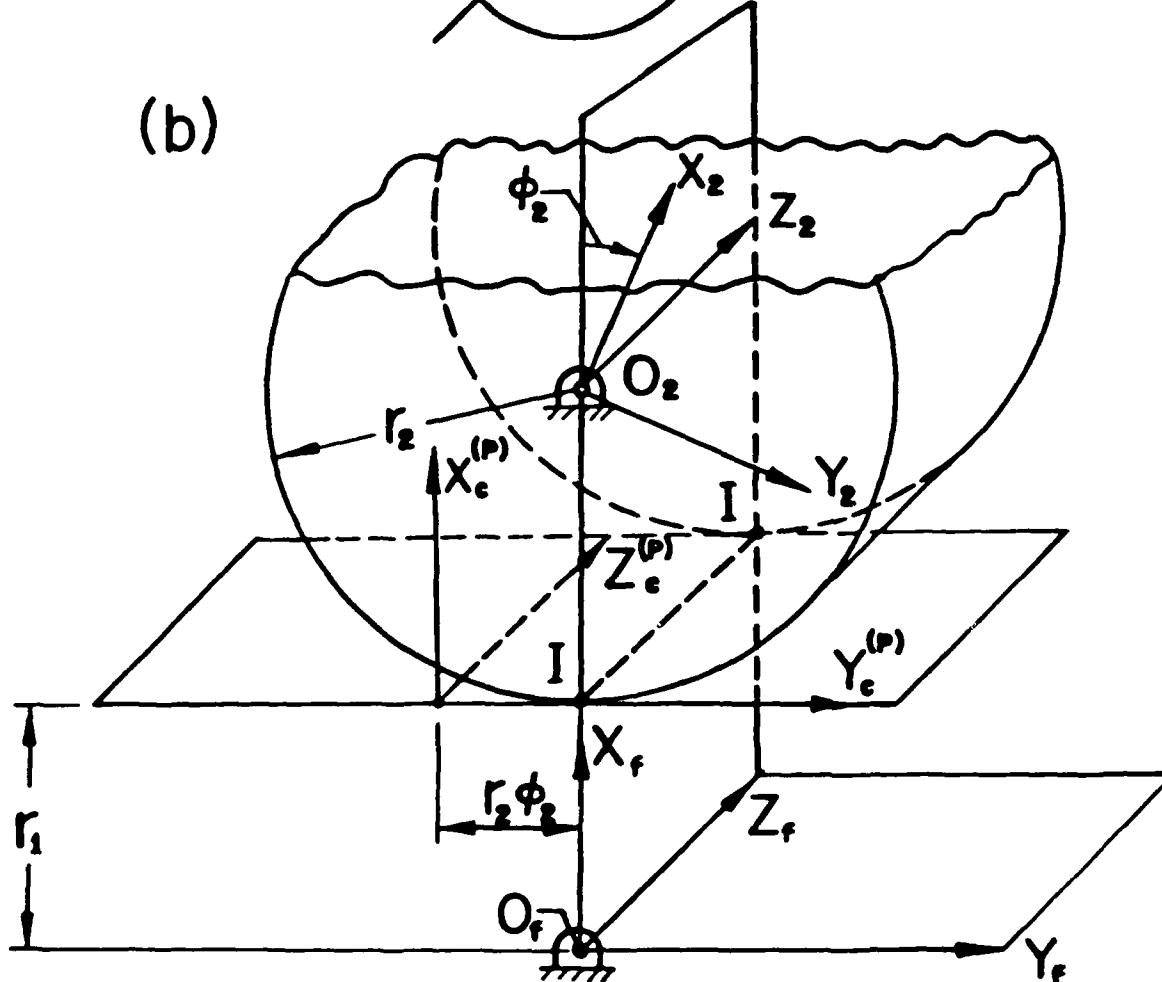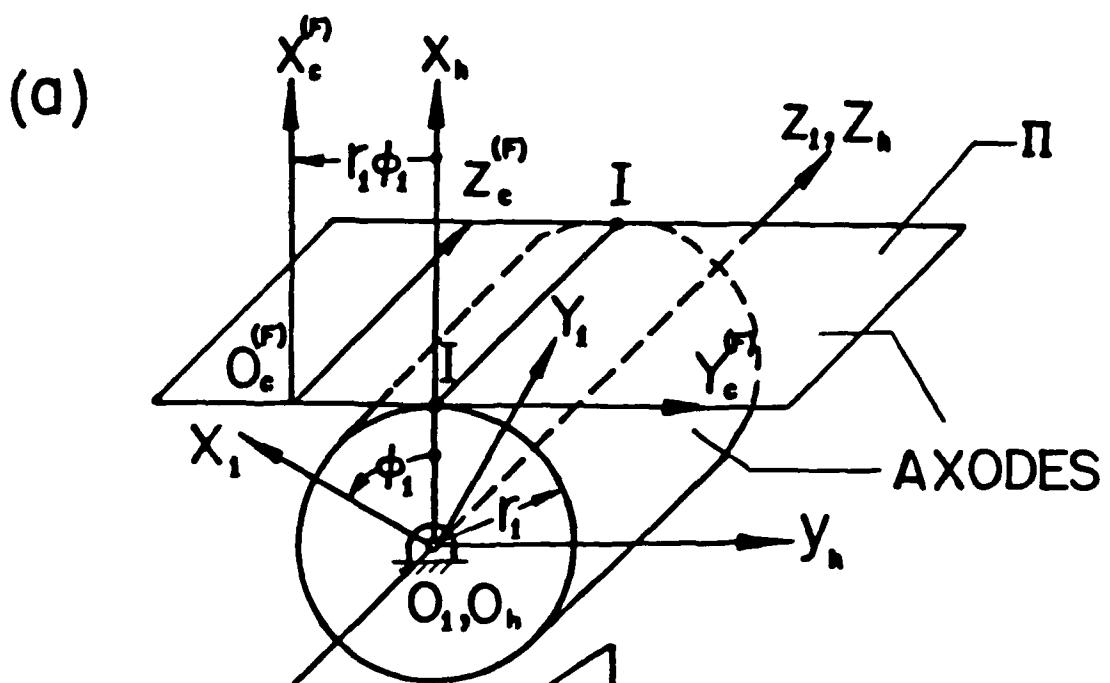
the equation of meshing as follows:

$$\frac{X_C - x_C}{N_{xc}} = \frac{Y_C - Y_C}{N_{yc}} = \frac{Z_C - z_C}{N_{zc}} \tag{3.2}$$

Equation (3.2) expresses that the normal to surfaces Σ_C and Σ_1 at their points of contact intersects the instantaneous axis of rotation, I-I. Here

$$X_C = 0, \ Y_C = r_1\phi_1, \ Z_C = \ell$$

are the coordinates of I-I.

Equations (3.2), (2.4) and (2.6) yield

$$(r_1\phi_1 - u_F\cos\lambda_F - a_F\sin\lambda_F)\sin\theta_F + b_F\cos\theta_F\sin\lambda_F =$$
$$f_F(u_F, \theta_F, \phi_1) = 0 \tag{3.3}$$

Here: $X_a^{(ci)} = -b_F$, $Y_a^{(ci)} = a_F$ are the coordinates of center C_F (Fig. 2.1)

The equation of meshing (3.3) and equations (2.4) of the generating surface Σ_C, considered simultaneously, represent a line on surface Σ_C (line L_F) which is the line of contact of Σ_C and Σ_1. The location of this line on Σ_C depends on the parameter of motion ϕ_1. In the case of $b_F = 0$ equation (3.3) yields that

$$u_F = \frac{r_1\phi_1 - a_F\sin\lambda_F}{\cos\lambda_F} \tag{3.4}$$

for any θ_F
Thus the line of contact is a circle of radius r_F (Fig. 3.2 a).

18

(a) Σ_c $U_F(\theta_F, \phi_1)$ ρ_F CONTACT LINES $(b_F = 0)$ θ_F

(b) Σ_c $U_F(\theta_F, \phi_1)$ ρ_F CONTACT LINES $(b_F \neq 0)$ θ_F
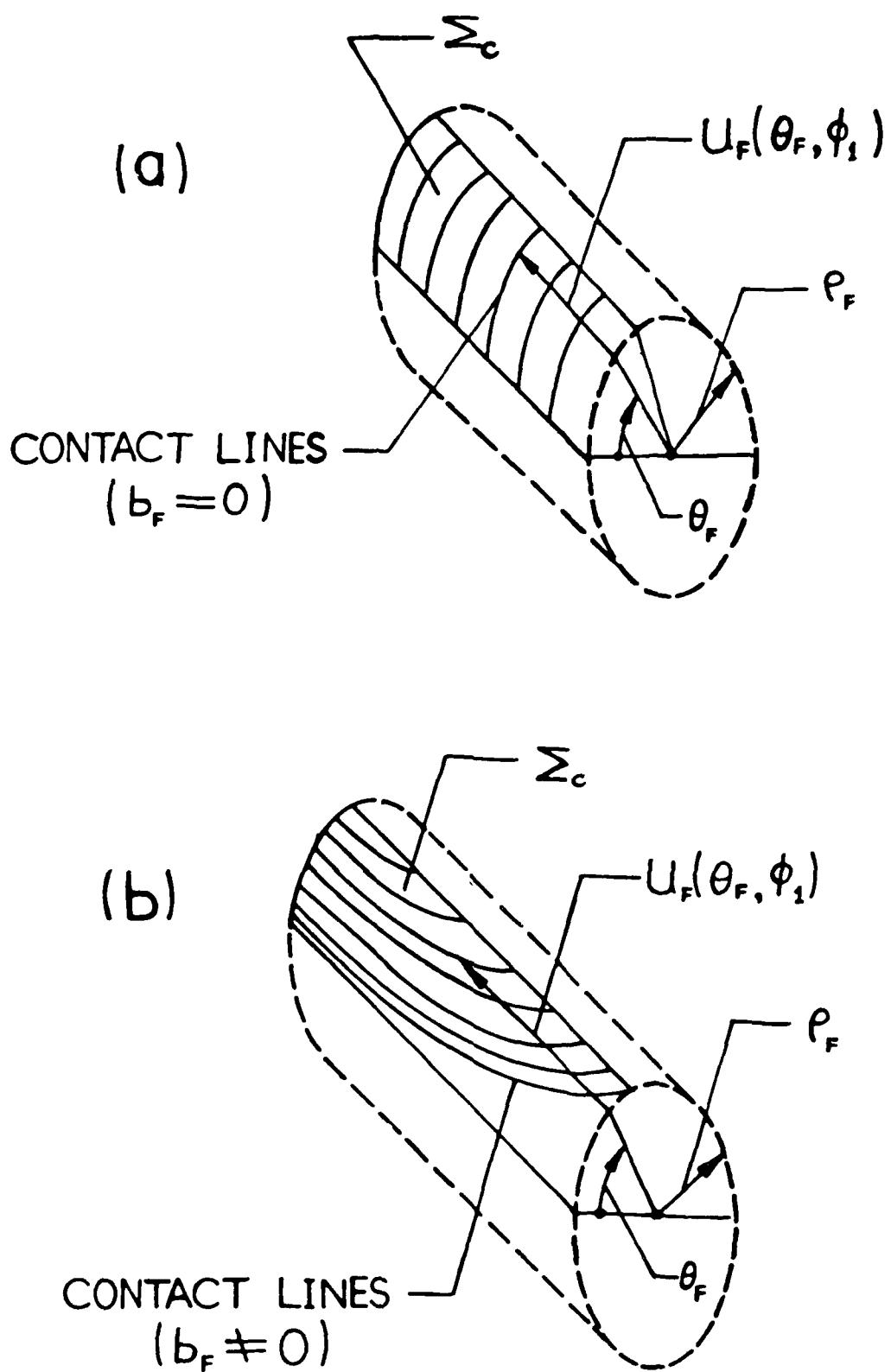
Fig. 3.2

Fig. 3.2 b shows the contact lines for the case with $b_F \neq 0$. It results from equation (3.3) that

$$u_F = b_F \cot\theta_F \tan\lambda_F + \frac{r_1\phi_1}{\cos\lambda_F} - a_F \tan\lambda_F \tag{3.4}$$

The contact lines approach infinity as θ_F approaches zero.

Surface Σ_1 may be determined with the family of contact lines represented in the coordinate system S_1. Using the matrix equation

$$\left[r_1 \right] = \left[M_{1c} \right]\left[r_c^{(F)} \right] = \left[M_{1f} \right]\left[M_{fc} \right]\left[r_c^{(F)} \right] =$$

$$\begin{bmatrix} \cos\phi_1 & -\sin\phi_1 & 0 & r_1(\cos\phi_1 + \phi_1 \sin\phi_1) \\ \sin\phi_1 & \cos\phi_1 & 0 & r_1(\sin\phi_1 - \phi_1 \cos\phi_1) \\ 0 & 0 & 1 & 0 \\ 0 & 0 & 0 & 1 \end{bmatrix} \begin{bmatrix} x_c^{(F)} \\ y_c^{(F)} \\ z_c^{(F)} \\ 1 \end{bmatrix} \tag{3.5}$$

and equations (2.4) and (3.4), we obtain

$$\begin{aligned} x_1 &= (\rho_F \sin\theta_F - b_F + r_1)\cos\phi_1 \\ &\quad + (\rho_F \cos\theta_F - b_F \cot\theta_F)\sin\phi_1 \sin\lambda_F \\ y_1 &= (\rho_F \sin\theta_F - b_F + r_1)\sin\phi_1 \\ &\quad - (\rho_F \cos\theta_F - b_F \cot\theta_F)\cos\phi_1 \sin\lambda_F, \\ z_1 &= \rho_F \cos\theta_F \cos\lambda_F - \frac{a_F}{\cos\lambda_F} + b_F \cot\theta_F \tan\lambda_F \sin\lambda_F + r_1\phi_1 \tan\lambda_F \end{aligned} \tag{3.6}$$

Equations (3.6) represent the tooth surfaces of gear 1 with surface coordinates θ_F and ϕ_1. To get the normal section of this

surface, we have to cut the gear tooth surface by the plane which
is drawn through the axis X_1 perpendicular to the tooth direc-
tion in plane π (Fig. 1.3, a)   The cutting plane is represented
in the coordinate system S_1 by the equation (Fig. 3.3)

$$y_1 = -z_1 \tan\lambda_F \tag{3.7}$$

Equations (3.6) and (3.7) considered simultaneously yield the
following relation between θ_F and ϕ_1 .

$$A_I \sin\phi_1 + B_I \cos\phi_1 + D_I \phi_1 = E_I \tag{3.8}$$

Here

$$A_I = \frac{\rho_F \sin\theta_F - b_F + r_1}{\sin\lambda_F} ,$$

$$B_I = -\rho_F \cos\theta_F + b_I \cot\theta_F$$

$$D_I = r_1 \frac{\tan^2\lambda_F}{\sin\lambda_F} \tag{3.9}$$

$$E_I = -\rho_F \cos\theta_F + \frac{a_F}{\cos^2\lambda_F} - b_F \cot\theta_F \tan^2\lambda_F$$

Considering that θ_F is given, we may determine ϕ_1 using equation
(3.8). It is easy to verify that $\phi_1 = 0$ with $\tan\theta_F = \dfrac{b_F}{a_F}$

We may represent the normal section of Σ_1 in the coordinate
system $S_1^*(x_1^*, y_1^*, z_1^*)$, where
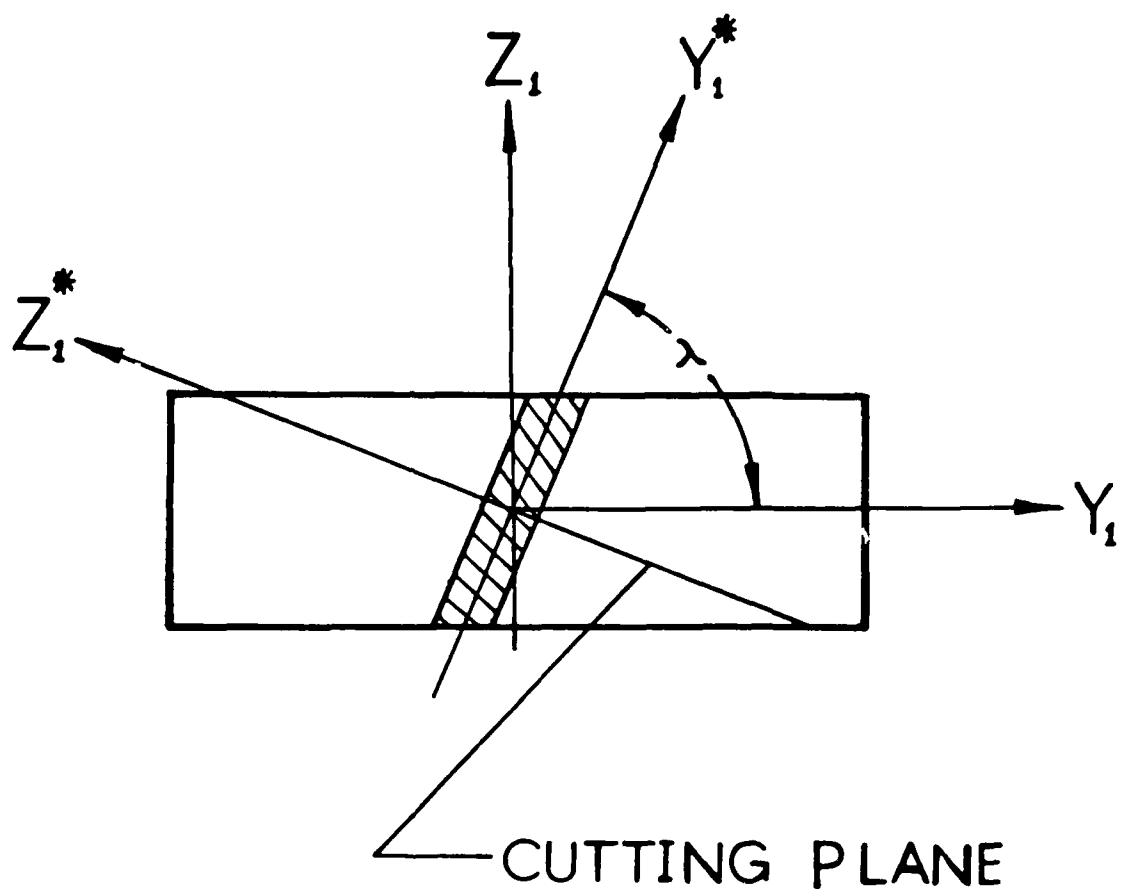
Fig. 3.3

$$x_1^* = x_1 , \quad y_1^* = y_1\cos\lambda_F + z_1\sin\lambda_F , \quad z_1^* = -y_1\sin\lambda_F + z_1\cos\lambda_F$$

$$(3.10)$$

Equations (3.7) and (3.10) yield

$$x_1^* = x_1 , \quad y_1^* = 0 , \quad z_1^* = \frac{z_1}{\cos\lambda_F} \qquad (3.11)$$

The sought-for normal section may now be represented by the following equations:

$$
\begin{aligned}
&A_I \sin\phi_1 + B_I \cos\phi_1 + D_I \phi_1 = E_I \\
&X_1^* = \sin\lambda_F (A_I \cos\phi_1 - B_I \sin\phi_1) \\
&y_1^* = 0 \\
&z_1^* = -E_I + D_I \phi_1
\end{aligned}
\qquad (3.12)
$$

Here A_I, B_I and E_I are functions of θ_F (see equations (3.9)). The x_1^* - axis is the axis of symmetry of the normal section.

Equations similar to (3.12) can be used for the determination of the normal section of the "fillet" surface, but we have to substitute ρ_F, θ_F, b_F and a_F by $\rho_F^{(f)}$, $\theta_F^{(f)}$, $b_F^{(f)}$ and $a_F^{(f)}$, respectively (Fig. 2.4 and Fig. 2.1). The circular arc $\overset{\frown}{DE}$ represents the fillet of the rack cutter in the normal section, points D and E are the points of tangency of this circular arc with the upper and lower parts of the shape of the rack cutter (Fig. 2.1).

Equations (3.12) are of a general nature and they can be used for all cases of the generation of gear 1 with a rack cutter

23

having the shape of a circular arc. In particular, these equations may be used in the case of generation of the "fillet" surface of involute gears.

Similarly, we can derive equations of the tooth surface of gear 2. The equation of meshing of the rack cutter P and gear 2 is given by

$$(r_2\phi_2 - u_p\cos\lambda_p - a_p\sin\lambda_p)\sin\theta_p + b_p\cos\theta_p\sin\lambda_p =$$

$$f_p(u_p, \theta_p, \phi_2) = 0 \qquad\qquad (3.13)$$

The line of contact of $\Sigma_c^{(P)}$ and Σ_2 is represented in S_c by equations

$$x_c^{(P)} = \rho_p\sin\theta_p - b_p$$

$$y_c^{(P)} = -(\rho_p\cos\theta_p - a_p)\sin\lambda_p + b_p\cot\theta_p\sin\lambda_p$$

$$\qquad\qquad -a_p\sin\lambda_p + r_2\phi_2 \qquad\qquad (3.14)$$

$$z_c^{(P)} = \rho_p\cos\theta_p\cos\lambda_p - \frac{a_p}{\cos\lambda_p} + b_p\cot\theta_p\tan\lambda_p\sin\lambda_p + r_2\phi_2\tan\lambda_p$$

The coordinate transformation from $S_c^{(P)}$ to S_2 is represented by the following matrix equation (Fig. 3.1 b):

$$\left[r_2\right] = \left[M_{2p}\right]\left[M_{pc}\right]\left[r_c^{(P)}\right] =$$

$$\begin{bmatrix} \cos\phi_2 & \sin\phi_2 & 0 & 0 \\ -\sin\phi_2 & \cos\phi_2 & 0 & 0 \\ 0 & 0 & 1 & 0 \\ 0 & 0 & 0 & 1 \end{bmatrix} \begin{bmatrix} 1 & 0 & 0 & -r_2 \\ 0 & 1 & 0 & -r_2\phi_2 \\ 0 & 0 & 1 & 0 \\ 0 & 0 & 0 & 1 \end{bmatrix} \begin{bmatrix} x_c^{(P)} \\ y_c^{(P)} \\ z_c^{(P)} \\ 1 \end{bmatrix} =$$

24

$$\begin{bmatrix} \cos\phi_2 & \sin\phi_2 & 0 & -r_2(\cos\phi_2 + \phi_2\sin\phi_2) \\ -\sin\phi_2 & \cos\phi_2 & 0 & r_2(\sin\phi_2 - \phi_2\cos\phi_2) \\ 0 & 0 & 1 & 0 \\ 0 & 0 & 0 & 1 \end{bmatrix} \begin{bmatrix} x_c^{(P)} \\ y_c^{(P)} \\ z_c^{(P)} \\ 1 \end{bmatrix} \quad (3.15)$$

Equations (3.15) and (3.14) yield

$$x_2 = (\rho_P\sin\theta_P - b_P - r_2)\cos\phi_2$$
$$- (\rho_P\cos\theta_P - b_P\cot\theta_P)\sin\phi_2 \sin\lambda_P$$

$$(3.16)$$

$$y_2 = -(\rho_P\sin\theta_P - b_P - r_2)\sin\phi_2$$
$$- (\rho_P\cos\theta_P - b_P\cot\theta_P)\cos\phi_2 \sin\lambda_P$$

$$z_2 = \rho_P\cos\theta_P\cos\lambda_P - \frac{a_P}{\cos\lambda_P} + b_P\cot\theta_P\sin\lambda_P\tan\lambda_P + r_2\phi_2 \tan\lambda_P$$

We will determine the normal section of Σ_2 by cutting the gear tooth surface by the same plane as we cut Σ_1. Considering simultaneously equation (3.16) with the equation

$$y_2 = -z_2\tan\lambda_P \quad (3.17)$$

we get

$$A_{II}\sin\phi_2 + B_{II}\cos\phi_2 + D_{II}\phi_2 = E_{II} \quad (3.18)$$

Here:

25

$$A_{II} = - \frac{\rho_P \sin\theta_P - b_P - r_2}{\sin\lambda_P}$$

$$B_{II} = -\rho_P \cos\theta_P + b_P \cot\theta_P$$

$$D_{II} = r_2 \frac{\tan^2\lambda_P}{\sin\lambda_P}$$

$$(3.19)$$

$$E_{II} = -\rho_P \cos\theta_P + \frac{a_P}{\cos^2\lambda_P} - b_P \cot\theta_P \tan^2\lambda_P$$

We may represent the sought-for normal section, in the coordinate system $S_2^*(x_2^*, y_2^*, z_2^*)$, whose orientation with respect to S_2 is similar to the orientation of S_1^* with respect to S_1 (Fig. 3.3). Using equations

$$x_2^* = x_2, \quad y_2^* = 0, \quad z_2^* = \frac{z_2}{\cos\lambda_P} \qquad (3.20)$$

which are similar to equations (3.11), we may represent the normal section of S_2 as follows

$$A_{II}\sin\phi_2 + B_{II}\cos\phi_2 + D_{II}\phi_2 = E_{II}$$
$$x_2^* = (-A_{II}\cos\phi_2 + B_{II}\sin\phi_2)\sin\lambda_P \qquad (3.21)$$
$$y_2^* = 0$$
$$z_2^* = -E_{II} + D_{II}\phi_2$$

Equations similar to (3.21) represent the normal section of the "fillet" surface. To derive these equations, we have to substitute ρ_P, θ_P, b_P and a_P by $\rho_P^{(f)}$, $\theta_P^{(f)}$, $b_P^{(f)}$, and $a_P^{(f)}$ in equations (3.19). The normal section of the "fillet" surface of the rack

26

cutter P is represented in Fig. 2.2.

4 Principal Curvatures and Directions of Gear Tooth Surfaces

The principal curvatures and directions of two contacting surfaces are necessary to define the size and direction of the contact ellipse at the contact point. If the relations between the principal curvatures and directions of two surfaces which are in mesh are known, the solution of this problem can be significantly simplified. Such relations were worked out first by Dr. F. L. Litvin.

Step 1: Principal curvatures and directions of the generating surfaces Σ_F and Σ_P

The rack cutter surface Σ_F and Σ_P and their unit normals are represented in the coordinate system S_c by equations (2.4) and (2.6), respectively. The principal curvatures and directions for a given surface may be obtained by using Rodrigues' equation [5]:

$$K_{I,II} \underset{\sim}{V}_r = -\dot{\underset{\sim}{n}}_r \qquad (4.1)$$

Here: $K_{I,II}$ are the principal curvatures; $\underset{\sim}{V}_r$ is relative velocity of the point of contact in its motion over the surface, and $\dot{\underset{\sim}{n}}_r$ is the velocity of the tip of the unit normal in the above motion. Equations (2.4) and (2.6) yield the following expressions for the principal directions and curvatures:

27

$$(1) \quad \frac{du_i}{dt} = 0, \quad \underset{\sim}{i}_I^{(i)} = \frac{\underset{\sim}{V}_{rI}^{(i)}}{\left|\underset{\sim}{V}_{rI}^{(i)}\right|} = \begin{bmatrix} \cos\theta_i \\ \sin\theta_i \sin\lambda_i \\ -\sin\theta_i \cos\lambda_i \end{bmatrix}, \quad \kappa_I^{(i)} = -\frac{1}{\rho_i}$$

$$(i = F, P) \tag{4.2}$$

$$(2) \quad \frac{d\theta_i}{dt} = 0, \quad \underset{\sim}{i}_{II}^{(i)} = \frac{\underset{\sim}{V}_{rII}^{(i)}}{\left|\underset{\sim}{V}_{rII}^{(i)}\right|} = \begin{bmatrix} 0 \\ \cos\lambda_i \\ \sin\lambda i \end{bmatrix}, \quad \kappa_{II}^{(i)} = 0, \quad (i = F, P) \tag{4.3}$$

Subscripts I and II designate the two principal directions and curvatures; the unit vectors $\underset{\sim}{i}_I^{(i)}$ and $\underset{\sim}{i}_{II}^{(i)}$ are given in the coordinate system S_c but they are represented in the coordinate system S_f by the same matrices. The above unit vectors may also be considered as the unit vectors of axes y_t and z_t of the coordinate system S_t which is rigidly connected to the rack cutter surfaces, Σ_F and Σ_P (Fig. 4.1). The unit vector of the x_t - axis coincides with the common unit normal to surfaces Σ_F and Σ_P along their line of tangency, axis z_t. Centers C_F and C_P are the centers of the principal curvatures $\kappa_I^{(F)}$ and $\kappa_I^{(P)}$ (Fig. 4.1 c).

The column matrices $[\underset{\sim}{i}_I^{(i)}]$ and $[\underset{\sim}{i}_{II}^{(i)}]$ may be also derived by using the matrix $[L_{ft}]$ which represents the transformation of direction cosines in transition from S_t to S_f. Using the drawings of Fig. 4.1 c, Fig. 2.3 and Fig. 3.1, we obtain

$$\begin{bmatrix} L_{ft} \end{bmatrix} = \begin{bmatrix} L_{fc} \end{bmatrix} \begin{bmatrix} L_{ca} \end{bmatrix} \begin{bmatrix} L_{at} \end{bmatrix} =$$

(a) TANGENT PLANE(T)

(b)

CONTACTING ELLIPSE

(c)
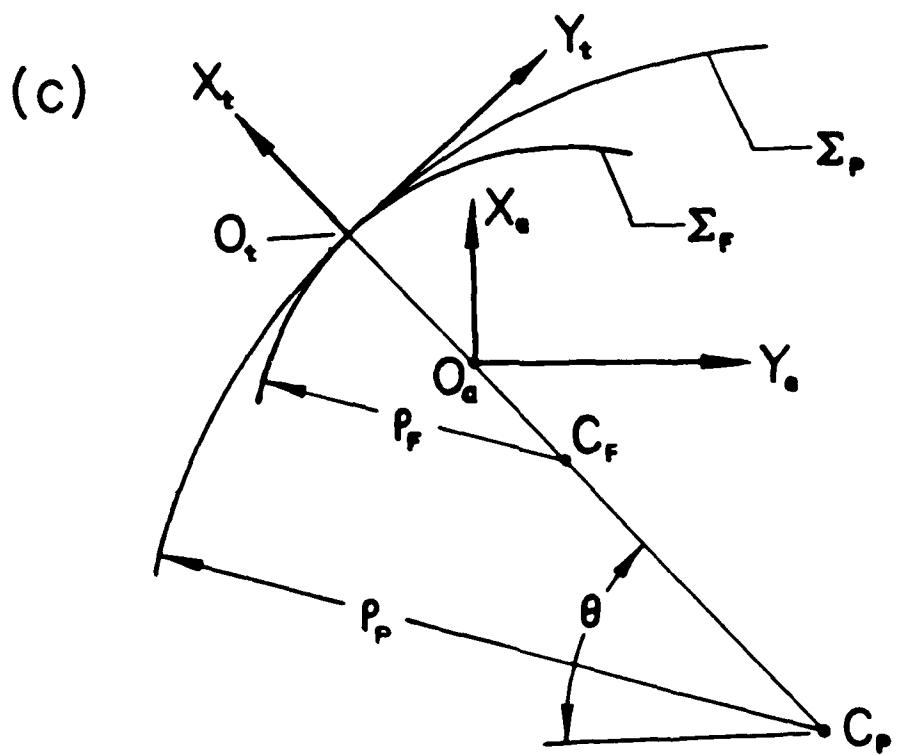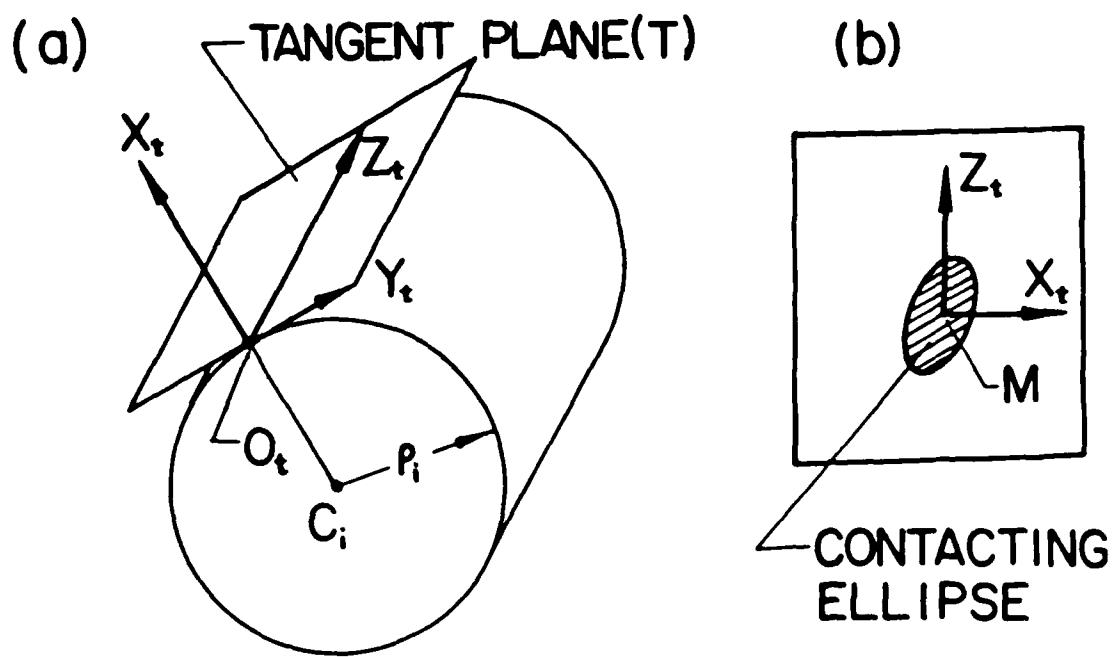
Fig. 4.1

$$= \begin{bmatrix} \sin\theta_i & \cos\theta_i & 0 \\ -\cos\theta_i\sin\lambda_i & \sin\theta_i\sin\lambda_i & \cos\lambda_i \\ \cos\theta_i\cos\lambda_i & -\sin\theta_i\cos\lambda_i & \sin\lambda_i \end{bmatrix} \; ; \; \begin{bmatrix} i_I^{(i)} \end{bmatrix} = \begin{bmatrix} L_{ft} \end{bmatrix} \begin{bmatrix} 0 \\ 1 \\ 0 \end{bmatrix} \; ;$$

$$\begin{bmatrix} i_{II}^{(i)} \end{bmatrix} = \begin{bmatrix} L_{ft} \end{bmatrix} \begin{bmatrix} 0 \\ 0 \\ 1 \end{bmatrix} \tag{4.4}$$

where: i = F, P and

θ_i is the pressure angle (FIg. 4.1 c)

Step 2: Principal curvatures and directions of Σ_1.

We may determine the principal curvatures and directions of Σ_1 by using the following equations:

$$\tan 2\sigma^{(F1)} = \frac{2F^{(1)}}{\kappa_I^{(F)} - \kappa_{II}^{(F)} + G^{(1)}} \tag{4.5}$$

$$\kappa_I^{(1)} + \kappa_{II}^{(1)} = \kappa_I^{(F)} + \kappa_{II}^{(F)} + S^{(1)} \tag{4.6}$$

$$\kappa_I^{(1)} - \kappa_{II}^{(1)} = \frac{\kappa_I^{(F)} - \kappa_{II}^{(F)} + G^{(1)}}{\cos 2\sigma^{(F1)}} \tag{4.7}$$

$$F^{(1)} = \frac{a_{31}^{(1)} a_{32}^{(1)}}{b_3^{(1)} + (\underset{\sim}{v}^{(F1)} \cdot \underset{\sim}{i}_I^{(F)}) a_{31}^{(1)} + (\underset{\sim}{v}^{(F1)} \cdot \underset{\sim}{i}_{II}^{(F)}) a_{32}^{(1)}} \tag{4.8}$$

$$G^{(1)} = \frac{[a_{31}^{(1)}]^2 - [a_{32}^{(1)}]^2}{b_3^{(1)} + (\underset{\sim}{v}^{(F1)} \underset{\sim}{i}_I^{(F)}) a_{31}^{(1)} + (\underset{\sim}{v}^{(F1)} \underset{\sim}{i}_{II}^{(F)}) a_{32}^{(1)}} \tag{4.9}$$

$$S^{(1)} = \frac{[a_{31}^{(1)}]^2 + [a_{32}^{(1)}]^2}{b_3^{(1)} + (\underset{\sim}{v}^{(F1)} \underset{\sim}{i}_I^{(F)}) a_{31}^{(1)} + (\underset{\sim}{v}^{(F1)} \underset{\sim}{i}_{II}^{(F)}) a_{32}^{(1)}} \tag{4.10}$$

30

$$a_{31}^{(1)} = [\underset{\sim}{n}^{(F)} \quad \underset{\sim}{^{(F1)}} \; \underset{\sim I}{i}^{(F)}] - K_I^{(F)} (\underset{\sim}{v}^{(F1)} \cdot \underset{\sim I}{i}^{(F)}) \qquad (4.11)$$

$$a_{32}^{(1)} = [\underset{\sim}{n}^{(F)} \quad \underset{\sim}{^{(F1)}} \; \underset{\sim II}{i}^{(F)}] - K_{II}^{(F)} (\underset{\sim}{v}^{(F1)} \cdot \underset{\sim II}{i}^{(F)}) \qquad (4.12)$$

$$b_3^{(1)} = [\underset{\sim}{n}^{(F)} \quad \underset{\sim}{^{(1)}} \; \underset{\sim tr}{v}^{(F)}] - [\underset{\sim}{n}^{(F)} \quad \underset{\sim}{^{(F)}} \; \underset{\sim tr}{v}^{(1)}] \qquad (4.13)$$

All the vectors of equations (4.5) - (4.13) are represented in the coordinate system S_f and the coordinate system S_h coincides with S_f (Fig. 3.1); $\kappa_I^{(1)}$ and $\kappa_{II}^{(1)}$ are the principal curvatures of Σ_1, $\sigma^{(F1)}$ is the angle which is formed by vectors $\underset{\sim 1}{i}^{(F)}$ and $\underset{\sim I}{i}^{(1)}$ where $\underset{I}{i}^{(1)}$ is the unit vector for the principal direction $I^{(1)}$ on surface Σ_1; $\kappa_I^{(F)} = -\dfrac{1}{\rho_F}$ and $\kappa_{II}^{(F)} = 0$ are the principal curvatures of Σ_F . Let us derive the following auxiliary equations

$$\underset{\sim}{^{(F1)}} = \underset{\sim}{^{(F)}} - \underset{\sim}{^{(1)}} = -\underset{\sim}{\omega}^{(1)} = \begin{bmatrix} 0 \\ 0 \\ \omega^{(1)} \end{bmatrix} \qquad (4.14)$$

Vector $\underset{\sim}{^{(F)}} = 0$ because the rack cutter performs translational motion (Fig. 3.1 a)

$$[\underset{\sim}{n}^{(F)} \quad \underset{\sim}{^{(F1)}} \; \underset{\sim I}{i}^{(F)}] = -\omega^{(1)} \sin\lambda_F \qquad (4.15)$$

$$[\underset{\sim}{n}^{(F)} \quad \underset{\sim}{^{(F1)}} \; \underset{\sim II}{i}^{(F)}] = -\omega^{(1)} \sin\theta_F \cos\lambda_F \qquad (4.16)$$

The point of contact of surfaces Σ_1 and Σ_2 lies on a straight line which passes through the point whose coordinates are given by

31

$$x_f^{(1)} = \rho_F \sin\theta_F - b_F + r_1 \tag{4.17}$$

$$y_f^{(1)} = -(\rho_F \cos\theta_F - b_F \cot\theta_F)\sin\lambda_F \tag{4.18}$$

$$z_f^{(1)} = \rho_F \cos\theta_F \cos\lambda_F - \frac{a_F}{\cos\lambda_F} + b_F \cot\theta_F \tan\lambda_F \sin\lambda_F + r_1 \phi_1 \tan\lambda_F \tag{4.19}$$

Here $\theta_F = \theta_p = \theta$ is the pressure angle at the point of contact of surfaces Σ_1 and Σ_2. Equations (4.17) - (4.19) may be derived from equations (I.9) with $\mu_1 = 0$ taking into account that the coordinate system S_h coincides with S_f. The transfer velocity of the rack cutter is (Fig. 3.1, a):

$$\underset{\sim}{v}_{tr}^{(F)} = \begin{bmatrix} 0 \\ -\omega^{(1)} r_1 \\ 0 \end{bmatrix} \tag{4.20}$$

The transfer velocity of a point of gear 1 is given by

$$\underset{\sim}{v}_{tr}^{(1)} = \underset{\sim}{\omega}^{(1)} \times \underset{\sim}{r}_f^{(1)} = \omega^{(1)} \begin{bmatrix} y_f^{(1)} \\ -x_f^{(1)} \\ 0 \end{bmatrix} =$$

$$-\omega^{(1)} \begin{bmatrix} (\rho_F \cos\theta_F - b_F \cot\theta_F)\sin\lambda_F \\ \rho_F \sin\theta_F - b_F + r_1 \\ 0 \end{bmatrix} \tag{4.21}$$

32

The sliding velocity is given by

$$v^{(F1)} = v^{(F)} - v^{(1)} = \omega^{(1)} \begin{bmatrix} (\rho_F \cos\theta_F - b_F \cot\theta_F)\sin\lambda_F \\ \rho_F \sin\theta_F - b_F \\ 0 \end{bmatrix} \quad (4.22)$$

Thus, we obtain (see equations (4.21), (4.2) and (4.3)):

$$v^{(F1)} \cdot i_I^{(F)} = \omega^{(1)}\left(\rho_F - \frac{b_F}{\sin\theta_F}\right)\sin\lambda_F \quad (4.23)$$

$$v^{(F1)} \cdot i_{II}^{(F)} = \omega^{(1)}\left(\rho_F - \frac{b_F}{\sin\theta_F}\right)\sin\theta_F\cos\lambda_F \quad (4.24)$$

Using equations (4.11), (4.12), (4.15), (4.16), (4.23), (4.24) (4.2), and (4.3), we obtain

$$a_{31}^{(1)} = -\omega^{(1)}\frac{b_F \sin\lambda_F}{\rho_F \sin\theta_F} \quad (4.25)$$

$$a_{32}^{(1)} = -\omega^{(1)}\sin\theta_F\cos\lambda_F \quad (4.26)$$

Using equations (4.13), (2.6), (4.20) and (4.21), we get

$$b_3^{(1)} = -\left(\omega^{(1)}\right)^2 r_1 \sin\theta_F \quad (4.27)$$

We may now derive the final expressions for $F^{(1)}$, $G^{(1)}$ and $S^{(1)}$ as follows:

$$F^{(1)} = -\frac{\dfrac{b_F}{r_F}\sin\lambda_F\cos\lambda_F}{A_1} \quad (4.28)$$

33

$$G^{(1)} = -\frac{\left[\frac{b_F \sin\lambda_F}{\rho_F \sin\theta_F}\right]^2 - \sin^2\theta_F\cos^2\lambda_F}{A_1} \tag{4.29}$$

$$S^{(1)} = -\frac{\left[\frac{b_F}{\rho_F}\frac{\sin\lambda_F}{\sin\theta_F}\right]^2 + \sin^2\theta_F\cos^2\lambda_F}{A_1} \tag{4.30}$$

Here

$$A_1 = r_1\sin\theta_F + \left[\rho_F - \frac{b_F}{\sin\theta_F}\right]\left[\frac{b_F\sin^2\lambda_F}{\rho_F\sin\theta_F} + \sin^2\theta_F\cos^2\lambda_F\right] \tag{4.31}$$

Equations (4.5) - (4.7) and (4.25) - (4.31) determine the
principal curvatures and directions of surface Σ_1 at the point
of contact of surfaces Σ_1 and Σ_2 .

Step 3: Principal curvatures and directions of Σ_2

The principal curvatures of the rack cutter Σ_P are: $\kappa_I^{(P)} = -\frac{1}{\rho_P}$,
$\kappa_{II}^{(P)} = 0$; the principal directions of Σ_P are the same as of Σ_F;
Using similar derivations, we obtain

$$\underset{\sim}{\omega}^{(P2)} = \begin{bmatrix} 0 \\ 0 \\ -\omega^{(2)} \end{bmatrix} \tag{4.32}$$

$$\left[\underset{\sim}{n}^{(P)} \quad \underset{\sim}{\omega}^{(P2)} \quad \underset{\sim}{i}_I^{(P)}\right] = \omega^{(2)}\sin\lambda_P \quad \left(\underset{\sim}{n}^{(P)} = \underset{\sim}{n}^{(F)}\right) \tag{4.33}$$

$$\left[\underset{\sim}{n}^{(P)} \quad \underset{\sim}{\omega}^{(P2)} \quad \underset{\sim}{i}_{II}^{(P)}\right] = \omega^{(2)}\sin\theta_P\cos\lambda_P \tag{4.34}$$

$$x_f^{(2)} = \rho_P\sin\theta_P - b_P - r_2 + C \tag{4.35}$$

$$y_f^{(2)} = -(\rho_P\cos\theta_P - b_P\cot\theta_P)\sin\lambda_P \tag{4.36}$$

34

$$z_f^{(2)} = \rho_P \cos\theta_P \cos\lambda_P - \frac{a_P}{\cos\lambda_P} + b_P \cot\theta_P \sin\lambda_P \tan\lambda_P + r_2\phi_2\tan\lambda_\Gamma \tag{4.37}$$

$$\underset{\sim}{v}_{tr}^{(P)} = \begin{bmatrix} 0 \\ -\omega^{(2)}r_2 \\ 0 \end{bmatrix} \tag{4.38}$$

$$\underset{\sim}{v}_{tr}^{(2)} = \underset{\sim}{\omega}^{(2)} \times \underset{\sim}{r}_f^{(2)} + \underset{\sim}{C} \times \underset{\sim}{\omega}^{(2)} = -\omega^{(2)}\begin{bmatrix} v_f^{(2)} \\ -x_f^{(2)} + C \\ 0 \end{bmatrix} \tag{4.39}$$

$$\underset{\sim}{v}^{(P2)} = \underset{\sim}{v}_{tr}^{(P)} - \underset{\sim}{v}_{tr}^{(2)} = -\omega^{(2)}\begin{bmatrix} (\rho_P\cos\theta_P - b_P\cot\theta_P)\sin\lambda_P \\ \rho_P\sin\theta_P - b_P \\ 0 \end{bmatrix} \tag{4.40}$$

$$\underset{\sim}{v}^{(P2)} \cdot \underset{\sim}{i}_I^{(P)} = -\omega^{(2)}\left(\rho_P - \frac{b_P}{\sin\theta_P}\right)\sin\lambda_P, \qquad (\underset{\sim}{i}_I^{(P)} = \underset{\sim}{i}_I^{(F)}) \tag{4.41}$$

$$\underset{\sim}{v}^{(P2)} \cdot \underset{\sim}{i}_{II}^{(P)} = -\omega^{(2)}\left(\rho_P - \frac{b_P}{\sin\theta_P}\right)\sin\theta_P\cos\lambda_P, \quad (\underset{\sim}{i}_{II}^{(P)} = \underset{\sim}{i}_{II}^{(F)}) \tag{4.42}$$

$$a_{31}^{(2)} = \left[\underset{\sim}{n}^{(P)} \quad \underset{\sim}{\omega}^{(P2)} \quad \underset{\sim}{i}_I^{(P)}\right] - \kappa_I^{(P)}(\underset{\sim}{v}^{(P2)} \cdot \underset{\sim}{i}_I^{(P)}) = \omega^{(2)}\frac{b_P\sin\lambda_P}{\rho_P\sin\theta_P} \tag{4.43}$$

$$a_{32}^{(2)} = \left[\underset{\sim}{n}^{(P)} \quad \underset{\sim}{\omega}^{(P2)} \quad \underset{\sim}{i}_{II}^{(P)}\right] - \kappa_{II}^{(P)}(\underset{\sim}{v}^{(P2)} \cdot \underset{\sim}{i}_{II}^{(P)}) = \omega^{(2)}\sin\theta_P\cos\lambda_P \tag{4.44}$$

$$b_3^{(2)} = \left[\underset{\sim}{n}^{(P)} \quad \underset{\sim}{\omega}^{(2)} \quad \underset{\sim}{v}_{tr}^{(P)}\right] - \left[\underset{\sim}{n}^{(P)} \quad \underset{\sim}{\omega}^{(P)} \quad \underset{\sim}{v}_{tr}^{(2)}\right] = \left(\omega^{(2)}\right)^2 r_2\sin\theta_P \tag{4.45}$$

$$F^{(2)} = \frac{a_{31}^{(2)} \, a_{32}^{(2)}}{b_3^{(2)} + \left(\underset{\sim}{v}^{(P2)} \cdot \underset{\sim}{i}_I^{(P)} \right) a_{31}^{(2)} + \left(\underset{\sim}{v}^{(P2)} \cdot \underset{\sim}{i}_{II}^{(P)} \right) a_{32}^{(2)}}$$

$$= \frac{\dfrac{b_P}{\rho_P} - \sin\lambda_P \cos\lambda_P}{A_2} \qquad (4.46)$$

$$G^{(2)} = \frac{\left(a_{31}^{(2)}\right)^2 - \left(a_{32}^{(2)}\right)^2}{\left(\omega^{(2)}\right)^2 A_2} = \frac{\left(\dfrac{b_P \sin\lambda_P}{\rho_P \sin\theta_P}\right)^2 - \sin^2\theta_P \cos^2\lambda_P}{A_2} \qquad (4.47)$$

$$S^{(2)} = \frac{\left(a_{31}^{(2)}\right)^2 + \left(a_{32}^{(2)}\right)^2}{\left(\omega^{(2)}\right)^2 A_2} = \frac{\left(\dfrac{b_P \sin\lambda_P}{\rho_P \sin\theta_P}\right)^2 + \sin^2\theta_P \cos^2\lambda_P}{A_2}$$

Here $\hspace{8cm} (4.48)$

$$A_2 = r_2 \sin\theta_P - \left(\rho_P - \frac{b_P}{\sin\theta_P}\right)\left(\frac{b_P \sin^2\lambda_P}{\rho_P \sin\theta_P} + \sin^2\theta_P \cos^2\lambda_P\right) \quad (4.49)$$

The principal curvatures and directions of Σ_2 are determined as follows

$$\tan 2\sigma^{(P2)} = \frac{2F^{(2)}}{-\dfrac{1}{\rho_P} + G^{(2)}} \qquad (4.50)$$

$$\kappa_I^{(2)} + \kappa_{II}^{(2)} = -\frac{1}{\rho_P} + S^{(2)} \qquad (4.51)$$

$$\kappa_I^{(2)} - \kappa_{II}^{(2)} = \frac{-\dfrac{1}{\rho_P} + G^{(2)}}{\cos 2\sigma^{(P2)}} \qquad (4.52)$$

Example 4.1: <u>Principal Curvatures and Directions of Gear Tooth</u>
<u>Surfaces</u>

Given: The rack parameters $\rho_F = 0.7^{\text{in.}}$, $\rho_P = 0.775^{\text{in.}}$ (See Fig. 2.1 and Fig. 2.2); the gear parameters: No. of teeth $N_1 =$

12, $N_2 = 94$; lead angle $\lambda_F = \lambda_P = 75°$; nominal pressure angle $\theta° = 30°$; normal diametral pitch $P_n = 2$;

(1) Pinion: By using equations (4.5) - (4.31) we obtain $A_1 = 1.70882$, $F^{(1)} = -0.02549$, $G^{(1)} = -0.05648$, $S^{(1)} = -0.07608$, principal direction $\sigma^{(F1)} = 0.98294°$ (Fig. 5.1), and two principal curvatures: $\kappa_I^{(1)} = -1.49529$, $\kappa_{II}^{(1)} = -0.00936$.

(2) Gear 2: By using equations (4.32) - (4.52), we obtain $A_2 = 11.98175$, $F^{(2)} = 0.00429$, $G^{(2)} = 0.01179$, $S^{(2)} = 0.01458$, principal direction $\sigma^{(P2)} = -0.19237°$ (See Fig. 5.1), and two principal curvatures: $\kappa_I^{(2)} = -1.27715$, $\kappa_{II}^{(2)} = 0.00141$.

5. Contacting Ellipse

The tangent plane to gear tooth surfaces is formed by axes y_t and z_t (Fig. 5.1 a). The unit vectors $\underset{\sim I}{i}^{(F,P)}$ and $\underset{\sim II}{i}^{(F,P)}$ represent the principal directions of surfaces Σ_F and Σ_P of the rack cutters. Angles $\sigma^{(F1)}$ and $\sigma^{(P2)}$, measured counter-clockwise from $\underset{\sim I}{i}^{(F,P)}$ determine the principal directions of gear tooth surfaces Σ_1 and Σ_2, respectively, with the unit vectors $\underset{\sim I}{i}^{(1)}$ and $\underset{\sim I}{i}^{(2)}$.

Consider that the principal curvatures $\kappa_I^{(1)}$, $\kappa_{II}^{(1)}$, $\kappa_I^{(2)}$, $\kappa_{II}^{(2)}$ of surfaces Σ_1 and Σ_2 are known. Also known are angles $\sigma^{(F1)}$ and $\sigma^{(P2)}$. We may then determine the dimensions of the axes of the contacting ellipse with respect to the elastic approach of gear tooth surfaces and the orientation of the contacting ellipse in the tangent plane T. The equations to be used are as follows [5,6]:

$$A = \frac{1}{4}\left[\kappa_\Sigma^{(1)} - \kappa_\Sigma^{(2)} - (g_1^2 - 2g_1g_2\cos2\sigma + g_2^2)^{\frac{1}{2}}\right]$$

37
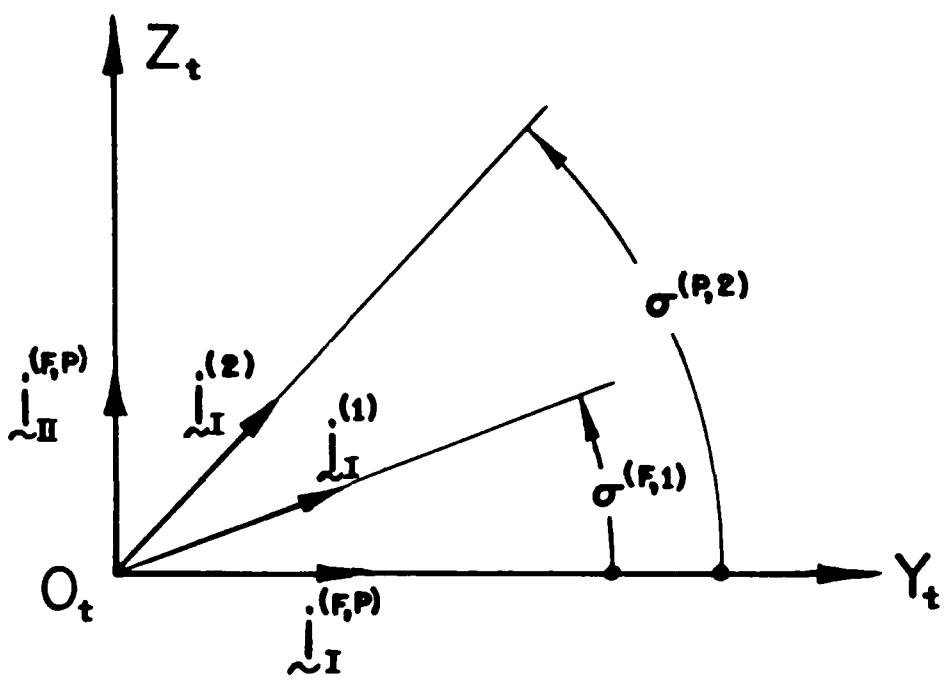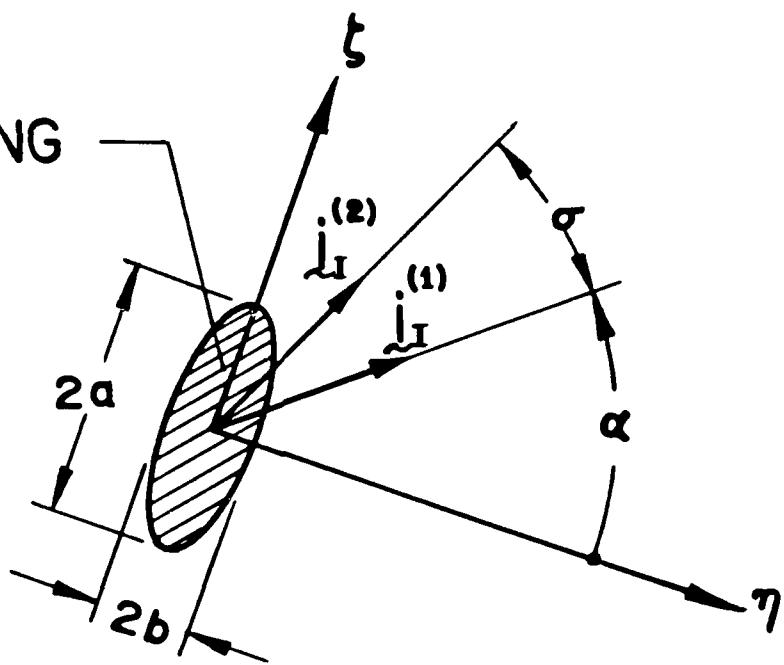
Fig. 5.1

$$B = \frac{1}{4}\left[\kappa_{\Sigma}^{(1)} - \kappa_{\Sigma}^{(2)} + (g_1^2 - 2g_1 g_2 \cos 2\sigma + g_2^2)^{\frac{1}{2}}\right]$$

$$\text{(5.1)}$$

$$a^2 = \left|\frac{\delta}{A}\right| \quad , \quad b^2 = \left|\frac{\delta}{B}\right| \; ;$$

$$\sin 2\alpha = g_2 \sin 2\sigma$$

$$\cos 2\alpha = g_1 - g_2 \cos 2\sigma$$

Here: $\kappa_{\Sigma}^{(1)} = \kappa_I^{(1)} + \kappa_{II}^{(1)}$; $\kappa_{\Sigma}^{(2)} = \kappa_I^{(2)} + \kappa_{II}^{(2)}$, $g_1 = \kappa_I^{(1)} - \kappa_{II}^{(1)}$, $g_2 = \kappa_I^{(2)} - \kappa_{II}^{(2)}$; $\sigma = \sigma^{(P2)} - \sigma^{(F1)}$; δ is

the elastic approach of gear tooth surfaces; a and b are the axes of the contacting ellipse and α is the angle which determines the orientation of contacting ellipse. Angle α is formed by the η - axis and unit vector $\underset{\sim I}{i}^{(1)}$ and measured counter-clockwise from axis η to $\underset{\sim I}{i}^{(1)}$ (Fig. 5.1 b). Axes η and ξ are directed along the b- and a-axis of the contacting ellipse. The magnitudes of a and b are expressed in terms of the elastic approach δ *which can be obtained from experiments or calculated.*

Example 5.1: <u>Dimension and Orientation of Contacting Ellipse</u>

The nominal rack and gear parameters are the same as given in Example 4.1. In Example 4.1, we found $\sigma^{(F1)} = 0.98294°$, $\sigma^{(P2)} = -0.19237°$; the two principal curvatures for pinion surface Σ_1 are $\kappa^{(1)} = 1.49529$ and $\kappa_{II}^{(1)} = -0.00936$, and two principal curvatures for gear surface Σ_2 are $\kappa_{II}^{(2)} = -1.27715$ and $\kappa_{II}^{(2)} = 0.00141$. By substituting these values into equation (5.1), we obtain A = 0.1110, B = 0.0035, a = 3.002δ, b = 16.9158δ and $\alpha = 82.9392°$.

6 Velocity of Motion of the Contacting Ellipse Over Gear Tooth Surface

The velocity of motion of the symmetry center of the contacting ellipse over surface Σ_1 is represented by the following equations [5,6]:

$$a_{11}x_1 + a_{12}x_2 = b_1$$
$$a_{21}x_1 + a_{22}x_2 = b_2 \tag{6.1}$$
$$a_{31}x_1 + a_{32}x_2 = b_3$$

Here:

$$a_{11} = -\kappa_I^{(1)} + \frac{1}{2}(\kappa_\Sigma^{(2)} + g_2\cos2\sigma);$$

$$a_{12} = a_{21} = \tfrac{1}{2}g_2\sin2\sigma$$

$$a_{22} = -\kappa_{II}^{(1)} + \frac{1}{2}(\kappa_\Sigma^{(2)} - g_2\cos2\sigma)$$

$$a_{31} = \left[n^{(1)}\ \omega^{(12)}\ i_I^{(1)}\right] - \kappa_I^{(1)}(v^{(12)} \cdot i_I^{(1)})$$

$$a_{32} = \left[n^{(1)}\ \omega^{(12)}\ i_{II}^{(1)}\right] - \kappa_{II}^{(1)}(v^{(12)} \cdot i_{II}^{(1)})$$

$$b_1 = \left[n^{(1)}\ \omega^{(12)}\ i_I^{(1)}\right] - \frac{1}{2}(v^{(12)} \cdot i_I^{(1)})(\kappa_\Sigma^{(2)} + g_2\cos2\sigma)$$
$$- \frac{1}{2}(v^{(12)} \cdot i_{II}^{(1)})g_2\sin2\sigma$$

$$b_2 = \left[n^{(1)}\ \omega^{(12)}\ i_{II}^{(1)}\right] - \frac{1}{2}(v^{(12)} \cdot i_I^{(1)})g_2\sin2\sigma$$
$$- \frac{1}{2}(v^{(12)} \cdot i^{(1)})(\kappa_\Sigma^{(2)} - g_2\cos2\sigma)$$

$$b_3 = \left[n^{(1)}\ \omega^{(2)}\ v_{tr}^{(1)}\right] - \left[n^{(1)}\ \omega^{(1)}\ v_{tr}^{(2)}\right]$$

$$\kappa_\Sigma^{(2)} = \kappa_I^{(2)} + \kappa_{II}^{(2)}; \quad g_2 = \kappa_I^{(2)} - \kappa_{II}^{(2)}$$

$$x_1 = v_r^{(1)} \cdot i_I^{(1)}; \quad x_2 = v_r^{(1)} \cdot i_{II}^{(1)}$$

$\kappa_I^{(i)}$ and $\kappa_{II}^{(i)}$ $(i = 1,2)$ are the principal curvatures of surface Σ_i; σ is the angle formed by the unit vectors $i_I^{(1)}$ and $i_I^{(2)}$,

and measured counter-clockwise from $\underset{\sim}{i}_I^{(1)}$ to $\underset{\sim}{i}_I^{(2)}$ (Fig. 5.1 a); $\underset{\sim}{i}_I^{(1)}$ and $\underset{\sim}{i}_I^{(2)}$ represent the principal directions of surfaces Σ_1 and Σ_2. $\underset{\sim}{n}$ is the unit normal to the contacting surfaces represented in the coordinate system S_f by equations (I.2); $\underset{\sim}{\omega}^{(1)}$ and $\underset{\sim}{\omega}^{(2)}$ are the angular velocities of gear 1 and 2, $\underset{\sim}{\omega}^{(12)} = \underset{\sim}{\omega}^{(1)} - \underset{\sim}{\omega}^{(2)}$; $\underset{\sim}{v}_{tr}^{(i)}$ is the transfer velocity of the contacting ellipse in the transfer motion, __with__ gear i (i = 1,2). Here: $\underset{\sim}{v}_{tr}^{(1)} = \underset{\sim}{\omega}^{(1)} \times \underset{\sim}{r}_f^{(1)}$; $\underset{\sim}{v}_{tr}^{(2)} = \underset{\sim}{\omega}^{(2)} \times \underset{\sim}{r}_f^{(1)} + \underset{\sim}{c} \times \underset{\sim}{\omega}^{(2)}$ where $\underset{\sim}{r}_f^{(1)}$ is the position vector of the point contact represented by equations (4.17) – (4.19); $\underset{\sim}{c} = (r_1 + r_2) \underset{\sim}{i}$; $v^{(12)} = \underset{\sim}{v}_{tr}^{(1)} - \underset{\sim}{v}_{tr}^{(2)}$ is the sliding velocity. Considering the coordinate system S_f, we have

$$
\underset{\sim}{r}_f^{(1)} = \begin{bmatrix} \rho_F\sin\theta_F - b_F + r_1 \\ -(\rho_F\cos\theta_F - b_F\cot\theta_F)\sin\lambda_F \\ \rho_F\cos\theta_F\cos\lambda_F - \dfrac{a_F}{\cos\lambda_F} + b_F\cot\theta_F\tan\lambda_F\sin\lambda_F + r_1\phi_1\tan\lambda_F \end{bmatrix}
\tag{6.2}
$$

$$
\underset{\sim}{\omega}_f^{(1)} = -\omega^{(1)}\underset{\sim}{k}
\tag{6.3}
$$

$$
\underset{\sim}{\omega}_f^{(2)} = \omega^{(2)}\underset{\sim}{k} = \left(\frac{r_1}{r_2}\right)\omega^{(1)}\underset{\sim}{k} = m_{21}\omega^{(1)}\underset{\sim}{k}
\tag{6.4}
$$

$$
\underset{\sim}{v}_{tr_{(f)}}^{(1)} = \underset{\sim}{\omega}^{(1)} \times \underset{\sim}{r}_f^{(1)} = \omega^{(1)}\begin{bmatrix} y_F^{(1)} \\ -x_f^{(1)} \\ 0 \end{bmatrix}
\tag{6.5}
$$

$$
\underset{\sim}{v}_{tr_{(f)}}^{(2)} = \underset{\sim}{\omega}^{(2)} \times \underset{\sim}{r}_f^{(1)} + \underset{\sim}{c} \times \underset{\sim}{\omega}^{(2)}
$$

41

$$= \omega^{(2)} \begin{bmatrix} -y_f^{(1)} \\ x_f^{(1)} - C \\ 0 \end{bmatrix} = m_{21}\,\omega^{(1)} \begin{bmatrix} -y_f^{(1)} \\ x_f^{(1)} - C \\ 0 \end{bmatrix} \quad (6.6)$$

$$\underset{\sim}{v}_f^{(12)} = \underset{\sim}{v}_{tr_{(f)}}^{(1)} - \underset{\sim}{v}_{tr_{(f)}}^{(2)}$$

$$= \omega^{(1)} \begin{bmatrix} y_f^{(1)}\,(1 + m_{21}) \\ -x_f^{(1)}\,(1 + m_{21}) + m_{21}c \\ 0 \end{bmatrix} \quad (6.7)$$

$$\underset{\sim}{\omega}_f^{(12)} = \underset{\sim}{\omega}_f^{(1)} - \underset{\sim}{\omega}_f^{(2)} = \omega^{(1)} \begin{bmatrix} 0 \\ 0 \\ -(1 + m_{21}) \end{bmatrix} \quad (6.8)$$

$$\underset{\sim}{n}_f^{(1)} = \begin{bmatrix} \sin\theta_F \\ -\cos\theta_F \sin\lambda_F \\ \cos\theta_F \cos\lambda_F \end{bmatrix} \quad (6.9)$$

Using coordinate transformation, we can transform $\underset{\sim}{\omega}_f^{(1)}$, $\underset{\sim}{\omega}_f^{(2)}$, $\underset{\sim}{v}_{tr_{(f)}}^{(1)}$, $\underset{\sim}{v}_{tr_{(f)}}^{(2)}$, $\underset{\sim}{v}_f^{(12)}$, $\underset{\sim}{\omega}_f^{(12)}$, and $\underset{\sim}{n}_q^{(1)}$ from coordinate system S_f to S_q by using Fig. 2.3, Fig. 3.1, Fig. 4.1 c and Fig. 6.1 a. We obtain:

$$\begin{bmatrix} L_{qf} \end{bmatrix} = \begin{bmatrix} L_{qt} \end{bmatrix} \begin{bmatrix} L_{ta} \end{bmatrix} \begin{bmatrix} L_{ac} \end{bmatrix} \begin{bmatrix} L_{cf} \end{bmatrix}$$

$$= \begin{bmatrix} \sin\theta_F & -\sin\lambda_F\cos\theta_F & \cos\theta_F\cos\lambda_F \\ \cos\theta_F\cos\sigma^{(F,1)} & \sin\theta_F\cos\sigma^{(F,1)}\sin\lambda_F + \sin\sigma^{(F,1)}\cos\lambda_F & -\sin\theta_F\cos\sigma^{(F,1)}\cos\lambda_F + \sin\sigma^{(F,1)}\sin\lambda_F \\ -\cos\theta_F\sin\sigma^{(F,1)} & -\sin\theta_F\sin\sigma^{(F,1)}\sin\lambda_F + \cos\sigma^{(F,1)}\cos\lambda_F & \sin\theta_F\sin\sigma^{(F,1)}\cos\lambda_F + \cos\sigma^{(F,1)}\sin\lambda_F \end{bmatrix}$$

$$(6.10)$$

42

(a)

(b)

Fig. 6.1

43

$$\underline{\omega}_q^{(1)} = \left[L_{qf} \right] \left[\omega_f^{(1)} \right]$$

$$= -\omega^{(1)} \begin{bmatrix} \cos\theta_F \ \cos\lambda_F \\ -\sin\theta_F \cos\sigma^{(F,1)} \cos\lambda_F + \sin\sigma^{(F,1)} \sin\lambda_F \\ \sin\theta_F \sin\sigma^{(F,1)} \cos\lambda_F + \cos\sigma^{(F,1)} \sin\lambda_F \end{bmatrix} \tag{6.11}$$

$$\underline{\omega}_q^{(2)} = \left[L_{qf} \right] \left[\omega_f^{(2)} \right]$$

$$= m_{21} \omega^{(1)} \begin{bmatrix} \cos\theta_F \cos\lambda_F \\ -\sin\theta_F \cos\sigma^{(F,1)} \cos\lambda_F + \sin\sigma^{(F,1)} \sin\lambda_F \\ \sin\theta_F \sin\sigma^{(F,1)} \cos\lambda_F + \cos\sigma^{(F,1)} \sin\lambda_F \end{bmatrix} \tag{6.12}$$

$$\underline{v}_{tr(q)}^{(1)} = \left[L_{qf} \right] \left[v_{tr(f)}^{(1)} \right]$$

$$= \begin{bmatrix} y_f^{(1)} \sin\theta_F + x_f^{(1)} \sin\lambda_F \cos\theta_F \\ y_f^{(1)} \cos\theta_F \cos\sigma^{(F,1)} - x_f^{(1)} \{ \sin\theta_F \cos\sigma^{(F,1)} \sin\lambda_F + \sin\sigma^{(F,1)} \cos\lambda_F \} \\ -y_f^{(1)} \cos\theta_F \sin\sigma^{(F,1)} - x_f^{(1)} \{ -\sin\theta_F \sin\sigma^{(F,1)} \sin\lambda_F + \cos\sigma^{(F,1)} \cos\lambda_F \} \end{bmatrix} \tag{6.13}$$

$$\underline{v}_{tr(q)}^{(2)} = \left[L_{qf} \right] \left[v_{tr(f)}^{(2)} \right]$$

$$= m_{21} \omega^{(1)} \begin{bmatrix} -y_f^{(1)} \sin\theta_F - (x_f^{(1)} - c) \sin\lambda_F \cos\theta_F \\ -y_f^{(1)} \cos\theta_F \cos\sigma^{(F,1)} + (x_f^{(1)} - c) \{ \sin\theta_F \cos\sigma^{(F,1)} \sin\lambda_F + \sin\sigma^{(F,1)} \cos\lambda_F \} \\ y_f^{(1)} \cos\theta_F \sin\sigma^{(F,1)} + (x_f^{(1)} - c) \{ -\sin\theta_F \sin\sigma^{(F,1)} \sin\lambda_F + \cos\sigma^{(F,1)} \cos\lambda_F \} \end{bmatrix} \tag{6.14}$$

$$\underline{v}_q^{(12)} = \left[L_{qf} \right] \left[v_f^{(12)} \right]$$

$$= \omega^{(1)} \begin{bmatrix} y_f^{(1)} (1 + m_{21}) \sin\theta_F - \{ -x_f^{(1)} (1 + m_{21}) + m_{21} c \} \sin\lambda_F \cos\theta_F \\ y_f^{(1)} (1 + m_{21}) \cos\theta_F \cos\sigma^{(F,1)} + \{ -x_f^{(1)} (1 + m_{21}) + m_{21} c \} (\sin\theta_F \cos\sigma^{(F,1)} \sin\lambda_F + \sin\sigma^{(F,1)} \cos\lambda_F) \\ -y_f^{(1)} (1 + m_{21}) \cos\theta_F \sin\sigma^{(F,1)} + \{ -x_f^{(1)} (1 + m_{21}) + m_{21} c \} (-\sin\theta_F \sin\sigma^{(F,1)} \sin\lambda_F + \cos\sigma^{(F,1)} \cos\lambda_F) \end{bmatrix} \tag{6.15}$$

$$\omega_{\sim q}^{(12)} = \left[L_{qf} \right] \left[\omega_{f}^{(12)} \right]$$

$$= -\omega^{(1)} \begin{bmatrix} (1 + m_{21}) \cos\theta_F \cos\lambda_F \\ (1 + m_{21})(-\sin\theta_F \cos\sigma^{(F,1)} \cos\lambda_F + \sin\sigma^{(F,1)} \sin\lambda_F) \\ (1 + m_{21})(\sin\theta_F \sin\sigma^{(F,1)} \cos\lambda_F + \cos\sigma^{(F,1)} \sin\lambda_F) \end{bmatrix} \quad (6.16)$$

$$\underset{\sim}{n}_q^{(1)} = \left[L_{qf} \right] \left[n_f^{(1)} \right]$$

$$= \begin{bmatrix} 1 \\ 0 \\ 0 \end{bmatrix} \quad (6.17)$$

Also, we may represent the unit vectors $\underset{\sim I}{i}^{(1)}$ and $\underset{\sim II}{i}^{(1)}$ of the principal directions of surface Σ_1 in coordinate system S_q as follows: (Fig. 6.1b):

$$\underset{\sim I}{i}^{(1)} = \begin{bmatrix} 0 \\ 1 \\ 0 \end{bmatrix} \quad (6.18)$$

$$\underset{\sim II}{i}^{(1)} = \begin{bmatrix} 0 \\ 0 \\ 1 \end{bmatrix} \quad (6.19)$$

$$\left[\underset{\sim}{n}^{(1)} \; \underset{\sim}{\omega}^{(12)} \; \underset{\sim I}{i}^{(1)} \right] = \underset{\sim}{n}^{(1)} \cdot (\underset{\sim}{\omega}^{(12)} \times \underset{\sim I}{i}^{(1)}) = -\omega_{zq}^{(12)}$$

$$= \omega^{(1)}(1 + m_{21})(\sin\theta_F \sin\sigma^{(F,1)} \cos\lambda_F + \cos\sigma^{(F,1)} \sin\lambda_F)$$
$$(6.20)$$

$$\left[\underset{\sim}{n}^{(1)} \; \underset{\sim}{\omega}^{(12)} \; \underset{\sim II}{i}^{(1)} \right] = \underset{\sim}{n}^{(1)} \cdot (\underset{\sim}{\omega}^{(12)} \times \underset{\sim I}{i}^{(1)}) = \omega_{yq}^{(12)}$$

$$= -\omega^{(1)}(1 + m_{21})(-\sin\theta_F \cos\sigma^{(F,1)} \cos\lambda_F + \sin\sigma^{(F,1)} \sin\lambda_F)$$
$$(6.21)$$

45

$$\left[\underset{\sim}{v}^{(12)} \cdot \underset{\sim}{i}^{(1)}_I\right] = \omega^{(1)}\left\{\left[-x_f^{(1)}(1 + m_{21}) + m_{21}c\right]\left[\sin\theta_F\cos\sigma^{(F,1)}\sin\lambda_F + \sin\sigma^{(F,1)}\cos\lambda_F\right]\right.$$

$$\left. + y_f^{(1)}(1 + m_{21})\cos\theta_F\cos\sigma^{(F,1)}\right\} \tag{6.22}$$

$$\left[\underset{\sim}{v}^{(12)} \cdot \underset{\sim}{i}^{(1)}_{II}\right] = \omega^{(1)}\left\{\left[-x_f^{(1)}(1 + m_{21}) + m_{21}c\right]\left[-\sin\theta_F\sin\sigma^{(F,1)}\sin\lambda_F + \cos\sigma^{(F,1)}\cos\lambda_F\right]\right.$$

$$\left. - y_f^{(1)}(1 + m_{21})\cos\theta_F\sin\sigma^{(F,1)}\right\} \tag{6.23}$$

$$\left[\underset{\sim}{n}^{(1)} \underset{\sim}{\omega}^{(2)} \underset{\sim}{v}^{(1)}_{tr}\right] = \underset{\sim}{n}_q^{(1)} \cdot (\underset{\sim}{\omega}_q^{(2)} \times \underset{\sim}{v}^{(1)}_{tr(q)})$$

$$= m_{21}\left(\omega^{(1)}\right)^2\left[-y_f^{(1)}\cos\theta_F\sin\lambda_F + x_f^{(1)}\sin\theta_F\right] \tag{6.24}$$

$$\left[\underset{\sim}{n}^{(1)} \underset{\sim}{\omega}^{(1)} \underset{\sim}{v}^{(2)}_{tr}\right] = \underset{\sim}{n}_q \cdot (\underset{\sim}{\omega}_q^{(1)} \times \underset{\sim}{v}^{(2)}_{tr(q)})$$

$$= m_{21}\left(\omega^{(1)}\right)^2\left[-y_f^{(1)}\cos\theta_F\sin\lambda_F + (x_f^{(1)} - c)\sin\theta_F\right] \tag{6.25}$$

An easier method of deriving equations (6.20) - (6.25) is to consider the tangent plane in Fig. 4.1a and the two unit vectors $\underset{\sim}{i}^{(1)}_I$ and $\underset{\sim}{i}^{(1)}_{II}$ along the two principal directions of gear surface Σ_1.

The projections of $\underset{\sim}{i}^{(1)}_I$ and $\underset{\sim}{i}^{(1)}_{II}$ along axis X_t, Y_t and Z_t are expressed as:

$$\underset{\sim}{i}^{(1)}_{It} = \begin{bmatrix} 0 \\ \cos\sigma^{(F,1)} \\ \sin\sigma^{(F,1)} \end{bmatrix} \tag{6.26}$$

$$\underset{\sim}{i}^{(1)}_{IIt} = \begin{bmatrix} 0 \\ -\sin\sigma^{(F,1)} \\ \cos\sigma^{(F,1)} \end{bmatrix} \tag{6.27}$$

46

using the matrix transformation of direction cosines in transition from S_t to S_f (Fig. 4.1 c), we obtain

$$\left[L_{ft}\right] = \left[L_{fc}\right]\left[L_{ca}\right]\left[L_{at}\right]$$

$$= \begin{bmatrix} \sin\theta_F & \cos\theta_F & 0 \\ -\cos\theta_F\sin\lambda_F & \sin\theta_F\sin\lambda_F & \cos\lambda_F \\ \cos\theta_F\cos\lambda_F & -\sin\theta_F\cos\lambda_F & \sin\lambda_F \end{bmatrix} \tag{6.28}$$

$$i_I^{(1)} = \left[L_{ft}\right] \begin{bmatrix} 0 \\ \cos\sigma^{(F,1)} \\ \sin\sigma^{(F,1)} \end{bmatrix}$$

$$= \begin{bmatrix} \cos\theta_F\cos\sigma^{(F,1)} \\ \sin\theta_F\sin\lambda_F\cos\sigma^{(F,1)} + \cos\lambda_F\sin\sigma^{(F,1)} \\ \sin\theta_F\cos\lambda_F\sin\sigma^{(F,1)} + \sin\lambda_F\cos\sigma^{(F,1)} \end{bmatrix} \tag{6.29}$$

$$i_{II}^{(1)} = \left[L_{ft}\right] \begin{bmatrix} 0 \\ -\sin\sigma^{(F,1)} \\ \cos\sigma^{(F,1)} \end{bmatrix}$$

$$= \begin{bmatrix} -\cos\theta_F\sin\sigma^{(F,1)} \\ -\sin\theta_F\sin\lambda_F\sin\sigma^{(F,1)} + \cos\lambda_F\cos\sigma^{(F,1)} \\ \sin\theta_F\cos\lambda_F\sin\sigma^{(F,1)} + \sin\lambda_F\cos\sigma^{(F,1)} \end{bmatrix} \tag{6.30}$$

47

$$\underset{\sim}{v}^{(12)} = \underset{\sim tr}{v}^{(1)} - \underset{\sim tr}{v}^{(2)} \tag{6.31}$$

$$= \underset{\sim}{\omega}^{(1)} \times \underset{\sim f}{r}^{(1)} - [\underset{\sim}{\omega}^{(2)} \times \underset{\sim f}{r}^{(1)} + \underset{\sim}{c} \times \underset{\sim}{\omega}^{(2)}]$$

where: $\quad \underset{\sim}{c} = (r_1 + r_2)\, \underset{\sim}{i}$

$$\underset{\sim f}{r}^{(1)} = [M_{fc}][r_c^{(F)}] \tag{6.32}$$

$$= \begin{bmatrix} 1 & 0 & 0 & r_1 \\ 0 & 1 & 0 & -r_1\phi_1 \\ 0 & 0 & 1 & 0 \\ 0 & 0 & 0 & 1 \end{bmatrix} \begin{bmatrix} x_c^{(F)} \\ y_c^{(F)} \\ z_c^{(F)} \\ 1 \end{bmatrix}$$

$$= \begin{bmatrix} \rho_F \sin\theta_F - b_F + r_1 \\ -(\rho_F \cos\theta_F - b_F \cot\theta_F)\sin\lambda_F \\ \rho_F \cos\theta_F \cos\lambda_F - \dfrac{a_F}{\cos\lambda_F} + b_F \cot\theta_F \tan\lambda_F \sin\lambda_F + r_1\phi_1 \tan\lambda_F \end{bmatrix} \tag{6.33}$$

$$\underset{\sim}{\omega}^{(1)} = -\omega^{(1)} \underset{\sim}{k}$$

$$\underset{\sim}{\omega}^{(2)} = \omega^{(2)} \underset{\sim}{k}$$

$$= m_{21}\, \omega^{(1)} \underset{\sim}{k} \tag{6.34}$$

where: $\quad m_{21} = \dfrac{\omega^{(2)}}{\omega^{(1)}} = \dfrac{r_1}{r_2}$

$$\underset{\sim tr}{v}^{(1)} = \underset{\sim}{\omega}^{(1)} \times \underset{\sim f}{r}^{(1)}$$

$$= -\omega^{(1)} \begin{bmatrix} (\rho_F \cos\theta_F - b_F \cot\theta_F)\sin\lambda_F \\ \rho_F \sin\theta_F - b_F + r_1 \\ 0 \end{bmatrix} \tag{6.35}$$

$$\underset{\sim tr}{v}^{(2)} = \underset{\sim}{\omega}^{(2)} \times \underset{\sim f}{r}^{(1)} + \underset{\sim}{c} \times \underset{\sim}{\omega}^{(2)} \tag{6.36}$$

$$\begin{bmatrix} \underset{\sim}{i} & \underset{\sim}{j} & \underset{\sim}{k} \\ 0 & 0 & \omega^{(2)} \\ x_f^{(1)} & y_f^{(1)} & z_f^{(1)} \end{bmatrix} + \begin{bmatrix} \underset{\sim}{i} & \underset{\sim}{j} & \underset{\sim}{k} \\ c & 0 & 0 \\ 0 & 0 & \omega^{(2)} \end{bmatrix}$$

$$= m_{21} \omega^{(1)} \begin{bmatrix} -y_f^{(1)} \\ x_f^{(1)} - c \\ 0 \end{bmatrix}$$

$$\underset{\sim}{v}^{(12)} = \underset{\sim}{v}_{tr}^{(1)} - \underset{\sim}{v}_{tr}^{(2)}$$

$$= \omega^{(1)} \begin{bmatrix} (1 + m_{21}) y_f^{(1)} \\ m_{21} c - (1 + m_{21}) x_f^{(1)} \\ 0 \end{bmatrix} \tag{6.37}$$

$$\underset{\sim}{\omega}^{(12)} = \underset{\sim}{\omega}^{(1)} - \underset{\sim}{\omega}^{(2)}$$

$$= \omega^{(1)} \begin{bmatrix} 0 \\ 0 \\ -(1 + m_{21}) \end{bmatrix} \tag{6.38}$$

$$\underset{\sim}{n}_f^{(1)} = \begin{bmatrix} L_{fc} \end{bmatrix} \begin{bmatrix} n_c^{(F)} \end{bmatrix} \tag{6.39}$$

$$= \begin{bmatrix} 1 & 0 & 0 \\ 0 & 1 & 0 \\ 0 & 0 & 1 \end{bmatrix} \begin{bmatrix} \sin\theta_F \\ -\cos\theta_F \sin\lambda_F \\ \cos\theta_F \cos\lambda_F \end{bmatrix}$$

$$= \begin{bmatrix} \sin\theta_F \\ -\cos\theta_F \sin\lambda_F \\ \cos\theta_F \cos\lambda_F \end{bmatrix}$$

49

$$\left[\underset{\sim}{n}^{(1)} \underset{\sim}{\omega}^{(12)} \underset{\sim}{i}_I^{(1)}\right] = \underset{\sim}{n}^{(1)} \cdot (\underset{\sim}{\omega}^{(12)} \times \underset{\sim}{i}_I^{(1)})$$
$$= \omega^{(1)}(1 + m_{21})[\sin\lambda_F\cos\sigma^{(F,1)} + \sin\theta_F\cos\lambda_F\sin\sigma^{(F,1)}] \quad (6.40)$$

$$\left[\underset{\sim}{n}^{(1)} \underset{\sim}{\omega}^{(12)} \underset{\sim}{i}_{II}^{(1)}\right] = \underset{\sim}{n}^{(1)} \cdot (\underset{\sim}{\omega}^{(12)} \times \underset{\sim}{i}_{II}^{(1)})$$
$$= \omega^{(1)}(1 + m_{21})[-\sin\lambda_F\cos\sigma^{(F,1)} + \sin\theta_F\cos\lambda_F\cos\sigma^{(F,1)}]$$
$$(6.41)$$

$$\underset{\sim}{v}^{(12)} \cdot \underset{\sim}{i}_I^{(1)} = \omega^{(1)}\{y_f^{(1)}(1 + m_{21})\cos\theta_F\cos\sigma^{(F,1)} + [m_{21}c - x_f^{(1)}(1 + m_{21})]$$
$$(\sin\theta_F\sin\lambda_F\cos\sigma^{(F,1)} + \cos\lambda_F\sin\sigma^{(F,1)})\} \quad (6.42)$$

$$\underset{\sim}{v}^{(12)} \cdot \underset{\sim}{i}_{II}^{(1)} = \omega^{(1)}\{-y_f^{(1)}(1 + m_{21})\cos\theta_F\sin\sigma^{(F,1)} + [m_{21}c - x_f^{(1)}(1 + m_{21})]$$
$$(\cos\theta_F\cos\sigma^{(F,1)} - \sin\theta_F\sin\lambda_F\sin\sigma^{(F,1)})\} \quad (6.43)$$

$$\left[\underset{\sim}{n}^{(1)} \underset{\sim}{\omega}^{(2)} \underset{\sim}{v}_{tr}^{(1)}\right] = \underset{\sim}{n}^{(1)} \cdot (\underset{\sim}{\omega}^{(2)} \times \underset{\sim}{v}_{tr}^{(1)})$$
$$= \begin{bmatrix} \sin\theta_F \\ -\cos\theta_F\sin\lambda_F \\ \cos\theta_F\cos\lambda_F \end{bmatrix} \begin{bmatrix} \underset{\sim}{i}_f & \underset{\sim}{j}_f & \underset{\sim}{k}_f \\ 0 & 0 & m_{21}\omega^{(1)} \\ \omega^{(1)}y_f^{(1)} & -\omega^{(1)}x_f^{(1)} & 0 \end{bmatrix}$$
$$= (\omega^{(1)})^2 m_{21}[\sin\theta_F x_f^{(1)} - \cos\theta_F\sin\lambda_F y_f^{(1)}] \quad (6.44)$$

$$\left[\underset{\sim}{n}^{(1)} \underset{\sim}{\omega}^{(1)} \underset{\sim}{v}_{tr}^{(2)}\right] = \underset{\sim}{n}^{(1)} \cdot (\underset{\sim}{\omega}^{(1)} \times \underset{\sim}{v}_{tr}^{(2)})$$
$$= \begin{bmatrix} \sin\theta_F \\ -\cos\theta_F\sin\lambda_F \\ \cos\theta_F\cos\lambda_F \end{bmatrix} \begin{bmatrix} \underset{\sim}{i}_f & \underset{\sim}{j}_f & \underset{\sim}{k}_f \\ 0 & 0 & -\omega^{(1)} \\ -\omega^{(1)}m_{21}y_f^{(1)} & \omega^{(1)}m_{21}(x_f^{(1)}-c) & 0 \end{bmatrix}$$
$$= (\omega^{(1)})^2 m_{21}[\sin\theta_F(x_f^{(1)} - c) - \cos\theta_F\sin\lambda_F y_f^{(1)}]$$
$$(6.45)$$

Comparing the expressions in equations (6.20) - (6.25) and (6.40)
- (6.45) we obtained the same results. Substituting these
expressions into equation (6.1), we get the coefficients a_{31}, a_{32}

b_1, b_2 and b_3. Equations (6.1) represent a system of three linear equations with two unknowns:

$$x_1 = \underset{\sim}{v}_r^{(1)} \cdot \underset{\sim}{i}_I^{(1)}, \quad x_2 = \underset{\sim}{v}_r^{(1)} \cdot \underset{\sim}{i}_{II}^{(1)} \tag{6.46}$$

where $\underset{\sim}{v}_r^{(1)}$ is the velocity of motion over the gear tooth surface Σ_1. These equations provide a unique solution for x_1 and x_2 if the following condition is observed [5,6]:

$$\begin{vmatrix} a_{11} & a_{12} & b_1 \\ a_{21} & a_{22} & b_2 \\ a_{31} & a_{32} & b_3 \end{vmatrix} = 0 \tag{6.47}$$

It is assumed that surfaces Σ_1 and Σ_2 are in point contact at every instant. Using any two equations of the system equations (6.1) we may determine x_1 and x_2 and thus $v_r^{(1)} = (x_1^{(2)} + x_2^{(2)})^{\frac{1}{2}}$

An alternative method of deriving the relative velocity $\underset{\sim}{v}_r^{(1)}$ at the point of contact M is:

Step 1   The point of contact of surface Σ_1 and Σ_2 lies on a straight line which passes through the following equations:

$$x_f^{(1)} = \rho_F \sin\theta_F - b_F + r_1$$
$$y_f^{(1)} = -(\rho_F \cos\theta_F - b_F \cot\theta_F)\sin\lambda_F$$
$$z_f^{(1)} = \rho_F \cos\theta_F \cos\lambda_F - \frac{a_F}{\cos\lambda_F} + b_F \cot\theta_F \tan\lambda_F \sin\lambda_F + r_1 \phi_1 \tan\lambda_F$$

$$\tag{6.48}$$

Here, $\theta_F = \theta_P = \theta = 30°$ is the pressure angle at the point of contact of surface Σ_1 and Σ_2

Step 2 The transfer velocity $\underset{\sim}{v}_{tr}^{(1)}$ of a point on gear 1 is:

$$\underset{\sim}{v}_{tr}^{(1)} = \underset{\sim}{\omega}^{(1)} \times \underset{\sim}{r}_f^{(1)}$$

$$= \omega^{(1)} \begin{bmatrix} y_f^{(1)} \\ -x_f^{(1)} \\ 0 \end{bmatrix} \tag{6.49}$$

Step 3 The direction of absolute velocity $\underset{\sim}{V}_{abs}$ of point M of gear 1 is parallel to the axes of gear rotation $z_f^{(1)}$. Hence

$$V_{abs}^{(1)} = \frac{dz_f^{(1)}}{dt}$$

$$= (-\rho_F \sin\theta_F \cos\lambda_F - \frac{b_F}{\sin^2\theta_F} \tan\lambda_F \sin\lambda_F) \frac{d\theta_F}{dt} + (r_1 \tan\lambda_F) \frac{d\phi_1}{dt} \tag{6.50}$$

Here: $\dfrac{d\theta_F}{dt} = 0$ and $\dfrac{d\phi_1}{dt} = \omega^{(1)}$. Therefore, we have:

$$V_{abs}^{(1)} = \begin{bmatrix} 0 \\ 0 \\ r_1 \omega^{(1)} \tan\lambda_F \end{bmatrix} \tag{6.51}$$

Step 4 The relative velocity $\underset{\sim}{v}_r^{(1)}$ of point M of gear 1 is:
($\underset{\sim}{v}_r^{(1)}$ is tangent to the helix of gear 1)

$$\underset{\sim}{v}_{tr}^{(1)} + \underset{\sim}{v}_{r}^{(1)} = \underset{\sim}{v}_{abs}^{(1)}$$

$$\underset{\sim}{v}_{r}^{(1)} = \underset{\sim}{v}_{abs}^{(1)} - \underset{\sim}{v}_{tr}^{(1)}$$

$$= \omega^{(1)} \begin{bmatrix} -y_f^{(1)} \\ x_f^{(1)} \\ r_1 \tan \lambda_F \end{bmatrix} \tag{6.52}$$

The velocity $\underset{\sim}{v}_{r}^{(2)}$ of the motion over surface Σ_2 may be determined by using the following equations [5]:

$$\underset{\sim}{v}_{r}^{(1)} + \underset{\sim}{v}_{tr}^{(1)} = \underset{\sim}{v}_{r}^{(2)} + \underset{\sim}{v}_{tr}^{(2)} \tag{6.53}$$

Equation (6.53) yields

$$\underset{\sim}{v}_{r}^{(2)} = \underset{\sim}{v}_{r}^{(1)} + \underset{\sim}{v}_{tr}^{(1)} - \underset{\sim}{v}_{tr}^{(2)} = \underset{\sim}{v}_{r}^{(1)} + \underset{\sim}{v}^{(12)} \tag{6.54}$$

where $\underset{\sim}{v}_{r}^{(2)}$ is the relative velocity of the contact point M of gear 2; $v^{(12)}$ is the sliding velocity expressed in equation (6.7).

Example 6.1: <u>Relative Velocity of Motion of the Contacting</u>
<u>Ellipse Over the Gear Tooth Surface</u>

The rack cutter and gear nominal parameters are the same as given in Example 4.1.

(1) We may determine the relative velocity in the motion of the contacting ellipse over the gear tooth surface Σ_1 by using equations (6.1) - (6.46). Then we obtain X_1 and X_2, thus

$$V_r^{(1)} = (X_1^2 + X_2^2)^{\frac{1}{2}} = 12.06574 \; \omega^{(1)}$$

and $\sigma = 16.1479°$ is the angle formed by $\underset{\sim}{V}_{r}^{(1)}$ and axis $z_f^{(1)}$.

53

(2) By using equations (6.48) - (6.52) to solve $V_{\sim r}^{(1)}$, we obtain

$$V_{\sim r}^{(1)} = V_{\sim abs}^{(1)} - V_{\sim tr}^{(1)} = 12.06706 \ \omega^{(1)}$$

(3) From equation (6.54), we have

$$V_{\sim r}^{(2)} = 11.99259 \ \omega^{(1)}$$

and $\beta = 14.8674°$ is the angle formed by $V_{\sim r}^{(2)}$ and axis $z_f^{(2)}$. Note: Due to a lot of computational procedures and matrix transformation for approach (1), there is a small difference between the approaches (1) and (2), and approach (2) is better than approach (1).

7 Computer Aided Simulation of Conditions of Meshing

We simulated the conditions of meshing of gears, which have some errors, using the equations of continuous tangency of gear tooth surfaces. We set up four coordinate systems: S_1 and S_2, rapidly connected to the gears and S_h and S_f, rigidly connected to the frames. By using the coordinate transformations from S_1 via S_h to S_f, we may represent the equations of the surfaces $\Sigma_i (i = 1,2)$ and its surface normal in coordinate system S_f.

The conditions of continuous tangency of gear tooth surfaces Σ_1 and Σ_2 are represented by the following equations [5,6]:

$$r_{\sim f}^{(1)} (\theta_F, \ \phi_1, \ \mu_1) = r_{\sim f}^{(2)} (\theta_p, \ \phi_2, \ \mu_2) \tag{7.1}$$

$$n_{\sim f}^{(1)} (\theta_F, \ \mu_1) = n_{\sim f}^{(2)} (\theta_p, \ \mu_2) \tag{7.2}$$

Equation (7.1) expresses that surfaces Σ_1 and Σ_2 have a common point determined with the position vectors $\underset{\sim}{r}_f^{(1)}$ and $\underset{\sim}{r}_f^{(2)}$. Equation (7.2) indicates that surfaces Σ_1 and Σ_2 have a common unit normal at their common point. Equations (7.1) and (7.2) when considered simultaneously yield a system of only five independent equations, since $\left|\underset{\sim}{n}_f^{(1)}\right| = \left|\underset{\sim}{n}_f^{(2)}\right| = 1$. These five equations relate six unknowns: θ_F, ϕ_1', ϕ_1, θ_p, ϕ_2, ϕ_2', and thus one of these unknowns may be considered as a variable.

8 Influence of Manufacturing and Assembly Errors, and Adjustment of Gears to the Errors

(i) Change of Axes Distance

Fig. 8.1a and Fig. 8.1b show that the operating center distance C' is not equal to the sum of the radic of pitch cylinders in this case; Thus $C' \neq r_1 + r_2$. Considering the gear tooth surface Σ_1 and its unit normal $\underset{\sim}{n}_1$, and gear tooth surface Σ_2 and its unit normal $\underset{\sim}{n}_2$ are represented in the coordinate systems S_1 and S_2, respectively. We may represent Σ_i and $\underset{\sim}{n}_i$ $(i = 1,2)$ in the coordinate system S_f using the following matrix equations:

$$\left[r_f^{(i)} \right] = \left[M_{fi} \right] \left[r_i \right] \tag{8.1}$$

where (Fig. 8.1):

$$\left[M_{f1} \right] = \begin{bmatrix} \cos\phi_1' & \sin\phi_1' & 0 & 0 \\ -\sin\phi_1' & \cos\phi_1' & 0 & 0 \\ 0 & 0 & 1 & 0 \\ 0 & 0 & 0 & 1 \end{bmatrix}$$

55
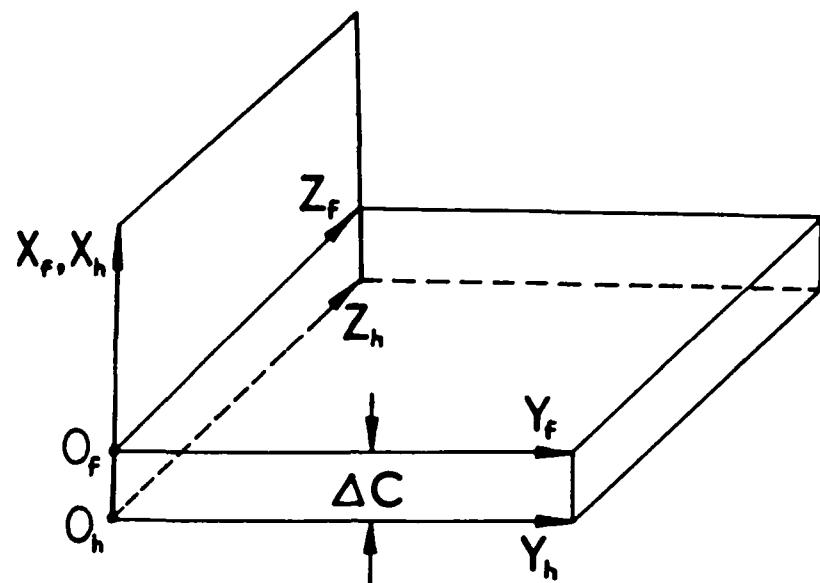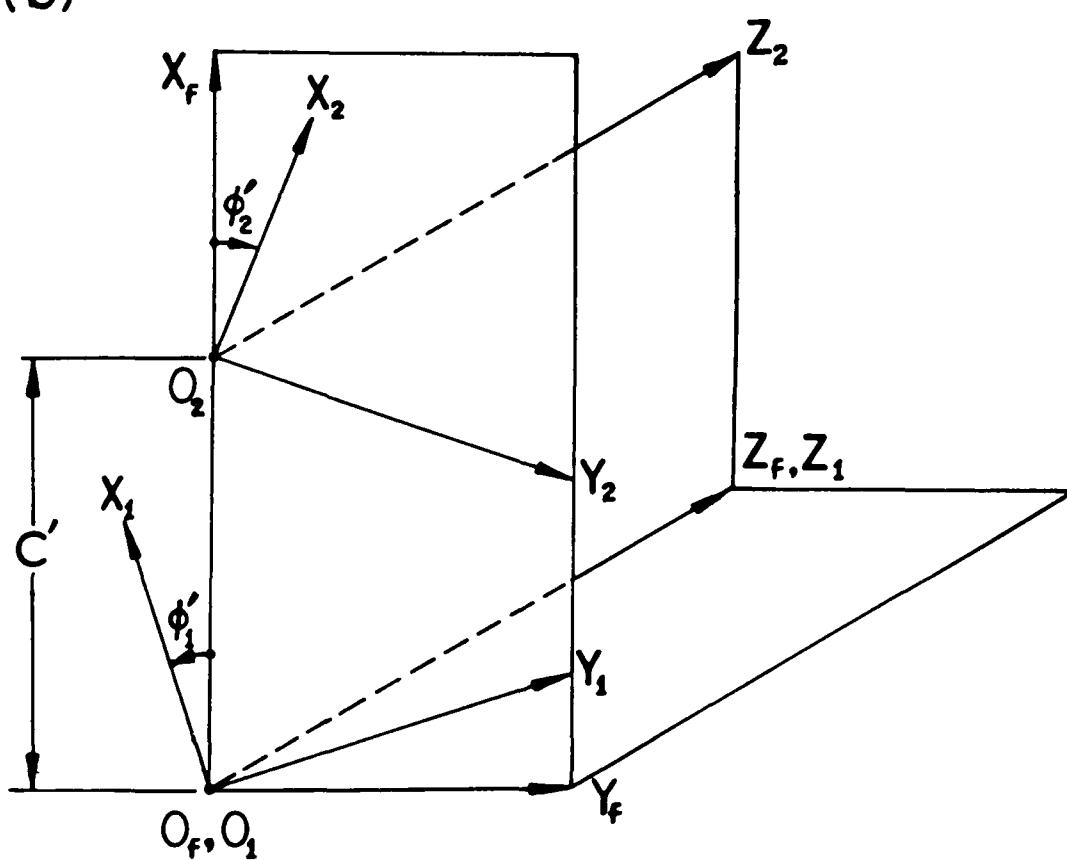
Fig. 8.1

$$
\left[M_{f2} \right] = \begin{bmatrix} \cos\phi_2' & -\sin\phi_2' & 0 & C' \\ \sin\phi_2' & \cos\phi_2' & 0 & 0 \\ 0 & 0 & 1 & 0 \\ 0 & 0 & 0 & 1 \end{bmatrix}
$$

and $\left[n_f^{(i)} \right] = \left[L_{fi} \right] \left[n_i \right]$ (8.2)

where:
$$
\left[L_{f1} \right] = \begin{bmatrix} \cos\phi_1' & \sin\phi_1' & 0 \\ -\sin\phi_1' & \cos\phi_1' & 0 \\ 0 & 0 & 1 \end{bmatrix}
$$

$$
\left[L_{f2} \right] = \begin{bmatrix} \cos\phi_2' & -\sin\phi_2' & 0 \\ \sin\phi_2' & \cos\phi_2' & 0 \\ 0 & 0 & 1 \end{bmatrix}
$$

ϕ_1' and ϕ_2' are the angles of rotation of the gear in mesh with the mating gear, while ϕ_1 and ϕ_2 are the angles of rotation of gear 1 and gear 2 in mesh with the corresponding rack cutter.

Using equations (8.1), (8.2) or (I.9) – (I.14) and (7.1), (7.2) yield the following procedure for computations:

Step 1: Using equations $n_{zf}^{(1)} = n_{zf}^{(2)}$, we obtain

$$
\cos\theta_F \cos\lambda_F = \cos\theta_P \cos\lambda_P \tag{8.3}
$$

57

Equation (8.3) with $\lambda_F = \lambda_P = \lambda$ yields that

$$\theta_F = \theta_P = \theta \qquad (8.4)$$

Step 2: Using equations $n_{yf}^{(1)} = n_{yf}^{(2)}$, $y_f^{(1)} = y_f^{(2)}$ and $x_f^{(1)} = x_f^{(2)}$, we obtain the following system of three equations in three unknowns (θ , μ_1 and μ_2):

$$\sin\theta\sin\mu_1 - \cos\theta\sin\lambda\cos\mu_1 = -\sin\theta\sin\mu_2 - \cos\theta\sin\lambda\cos\mu_2 \qquad (8.5)$$

$$(\rho_F\sin\theta - b_F)(\sin\theta\sin\mu_1 - \cos\theta\sin\lambda\cos\mu_1) + r_1\sin\theta\sin\mu_1 =$$
$$-(\rho_P\sin\theta - b_P)(\sin\theta\sin\mu_2 + \cos\theta\sin\lambda\cos\mu_2) + r_2\sin\theta\sin\mu_2 \qquad (8.6)$$

$$(\rho_F\sin\theta - b_F)(\sin\theta\cos\mu_1 + \cos\theta\sin\lambda\sin\mu_1) + r_1\sin\theta\cos\mu_1 =$$
$$(\rho_P\sin\theta - b_P)(\sin\theta\cos\mu_2 - \cos\theta\sin\lambda\sin\mu_2) - r_2\sin\theta\cos\mu_2 +$$
$$C'\sin\theta \qquad (8.7)$$

where: $C' = r_1 + r_2 + \Delta C$ and ΔC is the change of center distance.

The solution to these equations for θ , μ_1 and μ_2 provides constant values whose magnitude depends on the operating center distance C' only (the change of the center distance, ΔC). The location of the center of the contacting ellipse is determined by $\theta(\Delta C)$. Thus, the bearing contact also depends on ΔC.

We may check up the solution to equations (8.5), (8.6) and (8.7) using the equation $n_{xf}^{(1)} = n_{xf}^{(2)}$ which yields

$$\sin\theta\cos\mu_1 + \cos\theta\sin\lambda\sin\mu_1 = \sin\theta\cos\mu_2 - \cos\theta\sin\lambda\sin\mu_2$$

Step 3: Knowing θ , we may determine the relation between para-

58

meters ϕ_1 and ϕ_2 using equation $z_f^{(1)} = z_f^{(2)}$ which yields

$$\rho_F \cos\theta\cos\lambda - \frac{a_F}{\cos\lambda} + b_F \cot\theta\tan\lambda\sin\lambda + r_1\phi_1\tan\lambda =$$

$$\rho_p \cos\theta\cos\lambda - \frac{a_p}{\cos\lambda} + b_p \cot\theta\tan\lambda\sin\lambda + r_2\phi_2\tan\lambda \qquad (8.9)$$

Equation (8.9) provides a linear function which relates ϕ_1 and ϕ_2 since θ is constant.

Step 4: It is easy to prove that since θ, μ_1 and μ_2 have constant values, the angular velocity ratio for the gears does not depend on the center-distance. The proof is based on the following considerations: (i) Equation (8.9) with θ = const yields that $r_1 d\phi_1 = r_2 d\phi_2$ and $\frac{d\phi_1}{d\phi_2} = \frac{r_2}{r_1}$; (ii) Since $\mu_1 = \phi_1 - \phi_1'$ and $\mu_2 = \phi_2 - \phi_2'$ are constant, we obtain that $d\phi_1' = d\phi_1$, $d\phi_2' = d\phi_2$, and

$$m_{12} = \frac{\omega^{(1)}}{\omega^{(2)}} = \frac{d\phi_1'}{d\phi_2'} = \frac{r_2}{r_1} \qquad (8.10)$$

Step 5: It is evident that since θ, μ_1 and μ_2 have constant values, the line of action of the gear tooth surfaces represents, in the fixed coordinate system S_f, a straight line which is parallel to the z_f - axis. We may determine the coordinates $x_f^{(i)}$ and $y_f^{(i)}$ ($i = 1,2$) of the line of action using equations (I.9) or (I.12) (see Appendix I). The location of the instantaneous point of contact on the line of action may be represented as a function of ϕ_1':

59

$$z_f^{(1)} = \rho_F \cos\theta \cos\lambda - \frac{a_F}{\cos\lambda} + b_F \cot\theta \tan\lambda \sin\lambda + r_1(\mu_1 + \phi_1')\tan\lambda$$

(8.11)

Step 6: We may also derive an approximate equation which relates θ and the change of the center-distance, ΔC. Since μ_1 and μ_2 are small, we assume $\cos\mu_i = 1$ and $\sin\mu_i = 0$ in equation (8.7). We then obtain

$$\rho_F \sin\theta - b_F + r_1 = \rho_P \sin\theta - b_P - r_2 + C'$$

(8.12)

where $C' = r_1 + r_2 + \Delta C$

Equation (8.12) yields

$$\sin\theta = \frac{\Delta C + b_F - b_P}{\rho_F - \rho_P}$$

(8.13)

The nominal value of $\theta°$ which corresponds to the theoretical value of the center distance C, where $C = r_1 + r_2$, is given by

$$\sin\theta° = \frac{b_F° - b_P°}{\rho_F° - \rho_P°}$$

(8.14)

Compensation for the Location of Bearing Contact Induced by ΔC

The sensitivity of the gears to the change of center distance, ΔC, may be reduced by increasing the difference $\left|\rho_F - \rho_P\right|$. However, this results in the increase of contacting stresses.

The dislocation of the bearing contact may be compensated for by refinishing of one of the gears (preferably the pinion)

60

with new tool settings.

Consider that θ° is the nominal value for the pressure angle; b_F° and b_P° are the nominal values for the machine settings and ρ_F°, ρ_P° are the nominal values for the radii of circular arcs. These parameters are related by equation (8.14). The location of the bearing contact won't be changed if the pinion is refinished with a new tool setting b_F determined as follows (see equation (8.13):

$$\sin\theta^\circ = \frac{\Delta C + b_F - b_P^\circ}{\rho_F^\circ - \rho_P^\circ} \tag{8.15}$$

$$b_F = b_F^\circ - \Delta C \tag{8.16}$$

Change of Machine-Tool Settings b_F and b_P

The change of machine-tool settings b_F and b_P causes: (i) the change of gear tooth thickness and backlash between the mating teeth, and (ii) the dislocation of the bearing contact. The most dangerous result is the dislocation of the bearing contact.

Using similar principles of investigation, we may represent the new value of the pressure angle which corresponds to the changed machine-tool settings by using the following equation

$$\sin\theta = \frac{b_F - b_P}{\rho_F^\circ - \rho_P^\circ} \tag{8.17}$$

61

Here: b_F and b_P are the changed settings; $b_F \neq b_F^o$, $b_P \neq b_P^o$, where b_F^o and b_P^o are the nominal machine-settings; $\theta \neq \theta^o$ is the new pressure angle.

We may compensate for the dislocation of the bearing contact making $\theta = \theta^o$. This can be achieved by refinishing of the pinion with a corrected setting Δb_F. Similar to equation (8.15) we obtain

$$\sin\theta^o = \frac{b_F - b_P^o + \Delta b_F}{\rho_F^o - \rho_P^o} \tag{8.18}$$

(ii) <u>Misalignment of Crossed Axes of Gear Rotation</u>

Consider that the axis of rotation of gear 1 is not parallel to the axis of rotation of gear 2 and form an angle $\Delta\gamma$ (Fig. 8.2). The coordinate transformation from S_h to S_f is represented by the matrix equations

$$\left[r_f^{(1)} \right] = \left[M_{fh} \right] \left[r_h^{(1)} \right], \quad \left[n_f^{(1)} \right] = \left[L_{fh} \right] \left[n_h^{(1)} \right] \tag{8.19}$$

where:

$$\left[M_{fh} \right] = \begin{bmatrix} 1 & 0 & 0 & 0 \\ 0 & \cos\Delta\gamma & \sin\Delta\gamma & 0 \\ 0 & -\sin\Delta\gamma & \cos\Delta\gamma & 0 \\ 0 & 0 & 0 & 1 \end{bmatrix} ; \quad \left[L_{fR} \right] = \begin{bmatrix} 1 & 0 & 0 \\ 0 & \cos\Delta\gamma & \sin\Delta\gamma \\ 0 & -\sin\Delta\gamma & \cos\Delta\gamma \end{bmatrix}$$

Using equations (8.19), (I.9)-(I.12) and (7.1), (7.2), we may represent the tangency of surfaces Σ_1 and Σ_2 for crossed misaligned

62
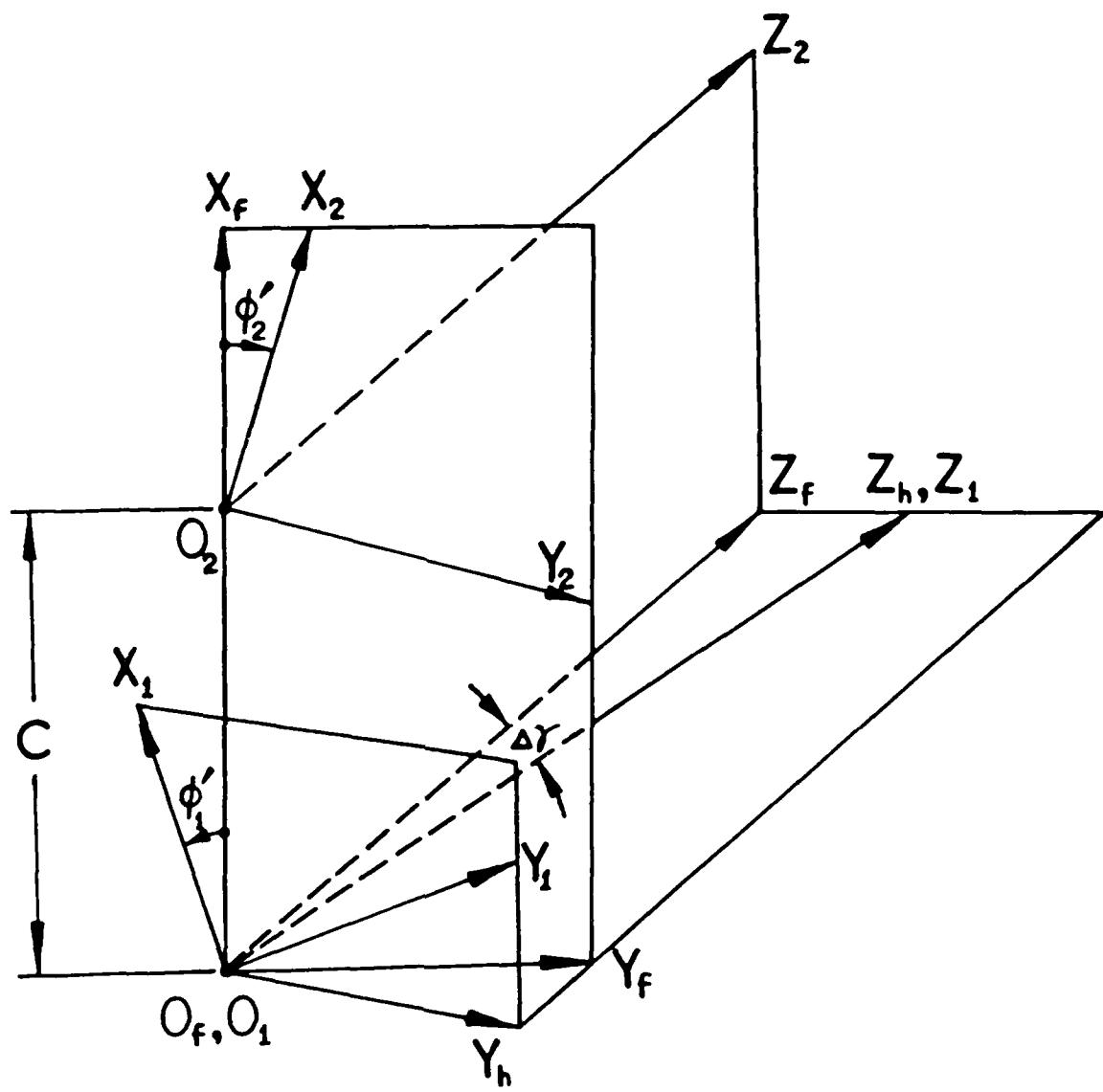
Fig. 8.2

gears as follows:

$$A_2\cos\mu_2 - B_2\sin\mu_2 + C = A_1\cos\mu_1 + B_1\sin\mu_1 \tag{8.20}$$

$$-A_2\sin\mu_2 - B_2\cos\mu_2 = (A_1\sin\mu_1 - B_1\cos\mu_1)\cos\Delta\gamma +$$

$$(f_F\cos\theta_F\cos\lambda_F - \frac{a_F}{\cos\lambda_F} + b_F\cot\theta_F\tan\lambda_F\sin\lambda_F + r_1\phi_1\tan\lambda_F)\sin\Delta\gamma$$

$$\tag{8.21}$$

(see expressions (I.11) and (I.14) in Appendix I)

$$f_F\cos\theta_p\cos\lambda_P - \frac{a_F}{\cos\lambda_p} + b_P\cot\theta_P\sin\lambda_P\tan\lambda_P + r_2\phi_2\tan\lambda_P =$$

$$-(A_1\sin\mu_1 - B_1\cos\mu_1)\sin\Delta\gamma + (f_F\cos\theta_F\cos\lambda_F - \frac{a_F}{\cos\lambda_F} +$$

$$b_F\cot\theta_F\tan\lambda_F\sin\lambda_F + r_1\phi_1\tan\lambda_F)\cos\Delta\gamma \tag{8.22}$$

$$\sin\theta_p\cos\mu_2 - \cos\theta_p\sin\lambda_P\sin\mu_2 = \sin\theta_F\cos\mu_1 + \cos\theta_F\sin\lambda_F\sin\mu_1 \tag{8.23}$$

$$-\sin\theta_p\sin\mu_2 - \cos\theta_p\sin\lambda_P\cos\mu_2 = (\sin\theta_F\sin\mu_1 - \cos\theta_F\sin\lambda_F\cos\mu_1)$$

$$\cos\Delta\gamma + \cos\theta_F\cos\lambda_F\sin\Delta\gamma \tag{8.24}$$

$$\cos\theta_p\cos\lambda_P = -(\sin\theta_F\sin\mu_1 - \cos\theta_F\sin\lambda_F\cos\mu_1)\sin\Delta\gamma +$$

$$\cos\theta_F\cos\lambda_F\cos\Delta\gamma \tag{8.25}$$

Equations (8.20) - (8.25) form a system of five independent
equations in six unknowns: θ_P, θ_F, μ_1, μ_2, ϕ_1 and ϕ_2. We remind
that only two equations from equation system (8.23) - (8.25) are
independent since $\left| n_f^{(1)} \right| = 1$ and $\left| n_f^{(2)} \right| = 1$.

The computational procedure is as follows: (i) We consider
equations (8.20), (8.21), (8.24) and (8.25) which form a system
of 4 equations in five unknowns: θ_F, θ_P, μ_1, μ_2 and ϕ_1. Fixing in ϕ_1
we may obtain the solutions by $\theta_F(\phi_1)$, $\theta_P(\phi_1)$, $\mu_1(\phi_1)$ and $\mu_2(\phi_1)$;

(ii) Using equation (8.22) we obtain $\phi_2(\phi_1)$; (iii) Then, using
the equations

$$\phi_1' = \phi_1 - \mu_1 \quad , \quad \phi_2' = \phi_2 - \mu_2 \tag{8.26}$$

64

we can obtain the relation between the angles ϕ_2' and ϕ_1' of gear rotation. Function $\phi_2'(\phi_1')$ is a non-linear function and its deviation from the linear function is given by

$$\Delta\phi_2'(\phi_1') = \phi_2'(\phi_1') - \frac{N_1}{N_2}\phi_1' \qquad (8.27)$$

Here: $\Delta\phi_2'(\phi_1')$ represents the kinematical errors of the gear train and $\theta_F(\phi_1')$ and $\theta_P(\phi_1')$ represent the change of location of the bearing contact induced by the misalignment of gear axes.

(iii) Misalignment of Intersected Axes of Gear Rotation

In the case of intersected axes of gear rotation, two axes form an angle $\Delta\gamma$ (Fig. 8.3). The coordinate transformation from S_h to S_f is represented by the matrix equations:

$$\left[r_f^{(1)}\right] = \left[M_{fh}\right]\left[r_h^{(1)}\right], \qquad \left[n_f^{(1)}\right] = \left[L_{fh}\right]\left[n_h^{(1)}\right] \qquad (8.28)$$

where

$$\left[M_{fh}\right] = \begin{bmatrix} \cos\Delta\gamma & 0 & -\sin\Delta\gamma & 0 \\ 0 & 1 & 0 & 0 \\ \sin\Delta\gamma & 0 & \cos\Delta\gamma & 0 \\ 0 & 0 & 0 & 1 \end{bmatrix}$$

65
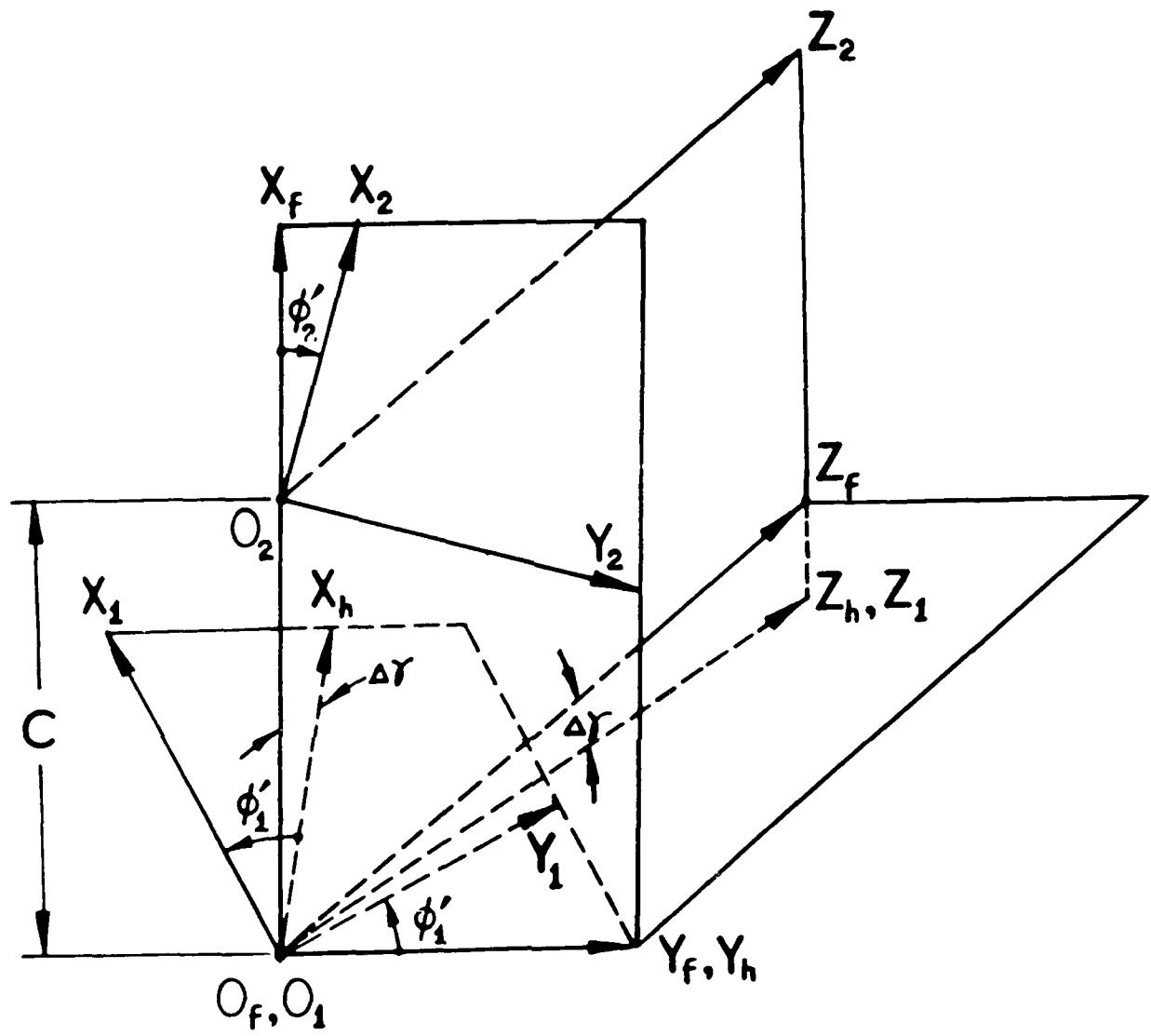
Fig. 8.3

$$\left[L_{fh}\right] = \begin{bmatrix} \cos\Delta\gamma & 0 & -\sin\Delta\gamma \\ 0 & 1 & 0 \\ \sin\Delta\gamma & 0 & \cos\Delta\gamma \end{bmatrix}$$

using equations (8.28), (I.9) - (I.12) and (7.1), (7.2), we may represent the tangency of surface Σ_1 and Σ_2 for intersected misaligned gear axes as follows:

$$A_2\cos\mu_2 - B_2\sin\mu_2 + C = (A_1\cos\mu_1 + B_1\sin\mu_1)\cos\Delta\gamma -$$

$$(\rho_F\cos\theta_F\cos\lambda_F - \frac{a_F}{\cos\lambda_F} + b_F\cot\theta_F\tan\lambda_F\sin\lambda_F + r_1\phi_1\tan\lambda_F)\sin\Delta\gamma \quad (8.29)$$

$$-A_2\sin\mu_2 - B_2\cos\mu_2 = A_1\sin\mu_1 - B_1\cos\mu_1 \quad (8.30)$$

$$\rho_P\cos\theta_P\cos\lambda_P - \frac{a_P}{\cos\lambda_P} + b_P\cot\theta_P\sin\lambda_P\tan\lambda_P + r_2\phi_2\tan\lambda_P =$$

$$(A_1\cos\mu_1 + B_1\sin\mu_1)\sin\Delta\gamma + (\rho_F\cos\theta_F\cos\lambda_F - \frac{a_F}{\cos\lambda_F} + b_F\cot\theta_F\tan\lambda_F$$

$$\sin\lambda_F + r_1\phi_1\tan\lambda_F)\cos\Delta\gamma \quad (8.31)$$

$$\sin\theta_P\cos\mu_2 - \cos\theta_P\sin\lambda_P\sin\mu_2 = (\sin\theta_F\cos\mu_1 + \cos\theta_F\sin\lambda_F\sin\mu_1)$$

$$\cos\Delta\gamma - \cos\theta_F\cos\lambda_F\sin\Delta\gamma \quad (8.32)$$

$$-\sin\theta_P\sin\mu_2 - \cos\theta_P\sin\lambda_P\cos\mu_2 = \sin\theta_F\sin\mu_1 - \cos\theta_F\sin\lambda_F\cos\mu_1 \quad (8.33)$$

$$\cos\theta_P\cos\lambda_P = (\sin\theta_F\cos\mu_1 + \cos\theta_F\sin\lambda_F\sin\mu_1)\sin\Delta\gamma + \cos\theta_F\cos\lambda_F\cos\Delta\gamma$$

$$(8.34)$$

Equations (8.29) - (8.34) form a system of five independent equations in six unknowns: θ_P, θ_F, μ_1, μ_2, ϕ_1 and ϕ_2. Only two equations from equation system (8.32) - (8.34) are independent. The computational procedure is the same as we discussed before.

Compensation for the Location of Bearing Contact Induced by the Gear Misalignment

The dislocation of the bearing contact induced by misalignment of the axes of gear rotation may be compensated for by the change of the lead angle λ_F (or λ_P). This can be done technologically by refinishing of the pinion.

Example 8.1:   The Influence of Change of Axes Distance

Given: the rack parameters (see Fig. 2.1 and Fig. 2.2); the gear parameters: No. of teeth $N_1 = 12$, $N_2 = 94$; lead angle $\lambda_F = \lambda_P = 75°$ nominal pressure angle $\theta° = 30°$; normal diametral pitch $P_n = 2$; nominal axes distance $C = 27.43482$ in.; change of axes distance $\Delta C = 0.021$ in. Due to the change of axes distance the new value of the pressure angle θ is: (i) $\theta = 12.82082°$ (exact solution provided by equation system (8.5) - (8.7)); (ii) $\theta = 12.70903°$ (approximate solution provided by equation (8.13))

The compensation for the dislocation of bearing contact is achieved by the new machine setting $b_F = b_F° - 0.021$ in. which provides $\theta = \theta° = 30°$ although $C = C° + \Delta C$.

Example 8.2:   The Influence of Misalignment of Crossed Gear Axes

The rack and gear nominal parameters are the same as shown in Example 8.1. The misalignment of crossed gear axes is given by $\Delta \gamma = 0.1°$ (Fig. 8.2). The kinematical errors $\Delta \phi_2'$ and the change of θ_F and θ_P are given in Table 1.

The compensation of kinematical errors is achieved with the change of the lead angle of the pinion $\lambda_F = 75.10°$ ($\Delta \lambda_F = 0.10°$). The kinematical errors after compensation are given in Table 2.

68

Table 1. Kinematical Errors

ϕ_1	θ_F	θ_P	$\Delta\phi_2'$ (seconds)
-20°	32.2603°	31.6606°	59.88"
-10°	32.2610°	31.6613°	29.94"
0°	32.2613°	31.6616°	0.00"
10°	32.2613°	31.6615°	-29.94"
20°	32.2609°	31.6611°	-59.89"

Table 2. Compensated Kinematical Errors

ϕ_1	θ_F	θ_P	$\Delta\phi_2'$ (seconds)
-20°	29.9988°	29.9989°	-0.00"
-10°	29.9996°	29.9996°	-0.00"
0°	29.9999°	29.9999°	0.00"
10°	30.0000°	29.9995°	-0.00"
20°	29.9996°	29.9995°	-0.00"

By using the proposed method of compensation we could reduce substantially the kinematical errors induced by the misalignment of crossed axes of gear rotation (kinematical errors approach zero).

Example 8.3: The Influence of Misalignment of Intersected Gear Axes

The rack and gear nominal parameters are the same as shown in Example 8.1. The misalignment of intersected gear axes is given by $\Delta\gamma = 0.1°$ (Fig. 8.3). The kinematical errors $\Delta\phi_2'$ and the change of θ_F and θ_P are given in Table 3. The compensation of kinematical errors is achieved with the change of the lead angle of the pinion $\lambda_F = 75.06°$ ($\Delta\lambda_F = 0.06°$). The kinematical errors with compensation are given in Table 4.

Table 3. Kinematical Errors

ϕ_1	θ_F	θ_P	$\Delta\phi_2'$ (seconds)
-20°	38.1358°	37.7508°	42.57"
-10°	34.7987°	34.4138°	19.98"
0°	31.5911°	31.2063°	-0.00"
10°	28.4910°	28.1062°	-17.65"
20°	25.4817°	25.0969°	-33.19"

Table 4. Compensated Kinematical Errors

ϕ_1	θ_F	θ_P	$\Delta\phi_2'$ (seconds)
-20°	37.1275°	37.0376°	5.17"
-10°	33.5327°	33.4847°	1.21"
0°	29.9883°	29.9898°	0.00"
10°	26.4191°	26.4823°	1.30"
20°	22.6873°	22.8334°	4.98"

By using the proposed method of compensation, we could reduce the kinematical errors induced by the misalignment of intersected axes of gear rotation.

9. Computer Aided Simulation of Bearing Contact (With Computer Graphics)

We simulated the bearing contact of gears by setting up two coordinate systems: S_1 and S_2, rigidly connected to the gear 1 (pinion) and gear 2, respectively (Fig. 3.1). Due to the computer graphics system, the figures showed in this section are two dimensional computer graphics.

Fig. 9.1 showed the normal crossed section of gear 1 (pinion) in coordinate system S_1 (Fig. 3.1 a), there are 12 teeth on the gear 1. We simulated gear 1 by considering the equations (3.6) - (3.12), the x_1 and y_1 axes are the axes of symmetry of the normal section. As we discussed in Chapter 3, it is important to mention that the normal section of the "fillet" of gear 1 can be simulated by using the same equations which we simulated the normal section of the working part and substituted ρ_F, θ_F, b_F and a_F by $\rho_F^{(f)}$, $\theta_F^{(f)}$, $b_F^{(f)}$, and $a_F^{(f)}$ in equations (3.6) - (3.12).

Fig. 9.2 showed the normal cross section of gear 2 in coordinate system S_2 (Fig. 3.1 b), there are 94 teeth on the

70

FILE NAME:G12P
PLOT OF GEAR 1

Y AXIS

X AXIS

Fig.9.1

FILE NAME:G12P
PLOT OF GEAR 2
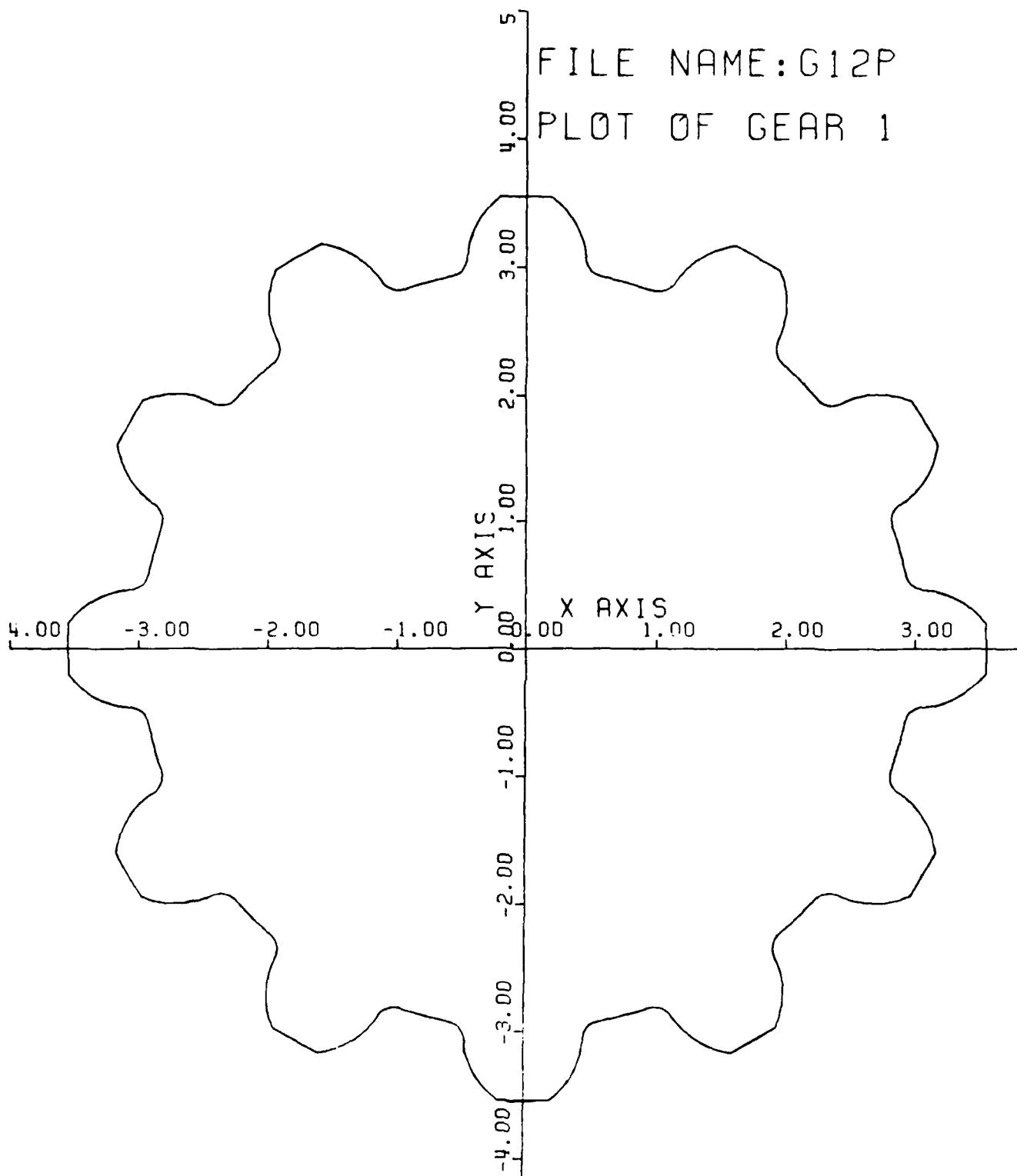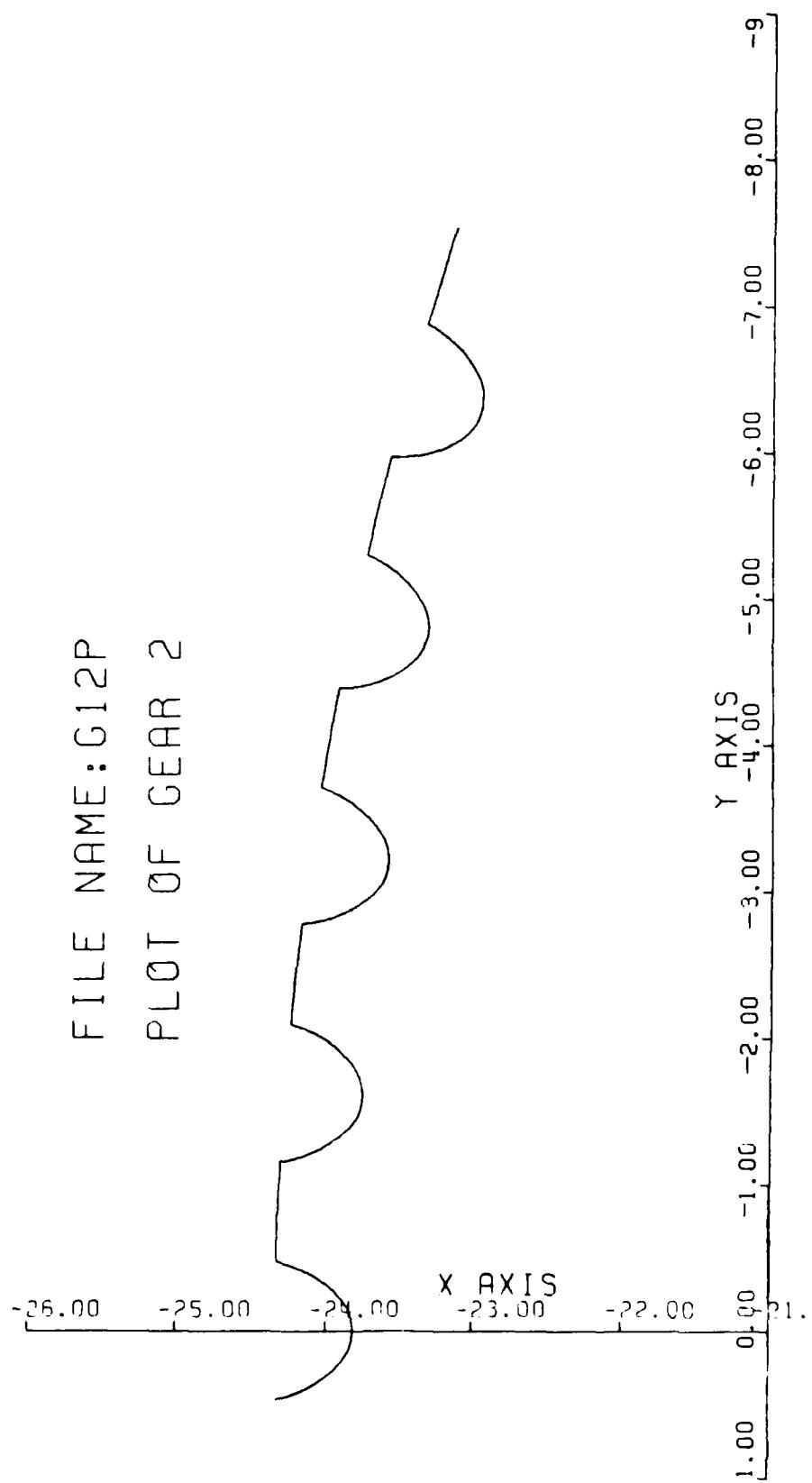
Fig.9.2

gear 2. We simulated gear 2 by considering the equations (3.16)
- (3.21), the x_2 and y_2 axes are the axes of symmetry of this
normal section. As we mentioned above, the normal section of the
"fillet" of gear 2 can be simulated by using the same equations
which we simulated the normal section of the working part, and
then substituted ρ_p, θ_p, b_p and a_p by $\rho_p^{(f)}$, $\theta_p^{(f)}$, $b_p^{(f)}$ and $a_p^{(f)}$
in equations (3.16) - (3.21)

Fig. 9.3 showed the front view of gear 1 and the orientation
of contacting ellipse of bearing contact when the center distance
did not change. It should be mentioned that the size of
contacting ellipse showed in Fig. 9.3 depended on the value of
elastic approach δ . Also, the contacting ellipses showed here
was a side view (the projection on x - z plane). Fig. 9.4 showed
the same case for the gear 2.

Fig. 9.5 showed the bearing contact of gear 1 due to an
increased of center distance 0.02 inches. Fig. 9.6 showed the
same case for the gear 2. From these two figures, we found that
the size and magnitudes of two axes of contacting ellipse are
changed a lot, this prove that circular arc helical gears are
very sensitive to the change of center-distance.

Fig. 9.7 showed the bearing contact of gear 1 due to the
misalignment of crossed axes of gear rotation for 1.0 degree.
The size and magnitudes of two axes of contacting ellipse were not
changed significantly. Fig. 9.8 showed the same case for the gear 2.
Fig. 9.9 showed the kinematical errors due to the misalignment of
crossed axes of gear rotation for 1.0 degree with and without

73

Y AXIS

FILE NAME:G1CC (TSO)

BEARING CONTACT OF GEAR 1 DUE TO
CHANGE OF CENTER DISTANCE=0.0 INCH

X AXIS

Fig.9.3

74

FILE NAME:G2CC (TSO)

BEARING CONTACT OF GEAR 2 DUE TO
CHANGE OF CENTER DISTANCE=0.0 INCH

Fig.9.4

X AXIS

Y AXIS

-25.00   -24.00   -23.00

0.00   1.00   2.00   3.00   4

-1.00

Y AXIS

FILE NAME:G1CC (TS0)

BEARING CONTACT OF GEAR 1 DUE TO
CHANGE OF CENTER DISTANCE=0.02 INCH

X AXIS
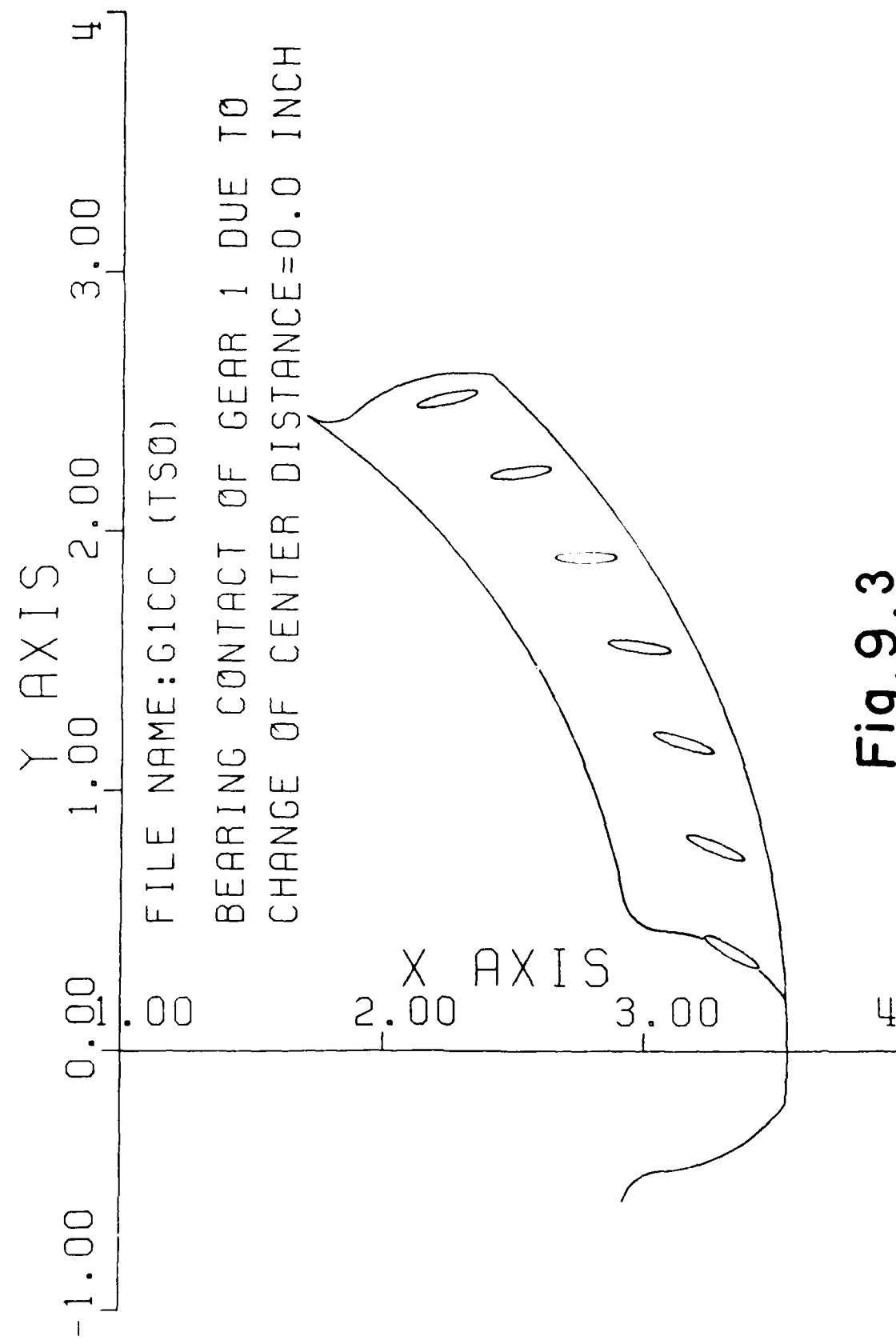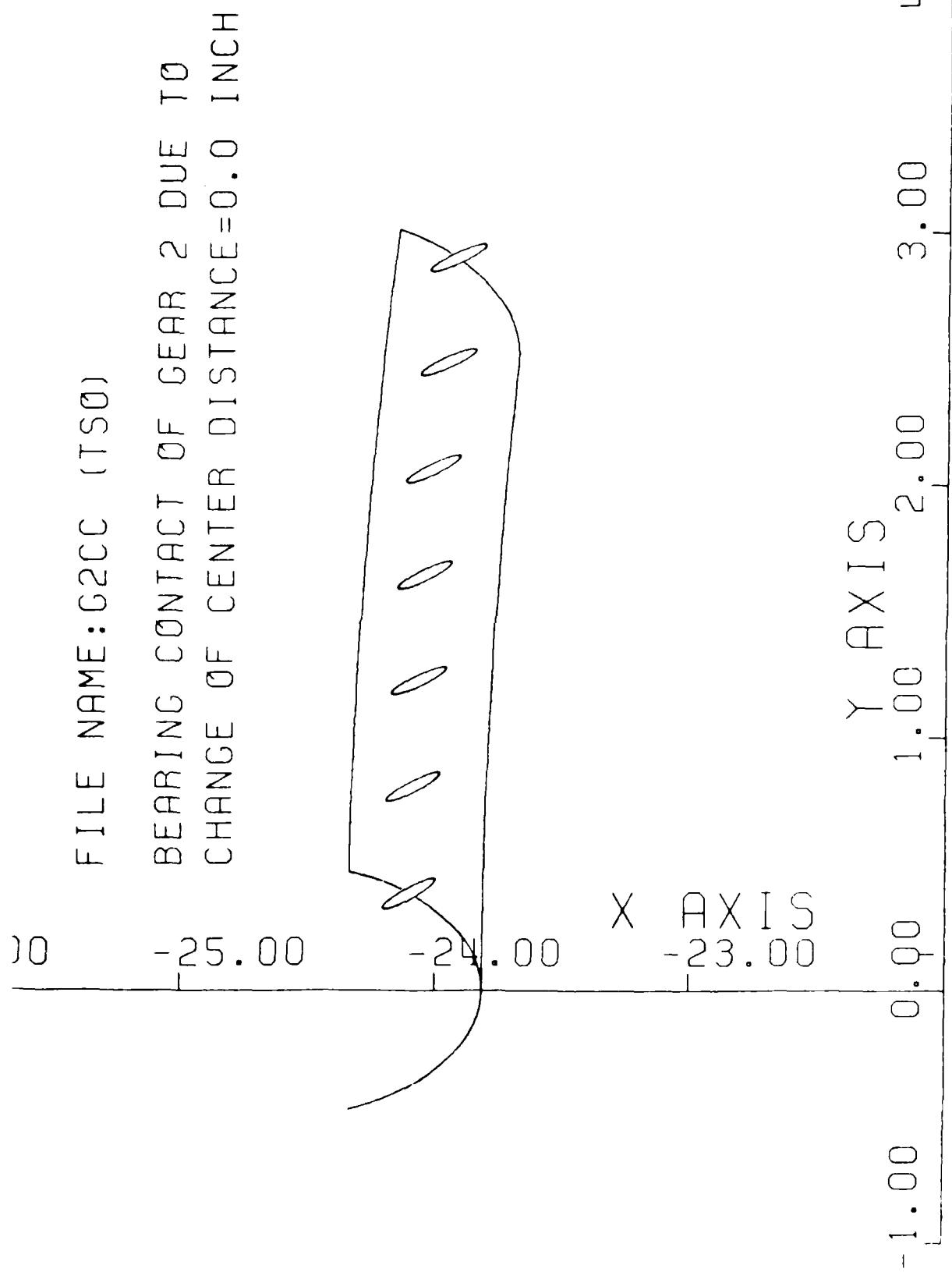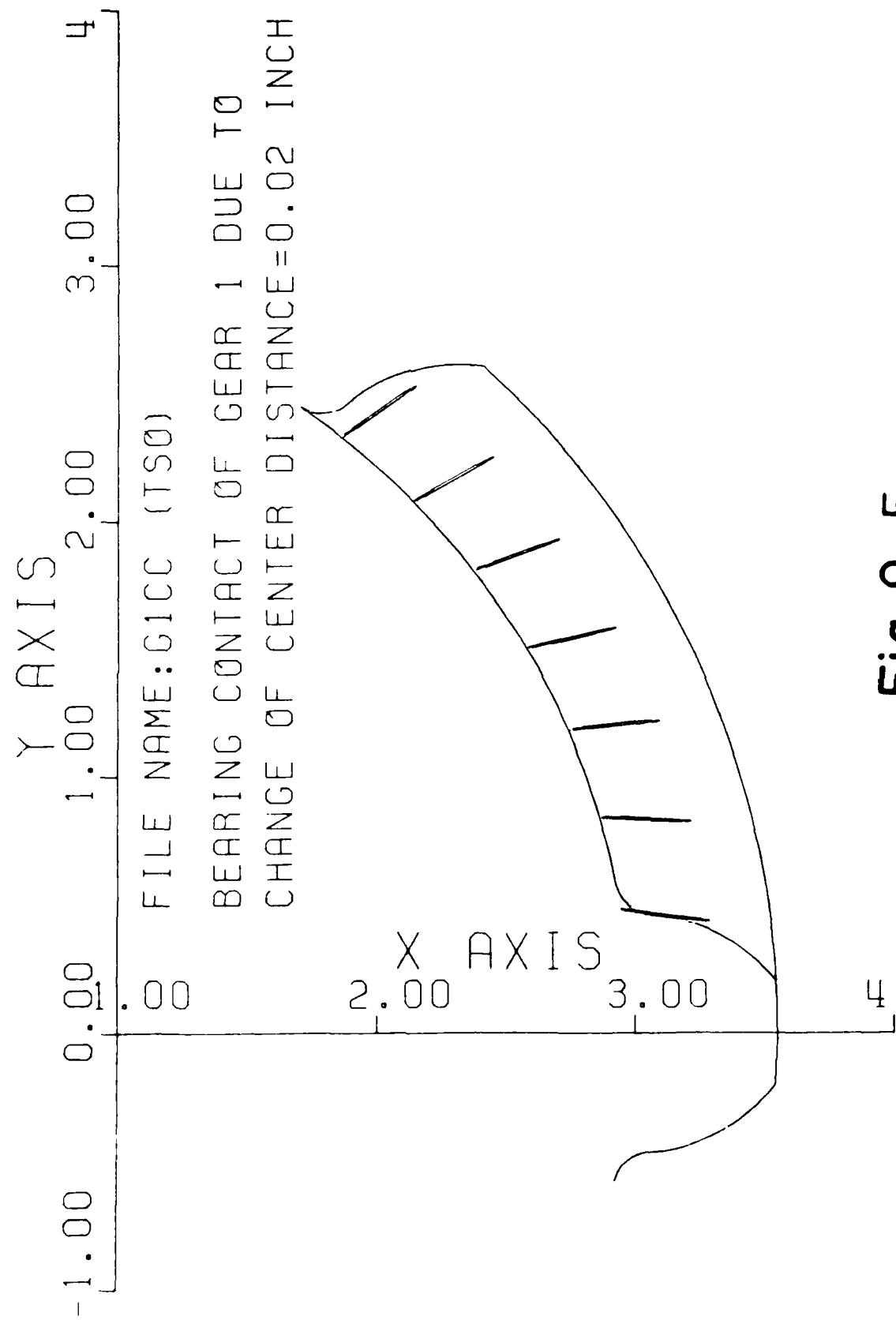
Fig.9.5

FILE NAME:G2CC (TS0)

BEARING CONTACT OF GEAR 2 DUE TO
CHANGE OF CENTER DISTANCE=0.02 INCH

Fig.9.6

Y AXIS

FILE NAME:G1MA (TS0)

BEARING CONTACT OF GEAR 1
DUE TO AXIAL MISALIGNMENT=1.0 DEG

Fig.9.7

FILE NAME:G2MA (TSO)

BEARING CONTACT OF GEAR 2
DUE TO AXIAL MISALIGNMENT=1.0 DEG

Fig.9.8

FILE NAME: KR (TSO)

KINEMATICAL ERRORS DUE TO
MISALIGNMENT OF AXIS =1.0 DEG

WITHOUT COMPENSATION:
WITH COMPENSATION:
(LAMDA==75.937 DEG)

KINEMATICAL ERRORS (×100 SEC)

ANGLE PHI1 (DEGREES)
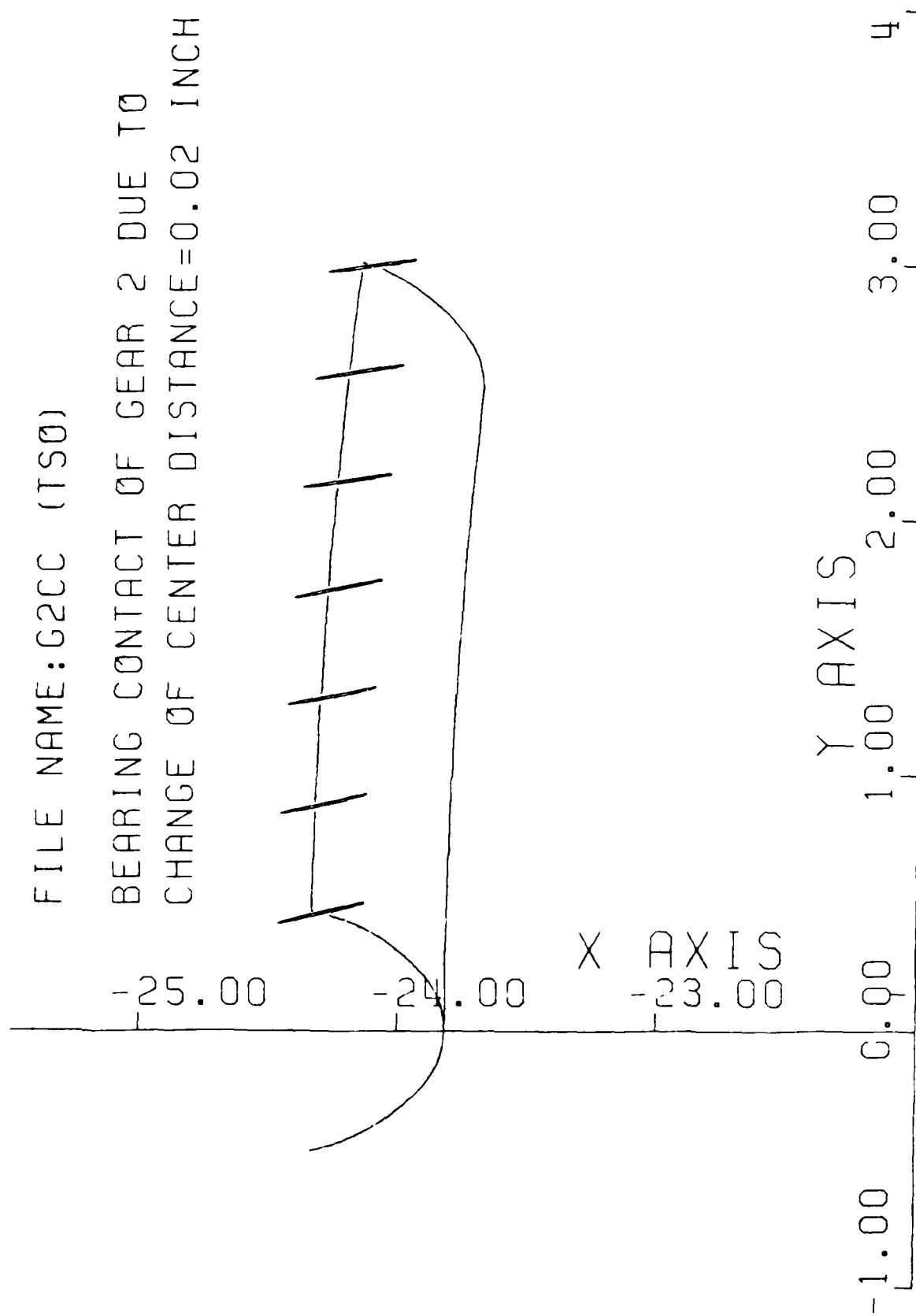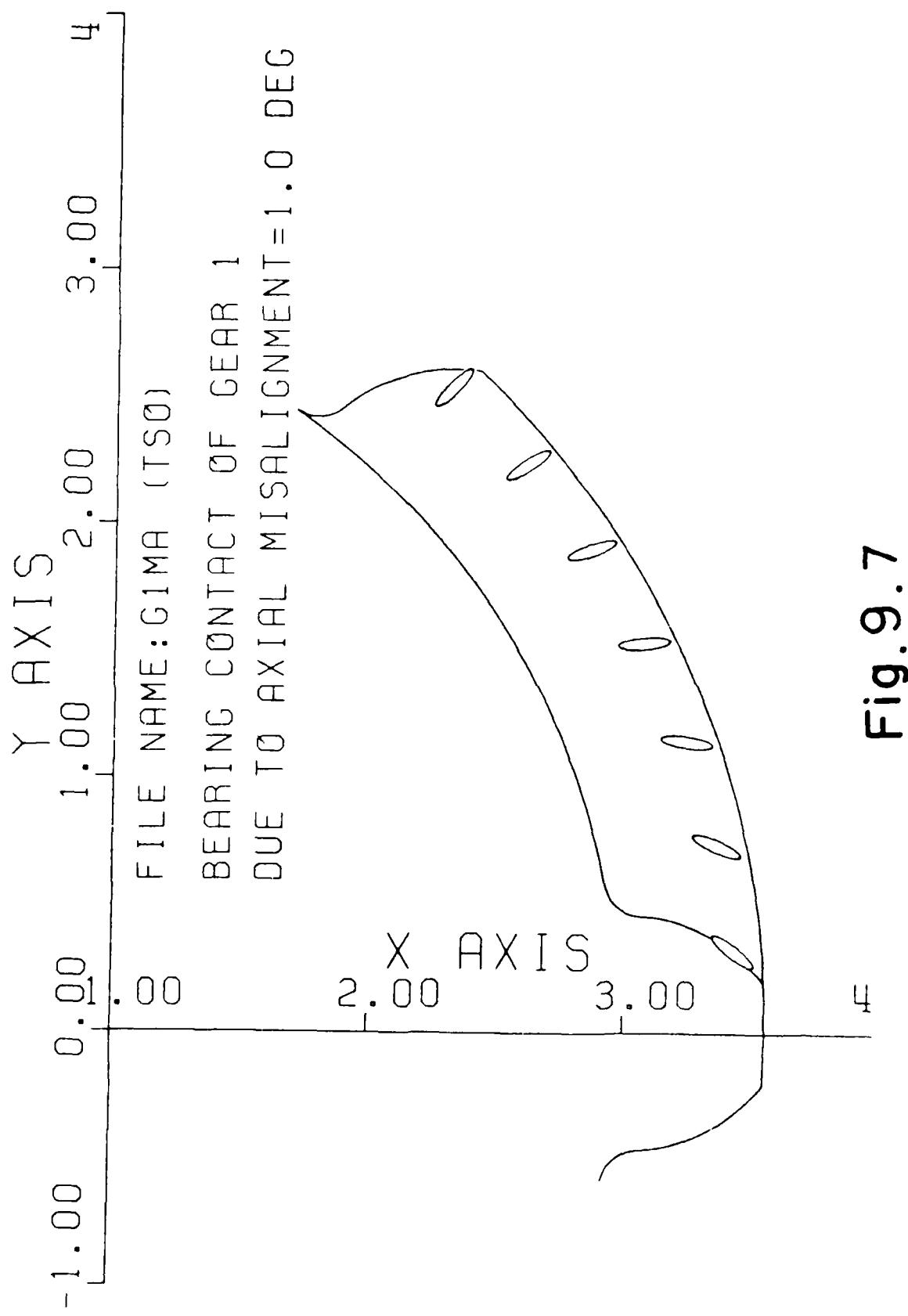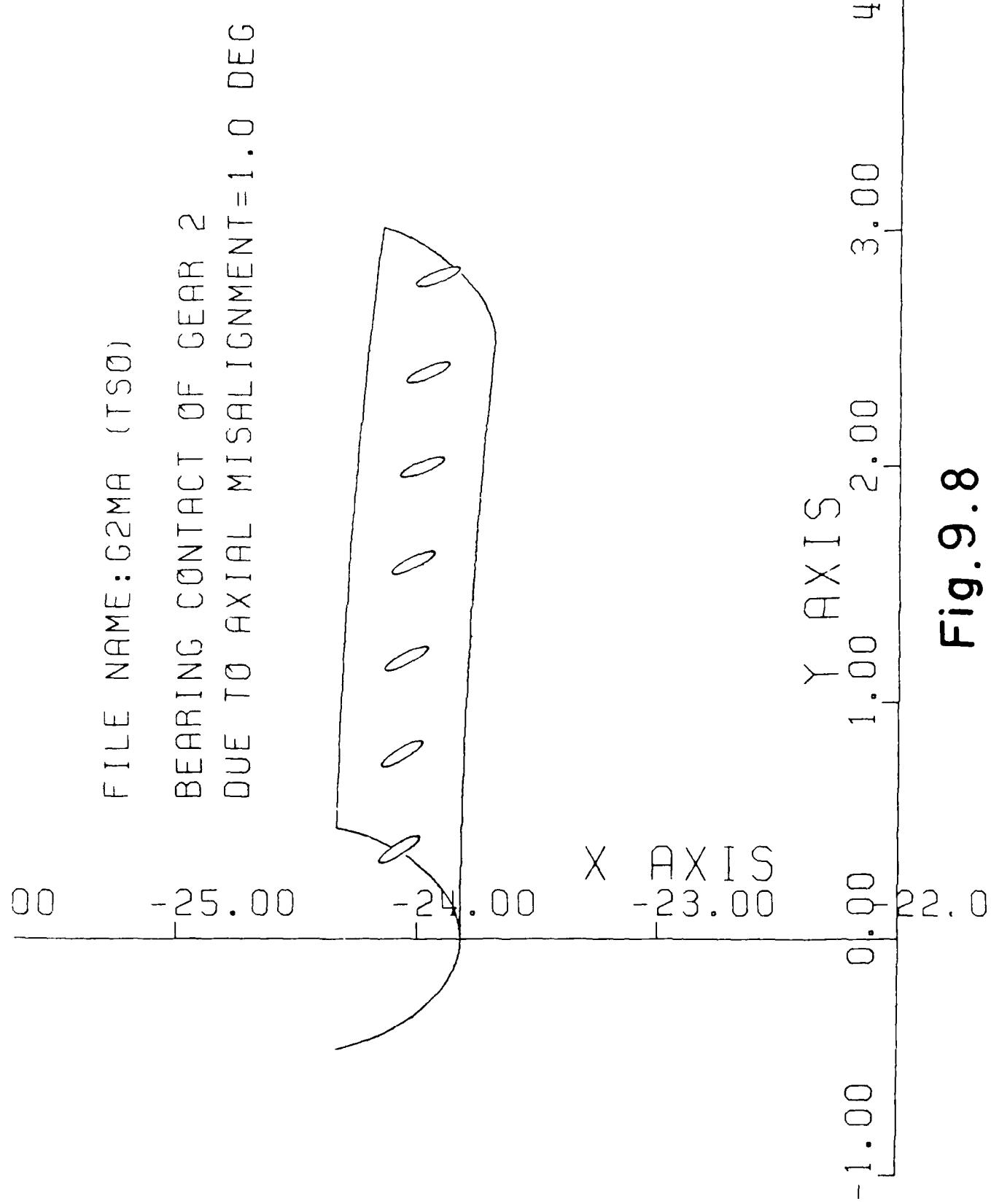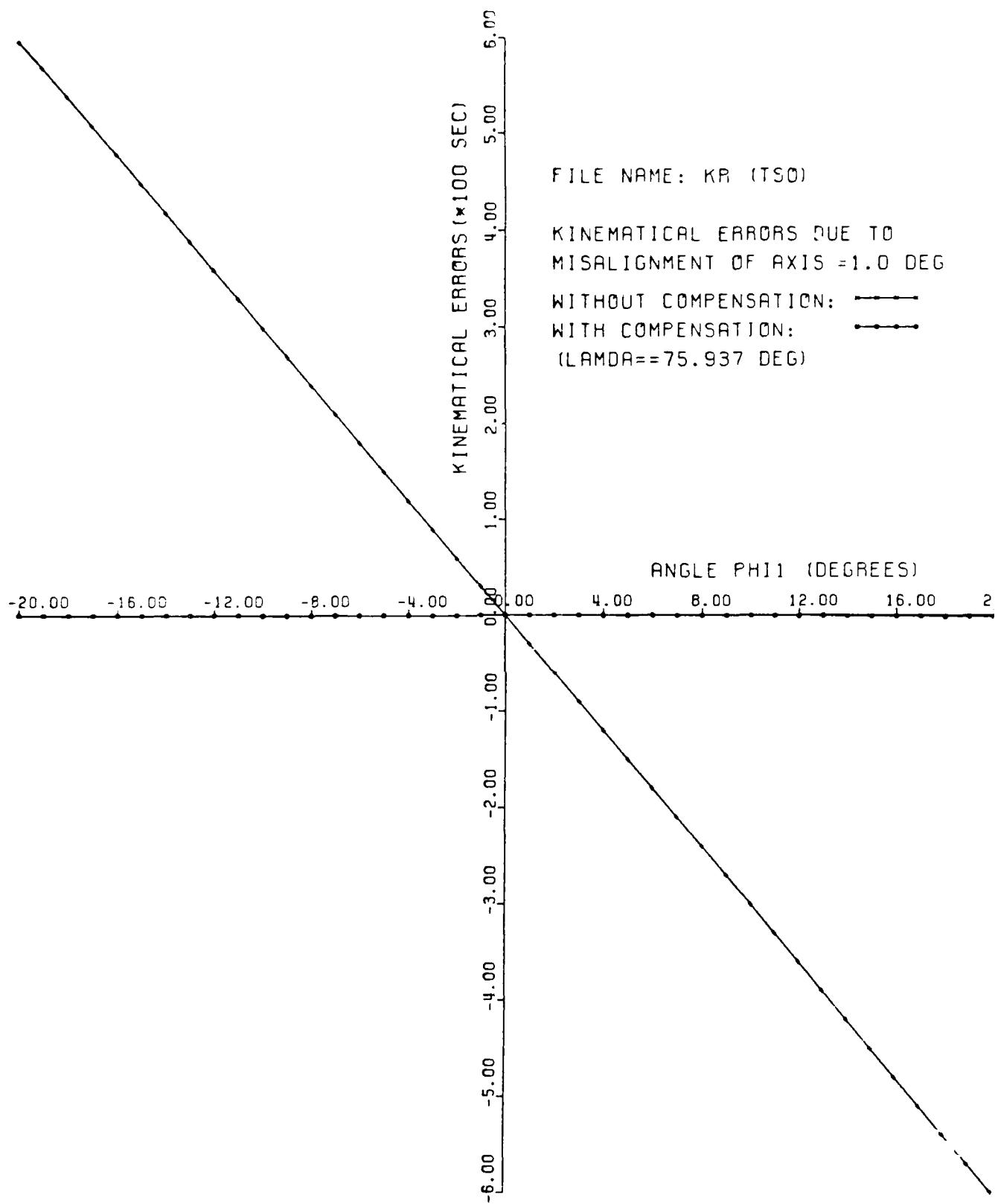
Fig.9.9

compensation. From this, we prove that using the proposed method of compensation discussed in Chapter 8, we can cause the kinematical errors to approach zero.

10. Conclusion

The authors have presented a method of generation of tooth surfaces for circular arc helical gears, derived the basic equations which represent the geometry of gears, and proposed a computer aided method for simulation of conditions of meshing and of the bearing contact for these gears. The sensitivity of the gears to the change of center-distance, machine-tool settings and to the misalignment of axes of gear rotation have been investigated. A technological technique for the compensation of the dislocation of the bearing contact induced by the above errors have been proposed.

11. References

1. N.P. Chironis, Design of Novikov Gears, in the book "Gear Design and Application," Editor N.P. Chironis, McGraw-Hill Book Company.

2. J.S. Davidov, "The Generation of Conjugate Surfaces by Two Rigidly Connected Tool Surfaces," Vestnik Mashinostroyenia, 1963, No. 2.

3. V.N. Kudrjavzev, Epicycloidal Trains, Mashgis, 1966.

4. F.L. Litvin, "The Investigation of the Geometric Properties of a Variety of Novikov Gearing", The Proceedings of Leningrad Mechanical Institute, 1962, No. 24 (in Russian)

5. F.L. Litvin, "Theory of Gearing," 2nd edition, Nauka, 1968 (in Russian).*

6. F.L. Litvin, P. Rahman and R.N. Goldrich, "Mathematical Models for the Synthesis and Optimization of Spiral Bevel Gear Tooth Surfaces," NASA Contractor Report 3553, 1982.

7. G. Niemann, "Novikov Gear System and Other Special Gear Systems for High Load Carrying Capacity," VDI Berichte, No. 47, 1961.

8. M.L. Novikov, USSR Patent No. 109, 750, 1956.

9. C.F. Wells and B.A. Shotter, "The Development of 'Circarc' Gearing," AEI Engineering, March-April 1962.

10. E. Wildhaber, The US Patent, No.1,601,750 issued Oct. 5, 1926, and "Gears with Circular Tooth Profile Similar to The Novikov System," VDI Berichte, No. 47, 1961.

11. H. Winter and J. Looman, "Tools for making Helical Circular Arc Spur Gears," VDI Berichte, No. 47, 1961.

*The new edition (in English), revised and completed, sponsored by NASA, is in press.

12. Appendix I Gear Tooth Surfaces

<u>Gear 1 Tooth Surface.</u> Substituting subscript "i" by "F" in equations (2.4) and (2.6) and taking into account that $b_F > 0$, we obtain:

$$
\left[r_C^{(F)} \right] =
\begin{bmatrix}
\rho_F \sin\theta_F - b_F \\[2mm]
-(\rho_F \cos\theta_F - a_F)\sin\lambda_F + u_F \cos\lambda_F \\[2mm]
(\rho_F \cos\theta_F - a_F)\cos\lambda_F + u_F \sin\lambda_F \\[2mm]
1
\end{bmatrix}
\tag{I.1}
$$

$$
\left[n_C^{(F)} \right] =
\begin{bmatrix}
\sin\theta_F \\[2mm]
-\cos\theta_F \sin\lambda_F \\[2mm]
\cos\theta_F \cos\lambda_F
\end{bmatrix}
\tag{I.2}
$$

Equations (I.1) and (I.2) represent the generating surface Σ_F and the unit normal to this surface. We may derive the equation of meshing using equations (I.1), (I.2) and (3.2) with

$$
X_C^{(F)} = 0, \quad Y_C^{(F)} = r_1 \phi_1, \quad Z_C^{(F)} = \ell
\tag{I.3}
$$

where $X_C^{(F)}$, $Y_C^{(F)}$ and $Z_C^{(F)}$ are coordinates of the point of intersection of the normal to Σ_F and the instantaneous axis of rotation, I-I (Fig. 3.1, a). We then obtain

$$
f_F(u_F, \theta_F, \phi_1) = (r_1\phi_1 - u_F \cos\lambda_F - a_F \sin\lambda_F)\sin\theta_F +
$$
$$
b_F \cos\theta_F \sin\lambda_F = 0
\tag{I.4}
$$

83

Equation of meshing (I.4) yields

$$u_F = \frac{r_1\phi_1 - a_F\sin\lambda_F}{\cos\lambda_F} + b_F\cot\theta_F\tan\lambda_F \qquad (I.5)$$

Equations (I.1) and (I.5) when considered simultaneously represent a family of contacting lines on surface Σ_F. Eliminating u_F, we may represent this family of lines of contact as follows:

$$\begin{bmatrix} x_c^{(F)} \\ y_c^{(F)} \\ z_c^{(F)} \end{bmatrix} = \begin{bmatrix} \rho_F\sin\theta_F - b_F \\ -(\rho_F\sin\theta_F - b_F)\cot\theta_F\sin\lambda_F + r_1\phi_1 \\ (\rho_F\sin\theta_F + b_F\tan^2\lambda_F)\cot\theta_F\cos\lambda_F - \dfrac{a_F}{\cos\lambda_F} + r_1\phi_1\tan\lambda_F \end{bmatrix} \qquad (I.6)$$

Using equations (I.6) and the coordinate transformation from $S_c^{(F)}$ to S_1 we obtain

$$x_1 = (\rho_F\sin\theta_F - b_F + r_1)\cos\phi_1 + (\rho_F\cos\theta_F - b_F\cot\theta_F)\sin\phi_1\sin\lambda_F$$

$$y_1 = (\rho_F\sin\theta_F - b_F + r_1)\sin\phi_1 - (\rho_F\cos\theta_F - b_F\cot\theta_F)\cos\phi_1\sin\lambda_F$$

$$z_1 = \rho_F\cos\theta_F\cos\lambda_F - \frac{a_F}{\cos\lambda_F} + b_F\cot\theta_F\tan\lambda_F\sin\lambda_F + r_1\phi_1\tan\lambda_F$$

$$(I.7)$$

The surface unit normal is given by

$$\begin{bmatrix} n_1 \end{bmatrix} = \begin{bmatrix} \sin\theta_F\cos\phi_1 + \cos\theta_F\sin\lambda_F\sin\phi_1 \\ \sin\theta_F\sin\phi_1 - \cos\theta_F\sin\lambda_F\cos\phi_1 \\ \cos\theta_F\cos\lambda_F \end{bmatrix} \qquad (I.8)$$

Using the coordinate transformation from S_1 to S_h we obtain

84

$$x_h^{(1)} = A_1\cos\mu_1 + B_1\sin\mu_1$$

$$y_h^{(1)} = A_1\sin\mu_1 - B_1\cos\mu_1$$

$$z_h^{(1)} = \rho_F\cos\theta_F\cos\lambda_F - \frac{a_F}{\cos\lambda_F} + b_F\cot\theta_F\tan\lambda_F\sin\lambda_F + r_1\phi_1\tan\lambda_F$$

$$(\text{I}.9)$$

$$\left[n_h^{(1)}\right] = \begin{bmatrix} \sin\theta_F\cos\mu_1 + \cos\theta_F\sin\lambda_F\sin\mu_1 \\ \sin\theta_F\sin\mu_1 - \cos\theta_F\sin\lambda_F\cos\mu_1 \\ \cos\theta_F\cos\lambda_F \end{bmatrix} \qquad (\text{I}.10)$$

Here:

$$A_1(\theta_F) = \rho_F\sin\theta_F - b_F + r_1, \quad B_1(\theta_F) = (\rho_F\cos\theta_F - b_F\cot\theta_F)\sin\lambda_F,$$

and $\mu_1 = \phi_1 - \phi_1'$ $\qquad (\text{I}.11)$

Equations (I.9) and (I.10) with a fixed value for ϕ_1', represent in the coordinate system S_h, surface Σ_1 and the unit normal to Σ_1. These equations with different values for ϕ_1', represent in S_h, a <u>family</u> of surfaces Σ_1 and the unit normals to these surfaces.

The derivation of equations for gear 2 surface Σ_2 and its unit normal is based on similar considerations. We may represent these equations in S_f as follows:

$$x_f^{(2)} = A_2\cos\mu_2 - B_2\sin\mu_2 + C$$

$$y_f^{(2)} = -A_2\sin\mu_2 - B_2\cos\mu_2$$

$$z_f^{(2)} = \rho_P\cos\theta_P\cos\lambda_P - \frac{a_P}{\cos\lambda_P} + b_P\cot\theta_P\sin\lambda_P\tan\lambda_P + r_2\phi_2\tan\lambda_P$$

$$(\text{I}.12)$$

$$\left[n_f^{(2)} \right] = \begin{bmatrix} \sin\theta_P\cos\mu_2 - \cos\theta_P\sin\mu_P\sin\mu_2 \\ -\sin\theta_P\sin\mu_2 - \cos\theta_P\sin\lambda_P\cos\mu_2 \\ \cos\theta_P\cos\lambda_P \end{bmatrix} \tag{I.13}$$

Here:

$$A_2(\theta_P) = \rho_P\sin\theta_P - b_P - r_2, \quad B_2(\theta_P) = (\rho_P\cos\theta_P - b_P\cot\theta_P)\sin\lambda_P,$$

$$\text{and } \mu_2 = \phi_2 - \phi_2' \tag{I.14}$$

The nominal value of the center distance is $C = r_1 + r_2$.

List of Symbols

(Note: $i = 1,2$; $d = F, P$)

a — Half the length of major axis of contacting ellipse.

a_d — Algebraic values which determine the location of the center of the circular arc.

$a_{31}^{(1)}$ — Auxiliary function defined in Eq. (4.11)

$a_{32}^{(1)}$ — " " Eq. (4.12)

$a_{31}^{(2)}$ — " " Eq. (4.43)

$a_{32}^{(2)}$ — " " Eq. (4.44)

A — " " Eq. (5.1)

A_I — " " Eq. (3.9)

A_{II} — " " Eq. (3.19)

b — Half the length of minor axis of contacting ellipse.

b_d — a parameter of tool setting

b_d° — Nominal value for the machine settings

$b_3^{(1)}$ — Auxiliary function defined in Eq. (4.13)

$b_3^{(2)}$ — " " Eq. (4.45)

B — " " Eq. (5.1)

B_I — " " Eq. (3.9)

B_{II} — " " Eq. (3.19)

87

C_F center of working part of circular arc rack cutter F

$C_F^{(f)}$ center of the fillet of circular arc rack cutter F

C_p center of working part of circular arc rack cutter P

$C_p^{(f)}$ center of the fillet of circular arc rack cutter P

D_I Auxiliary function defined in Eq. (3.9)

D_{II} "   "   Eq. (3.19)

E_I "   "   Eq. (3.9)

E_{II} "   "   Eq. (3.19)

$F^{(i)}$ Auxiliary function defined in Eq. (4.8), Eq. (4.46) to compute the principal directions of surface Σ_i

$g_1 = K_I^{(1)} - K_{II}^{(1)}$ Auxiliary function defined in Eq. (5.1) to determine the size of contacting ellipse

$g_2 = K_I^{(2)} - K_{II}^{(2)}$ Auxiliary function defined in Eq. (5.1) to determine the size of contacting ellipse

$G^{(i)}$ Auxiliary function defined in Eq. (4.9), Eq. (4.47) to compute the principal curvatures of surface Σ_i

$\underset{\sim}{i}_I^{(d)}, \underset{\sim}{i}_{II}^{(d)}$ unit vectors along principal direction of surface Σ_d

$\kappa_I^{(i)}, \kappa_{II}^{(i)}$ principal curvatures of surface Σ_i

$\kappa_{\Sigma}^{(1)} = \kappa_{I}^{(1)} + \kappa_{II}^{(1)}$ Auxiliary function defined in Eq. (5.1)

$\kappa^{(2)} = \kappa_{I}^{(2)} + \kappa_{II}^{(2)}$ Auxiliary function defined in Eq. (5.1)

$\left[L_{ij} \right]$ projection transformation matrix; transformation from S_j to S_i

M point of contact of tooth surface

$\left[M_{ij} \right]$ coordinate transformation matrix; transformation from S_j to S_i

$\underset{\sim}{n}^{(d)}$ surface d unit normal

$\underset{\sim}{\dot{n}}_r^{(i)}$ relative velocity of the tip of the unit normal vector $\underset{\sim}{n}_i$

$\underset{\sim}{N}^{(d)}$ surface d normal vector

P_n Diametral pitch in normal section

$\underset{\sim}{r}_c$ position vector represented in the coordinate system S_c

r_i Pitch radius of gear i

$\underset{\sim}{r}_i(u_i, \theta_i)$ surface Σ_i position vector with surface coordinates (u_i, θ_i)

S_f coordinate system rigidly connected with frame

S_h Auxiliary coordinate system h

$S_i(x_i, y_i, z_i)$ coordinate system rigidly connected with gear i

$s^{(i)}$ Auxiliary function defined in Eq. (4.10), Eq. (4.48)

89

u_d generating surface coordinate

$v_{abs}^{(1)}$ Absolute velocity of the point on the surface Σ_i

$v_f^{(12)}$ Relative velocity represented in coordinate system S_f of a contact point on surface Σ_1 with respect to contact point on surface Σ_2.

$v_r^{(i)}$ Relative velocity of contact point on surface Σ_i

$v_{tr}^{(i)}$ Transfer velocity of contact point on surface Σ_i

$v_1^{(i)}$ Transfer velocities of points on surface Σ_i in coordinate system 1.

$v_1^{(21)}$ Relative velocity of point 2 with respect to point 1 $\left(v_1^{(21)} = v_1^{(2)} - v_1^{(1)}\right)$

α Angle of the orientation of contacting ellipse measured from axis η to the unit vector $i_I^{(1)}$

ΔC Change of center distance (inches)

$\Delta \gamma$ misalignment of gear rotation axes

δ Approach of surface Σ_1 and Σ_2

ε° Nominal value of the pressure angle

θ_d pressure angle of gear d

θ_i variable parameter which determines the location of a point on circular arc gear i

λ_i helical gear i lead angle

$\mu_1 = \phi_1 - \phi_1'$ Auxiliary function

$\mu_2 = \phi_2 - \phi_2'$ Auxiliary function

ρ_d Radius of working part of circular arc rack cutter d

ρ_d^o Nominal value for the radius of circular arc

$\rho_d^{(f)}$ Radius of fillet of circular arc rack cutter d

Σ_d generating surface d

Σ_i generated surface of pinion and gear

σ Angle form by principal direction of two surfaces measured from $\underset{\sim}{i}_I^{(1)}$ to $\underset{\sim}{i}_I^{(2)}$ and positive angle for counterclockwise

$\sigma^{(F1)}$ Angle measured from $\underset{\sim}{i}_I^{(F)}$ to the unit vector $\underset{\sim}{i}_I^{(1)}$; positive if counterclockwise

$\sigma^{(P2)}$ Angle measured from $\underset{\sim}{i}_I^{(P)}$ to the unit vector $\underset{\sim}{i}_I^{(2)}$; positive if counterclockwise

ϕ_i gear i rotation angle in mesh with the corresponding rack cutter

ϕ_i' gear i rotation angle in mesh with the mating gear

$\Delta\phi_2'$ kinematical error function defined in Eq. (8.27)

ψ_c pressure angle

$\underset{\sim}{\omega}^{(i)}$ gear i angular velocity

NASA

Report Documentation Page

1. Report No.	2. Government Accession No.	3. Recipient's Catalog No.
NASA CR-4089 AVSCOM TR 87-C-18		

4. Title and Subtitle	5. Report Date
Helical Gears With Circular Arc Teeth: Generation, Geometry, Precision and Adjustment to Errors, Computer Aided Simulation of Conditions of Meshing, and Bearing Contact	OCTOBER 1987
	6. Performing Organization Code

7. Author(s)	8. Performing Organization Report No.
Faydor L. Litvin and Chung-Biau Tsay	None (E-3541)

	10. Work Unit No.
	1L161102AH45 505-63-51

9. Performing Organization Name and Address	11. Contract or Grant No.
University of Illinois at Chicago P.O. Box 4348 Chicago, Illinois 60680	NAG3-655

	13. Type of Report and Period Covered
12. Sponsoring Agency Name and Address	Contractor Report Final
U.S. Army Aviation Research and Technology Activity - AVSCOM, Propulsion Directorate, Lewis Research Center, Cleveland, Ohio 44135 and NASA Lewis Research Center, Cleveland, Ohio 44135	14. Sponsoring Agency Code

15. Supplementary Notes

Project Manager, John J. Coy, Propulsion Directorate, U.S. Army Aviation Research and Technology Activity - AVSCOM, Lewis Research Center.

16. Abstract

The authors have proposed a method for generation of circular arc helical gears which is based on application of standard equipment, worked out all aspects of the geometry of gears, proposed methods for the computer aided simulation of conditions of meshing and bearing contact, investigated the influence of manufacturing and assembly errors, and proposed methods for the adjustment of gears to these errors. The results of computer aided solutions are illustrated with computer graphics.

17. Key Words (Suggested by Author(s))	18. Distribution Statement
Gears; Circular arc gear teeth; Gear transmission error; Machine design; Kinematics	Unclassified - unlimited STAR Category 37

19. Security Classif. (of this report)	20. Security Classif. (of this page)	21. No of pages	22. Price*
Unclassified	Unclassified	93	A05

END

DATE

FILMED

MARCH

1988

DTIC